1976-06

# Study of an integrated circuit tapped delay line and its applications to signal processing

Ang Vong, Mongkol

Monterey, California. Naval Postgraduate School

# STUDY OF AN INTEGRATED CIRCUIT TAPPED DELAY LINE AND ITS APPLICATIONS TO SIGNAL PROCESSING

Ang Vong Mongkol

# NAVAL POSTGRADUATE SCHOOL
## Monterey, California


# THESIS

STUDY OF AN INTEGRATED CIRCUIT TAPPED DELAY
LINE AND ITS APPLICATIONS
TO SIGNAL PROCESSING

by


Ang Vong Mongkol


June 1976

Thesis Advisor: T. F. Tao

| REPORT DOCUMENTATION PAGE | | READ INSTRUCTIONS BEFORE COMPLETING FORM |
|---|---|---|
| 1. REPORT NUMBER | 2. GOVT ACCESSION NO. | 3. RECIPIENT'S CATALOG NUMBER |
| 4. TITLE (and Subtitle) Study of an Integrated Circuit Tapped Delay Line and its Applications to Signal Processing | | 5. TYPE OF REPORT & PERIOD COVERED Master's Degree; June 1976 |
| | | 6. PERFORMING ORG. REPORT NUMBER |
| 7. AUTHOR(s) Ang Vong Mongkol | | 8. CONTRACT OR GRANT NUMBER(s) |
| 9. PERFORMING ORGANIZATION NAME AND ADDRESS Naval Postgraduate School Monterey, California 93940 | | 10. PROGRAM ELEMENT, PROJECT, TASK AREA & WORK UNIT NUMBERS |
| 11. CONTROLLING OFFICE NAME AND ADDRESS Naval Postgraduate School Monterey, California 93940 | | 12. REPORT DATE June 1976 |
| | | 13. NUMBER OF PAGES |
| 14. MONITORING AGENCY NAME & ADDRESS(if different from Controlling Office) Naval Postgraduate School Monterey, California 93940 | | 15. SECURITY CLASS. (of this report) Unclassified |
| | | 15a. DECLASSIFICATION/DOWNGRADING SCHEDULE |

16. DISTRIBUTION STATEMENT (of this Report)

Approved for public release; distribution unlimited.

17. DISTRIBUTION STATEMENT (of the abstract entered in Block 20, if different from Report)

18. SUPPLEMENTARY NOTES

19. KEY WORDS (Continue on reverse side if necessary and identify by block number)

Sampled Analog Non-Recursive Filter

Reticon TAD-12 Tapped Delay Line

20. ABSTRACT (Continue on reverse side if necessary and identify by block number)

An integrated circuit tapped delay line and its applications to sampled analog processing are studied. The theoretical effort includes the design of sampled analog transversal filters using the techniques developed for digital non-recursive filters. The experimental study includes the evaluation of the new Reticon TAD-12 tapped delay line and its

applications as prewhitening, dewhitening and bandpass filters. The frequency domain response and the time domain response are evaluated. The limitations in the device performance and the deviations of filter performance from theoretical analysis are investigated.

# Study of an Integrated Circuit Tapped Delay Line and Its Applications to Signal Processing

by

Ang Vong Mongkol
LCDR, Cambodian Navy
B.S., Naval Postgraduate School, 1975

Submitted in partial fulfillment of the requirements for the degree of

MASTER OF SCIENCE IN ELECTRICAL ENGINEERING

from the

NAVAL POSTGRADUATE SCHOOL
June 1976

ABSTRACT

An integrated circuit tapped delay line and its applications to sampled analog processing are studied. The theoretical effort includes the design of sampled analog transversal filters using the techniques developed for digital non-recursive filters. The experimental study includes the evaluation of the new Reticon TAD-12 tapped delay line and its applications as prewhitening, dewhitening and bandpass filters. The frequency domain response and the time domain impulse response are evaluated. The limitations in the device performance and the deviations of filter performance from theoretical analysis are investigated.

TABLE OF CONTENTS

LIST OF FIGURES

LIST OF TABLES

ACKNOWLEDGEMENT

The author expresses his sincere appreciation to Dr. T. F. Tao for his guidance and assistance in this study, and to the other members of the research team for their time and support.

# I. INTRODUCTION

Signal processing covers a wide range of application in such diverse fields as biomedical engineering, acoustics, sonar, radar, speech communication, data communication, and many others. As an example, one may wish to remove interference, such as noise, from the signal or to modify the signal to present it in a form which is more easily interpreted by an expert. As another example, a signal transmitted over a communications channel is generally perturbed in a variety of ways, including channel distortion, fading, and the insertion of background noise. One of the objectives at the receiver is to compensate for these perturbances. In each case, processing of the signal is required.

Signal processing was carried out typically by using analog equipment before the advent of digital computers which promoted the intensive and successful development of digital signal processing in the past decade. At present, much of the digital signal processing is performed on general purpose digital computers using software. However, tremendous progress has also been made in other types of signal processors using electronic firmware and hardware. Particularly, using electronic technologies, a new class of sampled analog processors is being developed using charge transport devices. Their signals are analog but the independent variables are discrete which can be either time variable, spatial variables or other

transform variables. The signal processing implementations are illustrated in Table I.I.

Signal processors can be grouped into two classes: filtering and spectral analysis. This classification is highlighted in Figure 1.1. All of these signal processing systems require the basic essential functions, such as correlation, convolution and transformation (Fast Fourier transform). In other words, they are shown to be centered around four basic mathematical operations: delay (or shift), multiplication, summation and generation of special functions. These operations have been performed by digital techniques and it was probably the most convenient method. However, the new sampled analog signal processing systems only require a storage for discrete time analog samples and not discrete or quantized signal amplitudes; in fact, because of the computation time, frequency selectivity, and part counts, it is undesirable to quantize the signal. Therefore, discrete time analog devices are being developed to perform the convolution, correlation, etc., without the need to convert the signal to digital format.

There are several distinct advantages of using the discrete time analog devices over the digital techniques to perform the same algorithm:

(1) In general, the discrete time device system can perform the same computation with much greater speed over the digital technique.

(2) The device stores discrete time analog amplitudes; therefore, it does not have the quantization errors inherent in the digital system.

(3) The actual multiplying and summing operations are easily implemented, and with fewer components than the digital system.

To illustrate the advantages that these discrete time devices have over the digital technique, a simple system shown in Figure 1-2 is used. This is a model of a simple single pole, first order discrete time filter. To implement this system with a discrete time device such as the SAD (Serial Analog Delay), all that is required is a straight substitution of the analog device for the delay block, an operational amplifier for the adder and a potentiometer proportional to the weighting coefficient. This system is shown in Figure 1-3.

Comparing this system implementation to the digital form in Figure 1.4 demonstrates the difference between the two systems. It requires at least two memory registers, one to store the sampled data, the other to store the multiplying constant. In the figure it is seen that more devices are required, such as the adder and the costly analog to digital converters, as well as the digital to analog converter to complete this system.

The integrated circuit delay devices can perform in principle most of the necessary algorithms used in most equipment for signal processing today. However, due to the primitive nature of these new classes of devices, there are limitations in some fields of application.

The purpose of this study is to perform the evaluation of Reticon TAD-12 tapped delay lines available commercially and

to find out their performances and limitations in order to use them properly.

TABLE I.I Signal Processing Implementation

| Signal | Equipment | Implementation |
| --- | --- | --- |
| Analog | General Purpose Computer | Software |
| | Special Purpose Computer | |
| | Mini/Microcomputer (Microprocessor) | Firmware |
| Digital | | |
| | Signal Processing Function Modules: | |
| | Multiplier | |
| | Correlator | |
| Sampled Analog | Convolver (matched filter) | Hardware |
| | Filter | |
| | Discrete Fourier Transformer | |
| | Frequency synthesizer | |
| | etc. | |

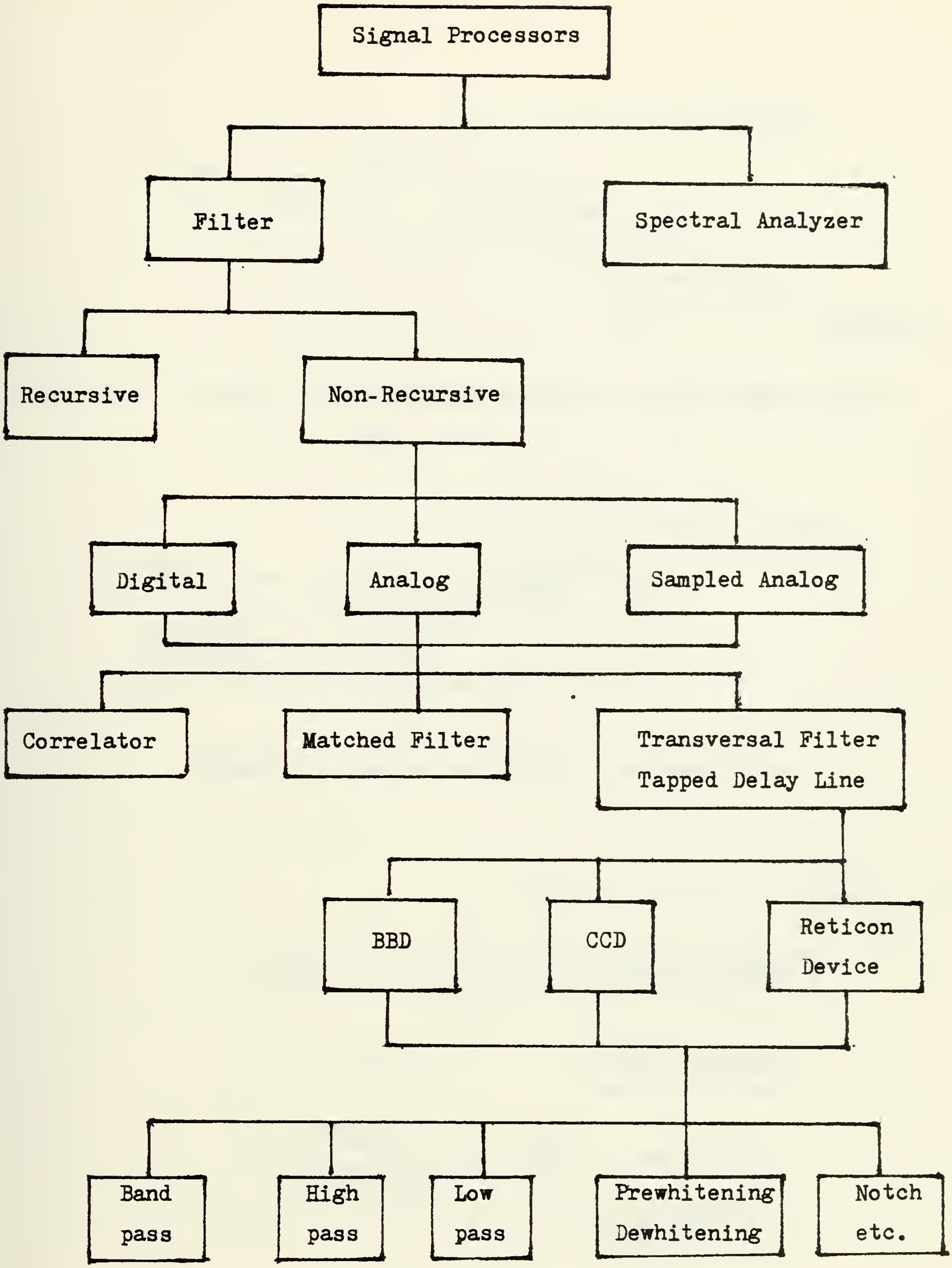


FIGURE 1.1 Classification of Signal Processors

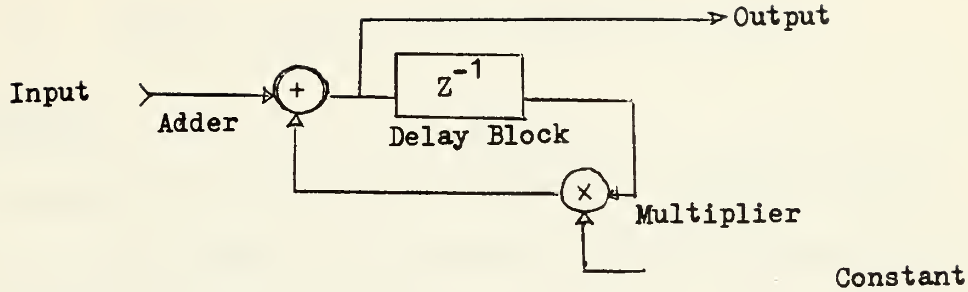


FIGURE 1.2 Equivalent Circuit of First Order Discrete Time Filter

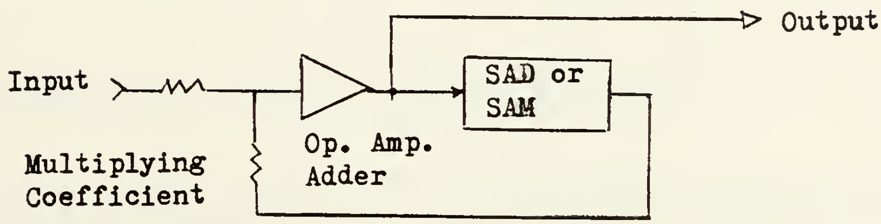


FIGURE 1.3 Equivalent Circuit Implementation

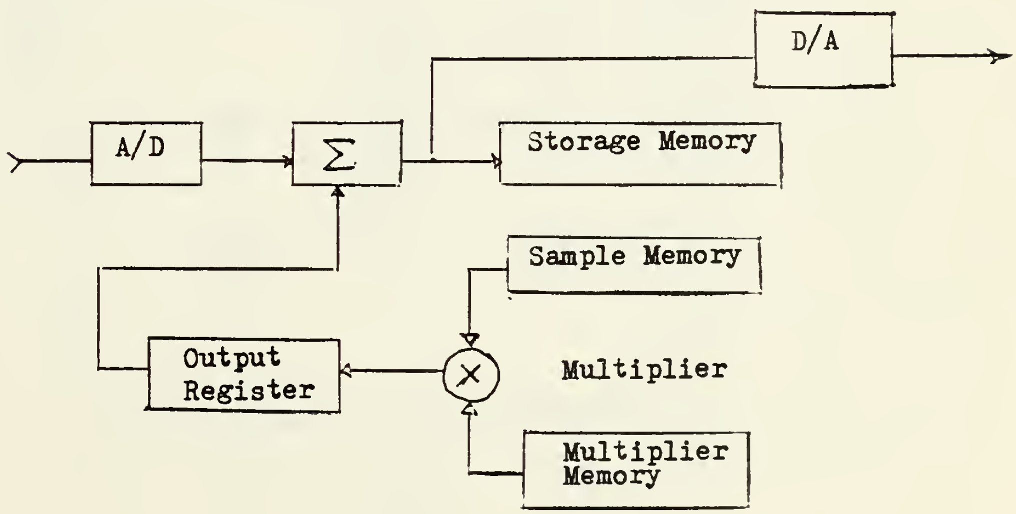


FIGURE 1.4 Digital Equivalent Circuit Implementation

## II. SAMPLED ANALOG NON-RECURSIVE FILTER

### A. PRINCIPLE

The transfer function of a digital or sampled analog filter can be expressed, in Z domain, by one of the following equations.

$$\text{Recursive filter:} \quad H(Z) = \frac{\Sigma_0^N \, a_n \, Z^{-n}}{1 + \Sigma_1^M \, b_m \, Z^{-n}} \qquad (2\text{-}1)$$

$$\text{Non-Recursive filter:} \quad H(Z) = \Sigma_0^N \, a_n \, Z^{-n} \qquad (2\text{-}2)$$

The block diagram of a sampled analog recursive filter is illustrated in Figure 2-1:

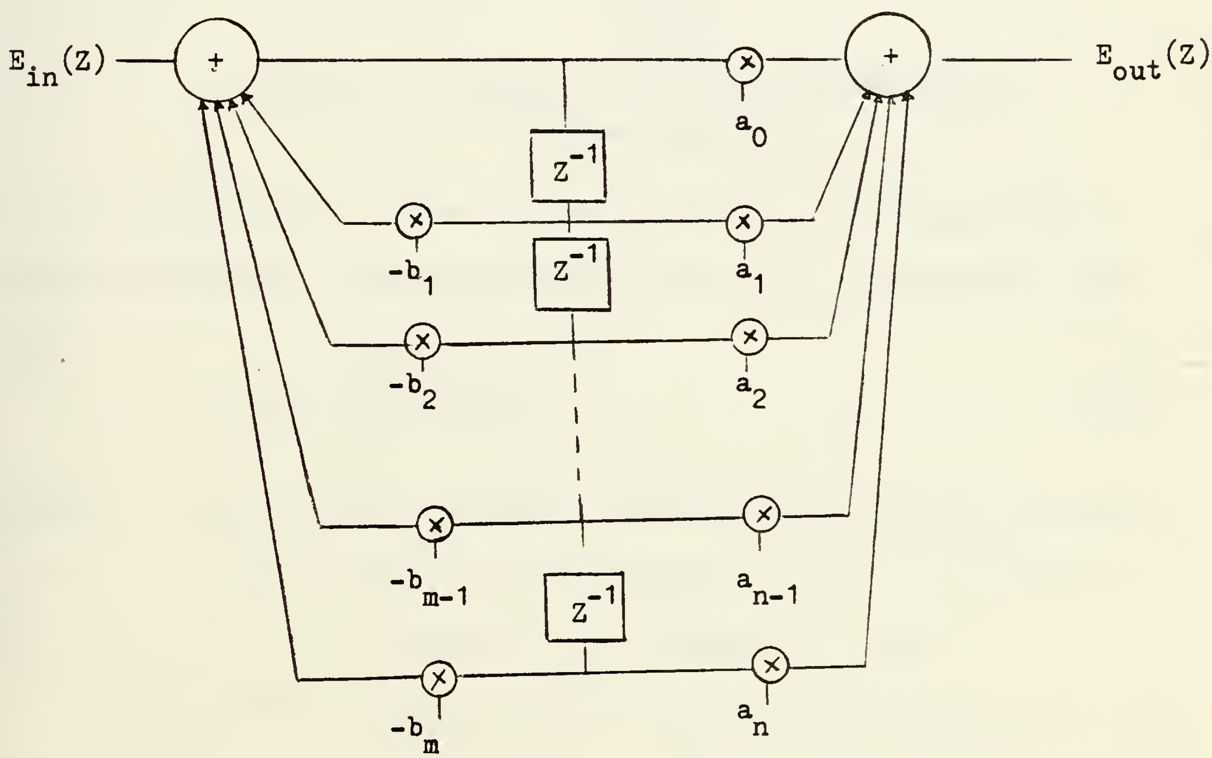


FIGURE 2.1 Schematics of a Recursive Filter (Tapped Delay Line)

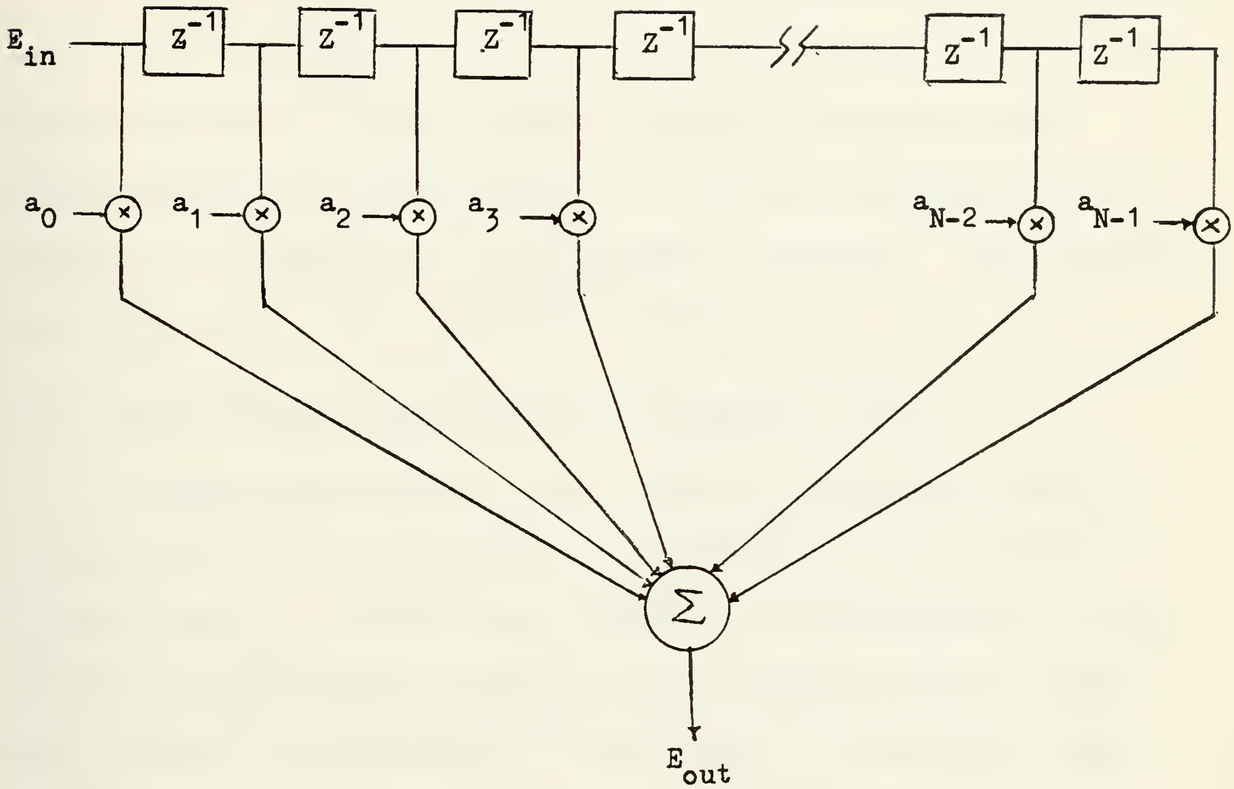


FIGURE 2.2 Schematic of a Non-Recursive Filter
(Tapped Delay Line)

In the case of causal system with finite duration of impulse response, the system function can be written in the form:

$$H(Z) = \sum_{n=0}^{N-1} h(n)\ Z^{-n} \tag{2-3}$$

$\{h(n)\}$ is the impulse response defined over the time interval $0 \leq nT \leq (N-1)T$, $H(Z)$ is a polynomial in $Z^{-1}$ of degree $N-1$. Thus, $H(Z)$ has $N-1$ zeroes in the finite Z- plane.

The frequency response $H(e^{jw})$ is obtained by substituting Z by $e^{jwT}$.

$$H(e^{jwT}) = \sum_{n=0}^{N-1} h(n)\, e^{-jwnT} \qquad (2\text{-}4)$$

We recall that any finite duration sequence is completely specified by N samples of its Fourier Transform [1], so that the design of a Finite Impulse Response Filter may be accomplished by finding either its impulse response coefficients or N samples of its frequency response. Both methods are discussed in the following section.

## B. LINEAR PHASE FINITE IMPULSE RESPONSE FILTER

In many applications, e.g., speech processing, data transmission, it is desirable to design filters to have linear phase. In this way, signals in the passband of the filter are reproduced exactly at the filter output except for a delay corresponding to the slope of the phase. One of the most important features of FIR systems is that they can be designed to have exactly linear phase. The unit impulse response for a causal FIR system with linear phase has the property that:

$$h(n) = h(N - 1 - n) \qquad (2\text{-}5)$$

To see that this condition implies linear phase, we write equation 2-4 as:

$$H(Z) = \sum_{n=0}^{(N/2)-1} h(n)\, Z^{-n} + \sum_{n=N/2}^{N-1} h(n)\, Z^{-n}$$

$$= \sum_{n=0}^{(N/2)-1} h(n)\, Z^{-n} + \sum_{n=0}^{(N/2)-1} h(N-1-n)\, Z^{-(N-1-n)}$$

where N is assumed to be even. Using equation 2-5, one can write:

$$H(Z) = \sum_{n=0}^{(N/2)-1} h(n)[Z^{-n} + Z^{-(N-1-n)}] \tag{2-6}$$

If N is odd, it is shown that

$$H(Z) = \sum_{n=0}^{[(N-1)/2]-1} h(n)[Z^{-n} + Z^{-(N-1-n)}] + h(\tfrac{N-1}{2})Z^{-[(N-1)/2]} \tag{2-7}$$

Evaluating equations 2-6 and 2-7 for $Z = e^{jw}$, one obtains, for N even,

$$H(e^{jw}) = e^{-jw[(N-1)/2]} \{ \sum_{n=0}^{(N/2)-1} 2h(n) \cos [w(n - \tfrac{N-1}{2})]\} \tag{2-8}$$

and for N odd,

$$H(e^{jw}) = e^{-jw[(N-1)/2]} \{h(\tfrac{N-1}{2}) + \sum_{n=0}^{[(N-3)/2]-1} 2h(n) \cos [w(n - \tfrac{N-1}{2})]\} \tag{2-9}$$

In both cases the sums in brackets are real, implying a linear phase shift corresponding to delay of (N-1)/2 samples. For N odd, the phase shift corresponds to an integer number of samples delay. For even N, the delay is an integer plus one-half of sampling period. This distinction between odd and even values of N is often of considerable importance in design and realization of FIR filter. Examples of impulse response having linear phase are shown in Figure 2-3.

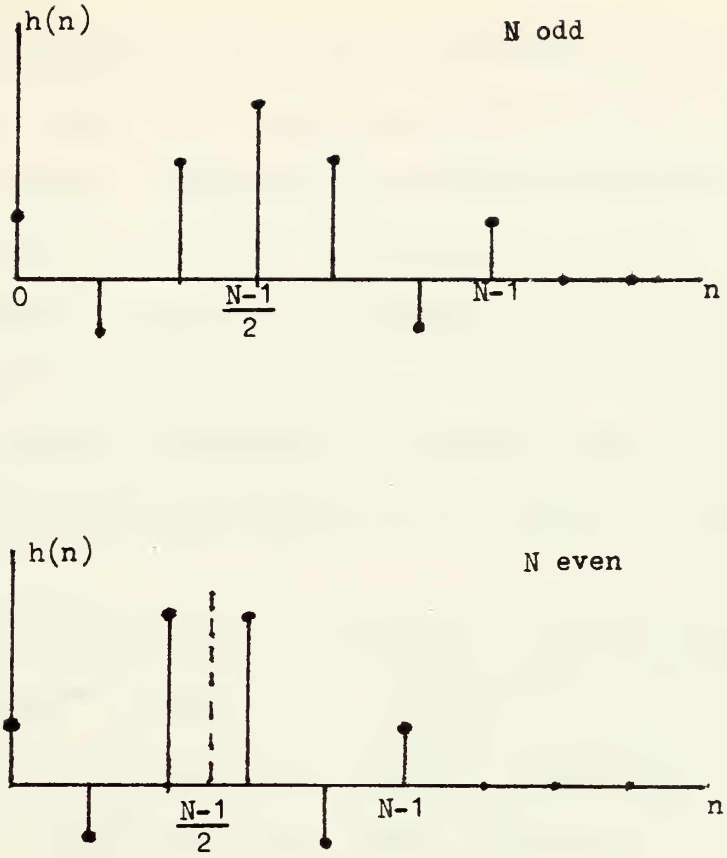


FIGURE 2.3 Typical Impulse Response for Linear Phase FIR Filters

## C. DESIGN TECHNIQUE OF FIR FILTERS

### 1. Determination of Impulse Response

Since the frequency response of $H(e^{jw})$ of any digital or sampled analog filter is periodic in frequency, it can be expanded in Fourier series of the form:

$$H(e^{jw}) = \sum_{n=-\infty}^{\infty} h(n)\ e^{-jwn} \tag{2-10}$$

where the sequence h(n) playing the role of the "Fourier coefficients," i.e.,

$$h(n) = \frac{1}{2\pi} \int_{-\pi}^{\pi} H(e^{jw})\ e^{jwn}\ dw \tag{2-11}$$

One can easily recognize that the coefficients of the Fourier series, h(n), are identical to the impulse response of a digital filter. There are two difficulties with the representation of (2-10) for designing FIR filters. First, the filter impulse response is infinite in duration since the summation in (2-10) extends to $\pm\infty$. Second, the filter is unrealizable because the impulse response begins at $-\infty$; i.e., no finite amount of delay can make the impulse response realizable.

One possible way of obtaining an FIR filter that approximates $H(e^{jw})$ would be to truncate the infinite Fourier series (2-10), at $n = \pm M$. But direct truncation of the series leads to the well known Gibbs phenomenon. However, the non-uniform convergence phenomenon can be moderated through the use of a less abrupt truncation of the Fourier series by applying the so-called "windowing" or "weighting function."

2. Effect of Window

A more successful way of obtaining an FIR filter is to use a finite weighting sequence W(n), called window, to modify the Fourier coefficients h(n) in (2-10) to control the convergence of the Fourier series. The technique of windowing is illustrated in Figure 2-4. At the top of this figure is shown the desired periodic frequency response $H(e^{jw})$ and its Fourier series coefficients {h(n)}. The next row shows a finite duration weighting sequence W(n) with Fourier transform $W(e^{jw})$. $W(e^{jw})$, for most reasonable windows, consists

of a central lobe which contains most of the energy of the windows and side lobes which generally decay rapidly. To produce an FIR approximation to $H(e^{jw})$, the sequence

$$\hat{h}(n) = \begin{cases} h(n) \cdot W(n) & , -M \leq n \leq M \\ 0 & , \text{elsewhere} \end{cases} \qquad (2\text{-}12)$$

is formed. The third row of Figure 2.4 shows $\hat{h}(n)$ and its Fourier transform $\hat{H}(e^{jw})$, which is the convolution of $H(e^{jw})$ and $W(e^{jw})$, since h(n) is the product of the sequences h(n) and w(n). The last row of Figure 2-4 shows the realizable sequence g(n), which is a shifted version of h(n) and may be used as the desired filter impulse response.

As seen in the example of Figure 2-4, there are several effects on the resulting frequency response of windowing the Fourier coefficients of the filter. A major effect is that discontinuities in $H(e^{jw})$ become a transition band between values on either side of the discontinuity. Since the final frequency response of the filter is the circular convolution of the ideal frequency response with the window's frequency response, it is clear that the width of these transition bands depend on the width of the main lobe of $W(e^{jw})$. A secondary effect of windowing is that ripple from the side lobes of $W(e^{jw})$ produces approximation errors (ripple in the resulting frequency response) for all w.

There are many windows proposed that approximate the desired characteristics. But, in general, the desirable window should have the following characteristics:

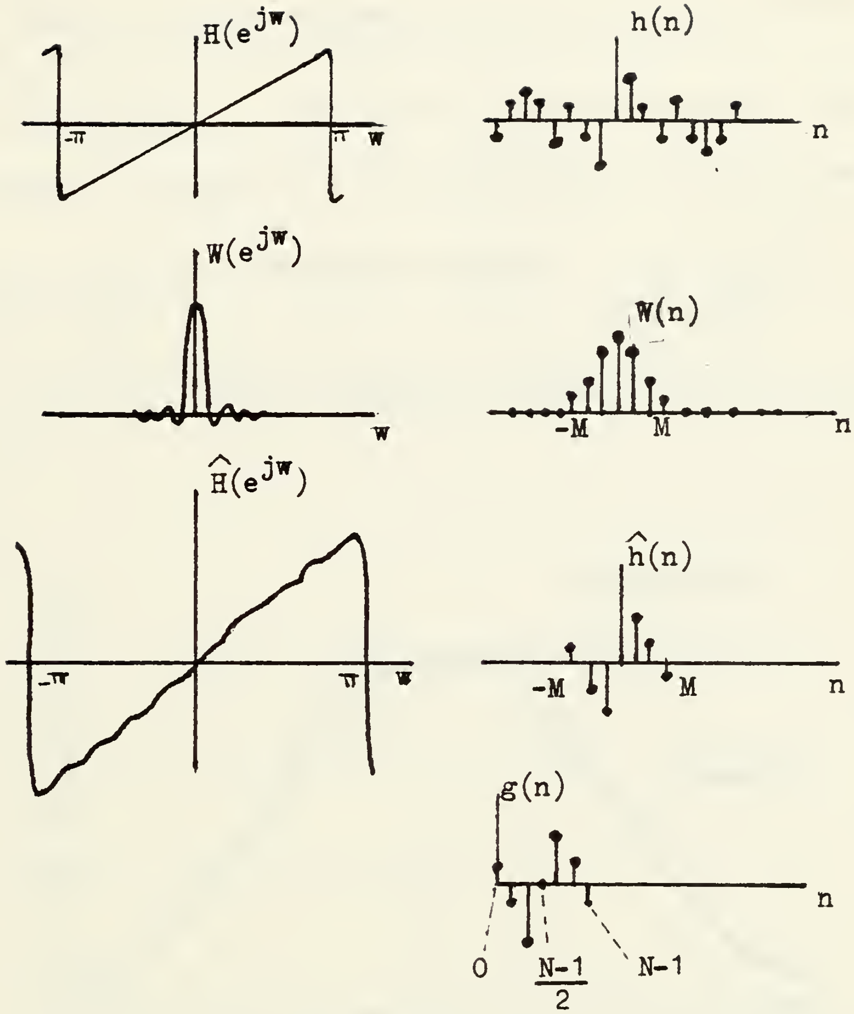


FIGURE 2.4 Illustration of windowing

$H(e^{jw})$ Desired periodic frequency response

$h(n)$ Its Fourier series coefficients

$w(n)$ Finite duration weighting sequence

$W(e^{jw})$ Its Fourier transform

$\hat{h}(n) = h(n) \cdot w(n)$

$\hat{H}(e^{jw}) = H(e^{jw}) * W(e^{jw})$

1. Small width of main lobe of the frequency response of the window containing as much of the total energy as possible.

2. Side lobes of the frequency response that decrease in energy rapidly as w tends to $\pi$.

In the design of the filters in this study, the Hamming window is chosen. It is specified by the equation:

$$w(n) = \begin{cases} 0.54 - 0.46 \cos\left(\frac{2\pi n}{N-1}\right), & 0 \le n \le N-1 \\ 0 & , \text{elsewhere} \end{cases} \tag{2-13}$$

Figure 2-5 illustrates the Hamming window and the rectangular window.

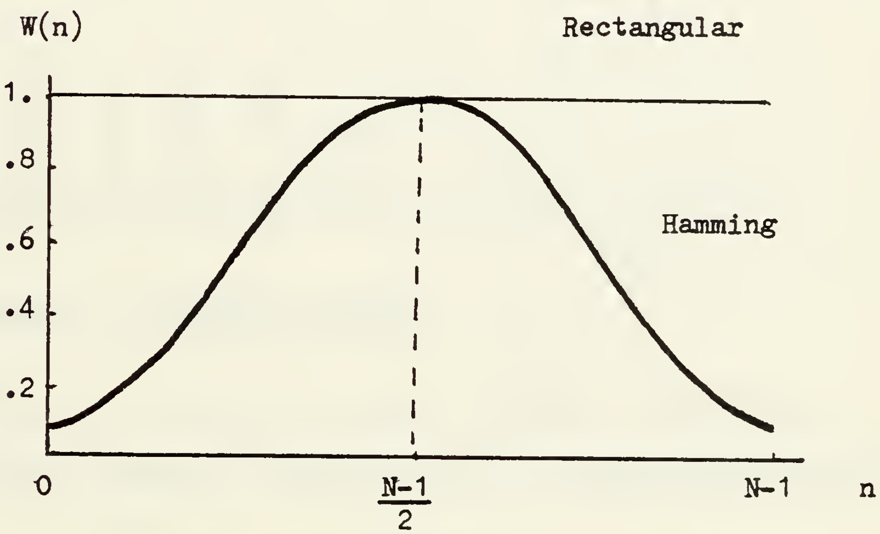


FIGURE 2.5 Hamming Window and Rectangular Window

3. Frequency Sampling Technique

Figure 2-6 shows an arbitrary frequency response (solid curve) that one wants to approximate and a sequence of N frequency samples $H_k$ (Figure 2-7) that can be represented as

$$H(k) = |H(k)|e^{j\theta(k)}, \qquad k = 0, 1..., N-1$$

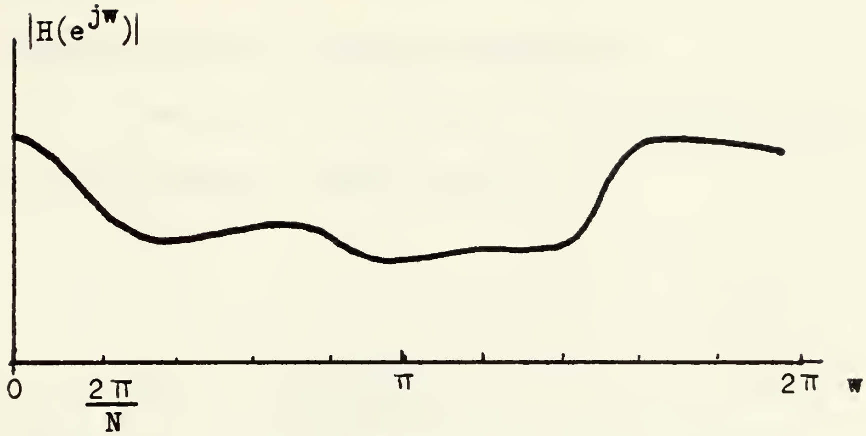


FIGURE 2.6 Desired Continous Frequency Response

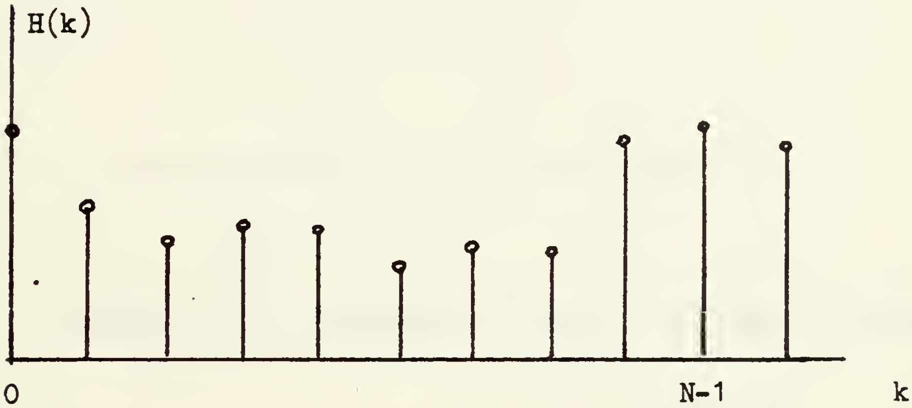


FIGURE 2.7 Frequency Samples

Using the inverse discrete Fourier transform, a finite duration impulse response can be determined from H(k)

$$h(n) = \frac{1}{N} \sum_{k=0}^{N-1} H(k)\ e^{j(2\pi/N)nk} \tag{2-14}$$

where H(k) can also be written in the form:

$$H(k) = \sum_{n=0}^{N-1} h(n)\ e^{-j(2\pi/N)nk} \tag{2-15}$$

## D. APPLICATIONS

### 1. Bandpass Filter Design Algorithm

In the analog or continuous time system, the bandpass filter has the transfer function H(f).

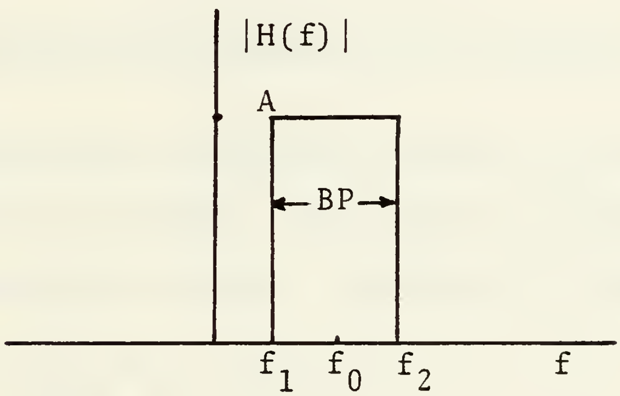


FIGURE 2.8 Bandpass filter frequency response

$$H(f) = \begin{cases} A, & f_1 < f < f_2 \\ 0, & \text{otherwise} \end{cases}$$

In the discrete time system, a rectangular bandpass filter has the frequency response $H(e^{jw})$ as shown in Figure 2-9. It is periodic of period $2\pi$.

$$H(e^{j\frac{w}{w_s}}) = \begin{cases} A, & |w_1| < |\frac{w}{w_s}| < |w_2| \\ 0, & \text{otherwise.} \end{cases}$$

with $f_2 = \frac{w_s}{2\pi}$ sampling frequency.

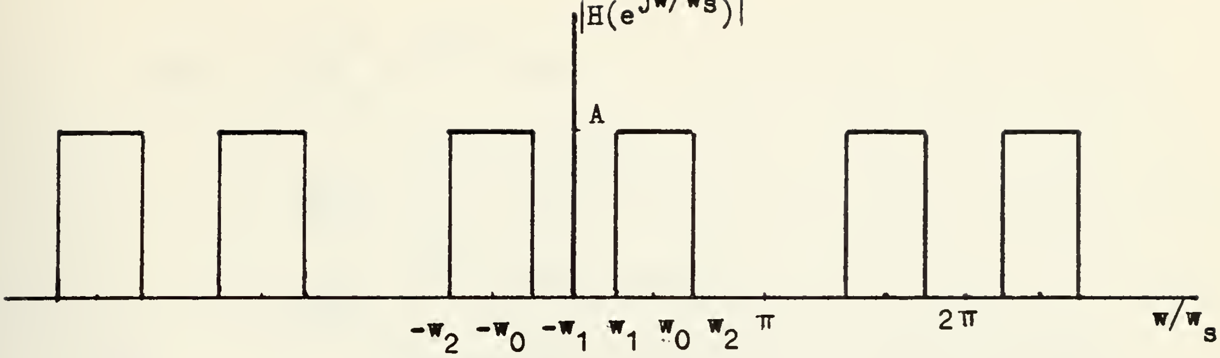


FIGURE 2.9 Discrete Time Bandpass Filter Frequency Response

Basing upon the periodic nature of a discrete time filter frequency response, the impulse response can be computed by finding the Fourier coefficient, using equation 2-11.

$$h(n) = \frac{2}{2\pi} \int_{w_1}^{w_2} A\, e^{jwn}\, dw \qquad (2\text{-}16)$$

$$= \frac{1}{\pi} \int_{w_1}^{w_2} A\,(\cos wn + j \sin wn)\, dw.$$

Since only real term may be implemented, the series coefficients are:

Case I: $n \neq 0$

$$h(n) = \frac{1}{\pi} \int_{w_1}^{w_2} A \cos (wn)\, dw$$

$$= \frac{A}{\pi n} (\sin 2\pi f_2 - \sin 2\pi f_1) \qquad (2\text{-}17)$$

Case 2: $n = 0$

Let $w_2 = 2\pi\,(fo + \frac{\Delta f}{2})$

$w_1 = 2\pi\,(fo + \frac{\Delta f}{2})$

One can write using equation (2-16):

$$h(n) = \frac{A}{\pi} \int_{w_1}^{w_2} e^{jwn}\, dw$$

$$= \frac{A}{jn\pi} [e^{jw_2 n} - e^{jw_1 n}]$$

$$= \frac{A}{jn\pi} e^{j2\pi f_o} (\sin \pi n \Delta f)$$

$$= 2A\,\Delta f \frac{\sin \pi n \Delta f}{\pi n \Delta f} (\cos 2\pi n f_o + j \sin 2\pi n f_o) \tag{2-18}$$

When n tends to 0, the real part of equation (2-18) tends to:

$$h(0) = 2A\Delta f(1.)(1.) = 2A\Delta f \tag{2-19}$$

Window weighting functions are used to modify the coefficients in order to improve the filter characteristics. If the Hamming window is used, the weighted coefficients A(n) become

$$A(n) = h(n)(0.54 + 0.46 \cos (\tfrac{k}{N} \pi)) \tag{2-20}$$

A computer program shown in Appendix C was established to design the non-recursive bandpass filter. It was based upon the equations 2-17, 2-19, 2-20.

2. Prewhitening and Dewhitening Filters in Communication System

The prewhitening and dewhitening filters are also called preemphasis and deemphasis filters in the communication field.

Suppose one desires to transmit a baseband signal using FM modulation and requires the best possible signal to noise ratio. One possible solution is to raise the level of

modulating baseband signal to the maximum extent possible in order to modulate the carrier as vigorously as possible. But the modulating signal level may be raised only until the distortion exceeds a specified value (maximum allowable value).

However, the baseband signal happens to be an audio signal; it turns out that something further can be done. An audio signal usually has the characteristic that its power spectral density is relatively high in the low frequency range and falls off rapidly at higher frequencies. For example, speech has little power spectral density above about 3 kHz. Music extends farther into the high frequency range, the feature still persists that most of its power is in the low frequency region. As a consequence, when one examines the spectrum of the sidebands associated with a carrier which is frequency modulated by an audio signal, one finds that the power spectral density of the sidebands is greatest near the carrier and relatively small near the limits of the allowable frequency band allocated to the transmission. The manner in which one may take advantage of these spectral features, which are characteristic of audio signals, in order to improve the performance of an FM system is shown in Figure 2-10.

At the transmitting end, in Figure 2-10, the baseband signal m(t) is not applied directly to the FM modulator but is first passed through a filter of transfer characteristic $H_p(w)$, so that the modulating signal is $m_p(t)$. The modification introduced into the baseband signal by the first filter is undone by the receiver filter which follows the

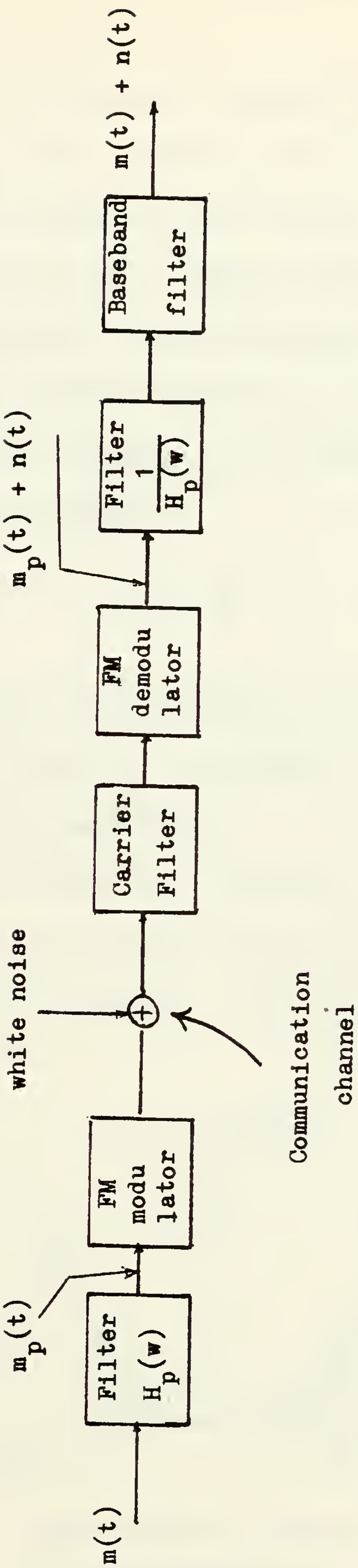


FIGURE 2.10 Preemphasis and Deemphasis in an FM system

discriminator and has transfer characteristic $1/H_p(w)$. The noise passes through only the receiver filter which may be used to suppress the noise to some extent.

The selection of the transfer characteristic $H_p(w)$ is based on the following considerations. At the output of the demodulator, the spectral density of the noise increases with the square of the frequency, as shown in Figure 2-11. It is given by the equation:

$$G_n(f) = \frac{\alpha^2 \eta}{A^2} w^2 \quad , \quad |f| \leq \frac{B}{2} \tag{2-21}$$

where $\alpha$ = constant proportional to limited amplitude of the carrier obtained with the hard limiter in the demodulator

$A$ = amplitude of the carrier

$\eta$ = power spectral density of the white noise over the range $|f| < \frac{B}{2}$.

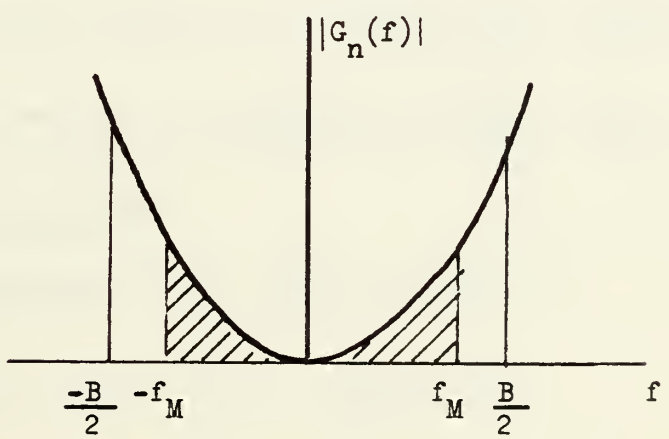


FIGURE 2.11 Power Spectral Density at the Output of an FM Demodulator

Hence the receiver filter will be most effective in suppressing noise if the response of the filter falls off with increasing frequency. In such a case the transmitter filter must exhibit a rising response with increasing frequency. The premodulation filtering in the transmitter, to raise the power spectral density of the baseband signal in its upper frequency range, is called preemphasis. The filtering at the receiver to undo the signal preemphasis and to suppress noise is called deemphasis.

Referring to Figure 2-10, one requires that the normalized power of the baseband signal m(t) must be the same as the normalized power of the preemphasized signal $m_p(t)$. If $G_m(f)$ is the power spectral density of m(t), the density of $m_p(t)$ is $|H_p(f)|^2\, G_m(f)$, and one requires that:

$$P_m = \int_{-fm}^{fm} G_m(f)\, df = \int_{-fm}^{fm} |H_p(f)|^2 G_m(f)\, df \tag{2-22}$$

where

fm = maximum frequency of modulating signal.

In the absence of deemphasis, output noise is:

$$N_O = \frac{8\pi^2}{3} \frac{\alpha^2 \eta}{A^2} fm^3$$

With deemphasis, the output noise is:

$$N_{od} = \left(\frac{\alpha}{A}\right)^2 4\pi^2 \eta \int_{-fm}^{fm} f^2 \left|\frac{1}{H_p(f)}\right|^2 df \tag{2-23}$$

The ratio, $R = \frac{N_o}{N_{od}}$, is

$$R = \frac{fm^3/3}{\int_0^{fm} f^2 df/|H_p(f)|^2} \tag{2-24}$$

Since the signal itself is unaffected in the overall process, the quantity R is the ratio by which preemphasis-deemphasis improves the signal to noise ratio.

The prewhitening filter has the transfer characteristic illustrated in Figure 2-12. The dewhitening filter has the transfer characteristic illustrated in Figure 2-13. The relation between these two filters is:

$$H_D(e^{jw}) = \frac{1}{H_p(e^{jw})} \tag{2-25}$$

where

$H_p(e^{jw})$ = transfer function of prewhitening filter

$H_D(e^{jw})$ = transfer function of dewhitening filter.

3. <u>Prewhitening Filter Design Algorithm</u>

a. In the analog or continuous time system, the prewhitening filter has the transfer characteristic shown in Figure 2-12 and has the transfer function,

$$H_p(f) = \begin{cases} R & , \quad |f| \leq f_o \\ R + A(f - f_o) & , \quad f_o \leq |f| \leq f_p \end{cases} \tag{2-26}$$

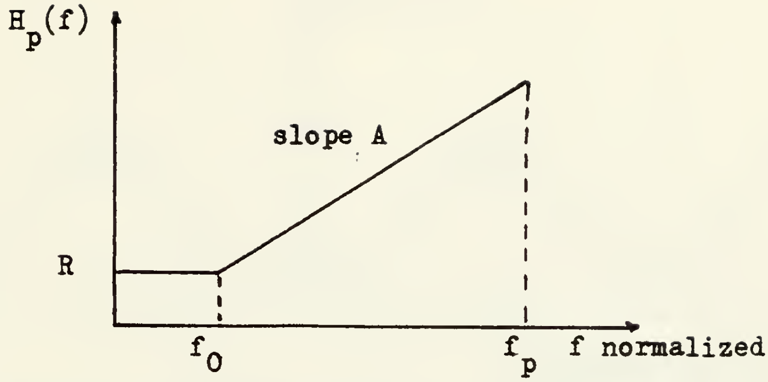


FIGURE 2.12 Prewhitening Filter Transfer Function

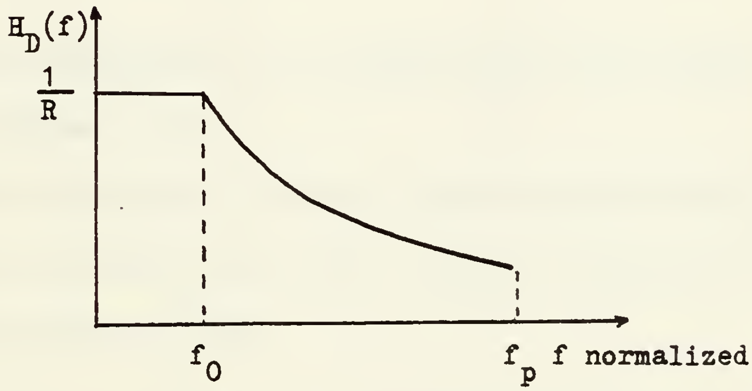


FIGURE 2.13 Dewhitening Filter Transfer Function

b. In the sampled analog or digital system, the frequency response of the prewhitening filter is periodic. It is illustrated in Figure 2-14.

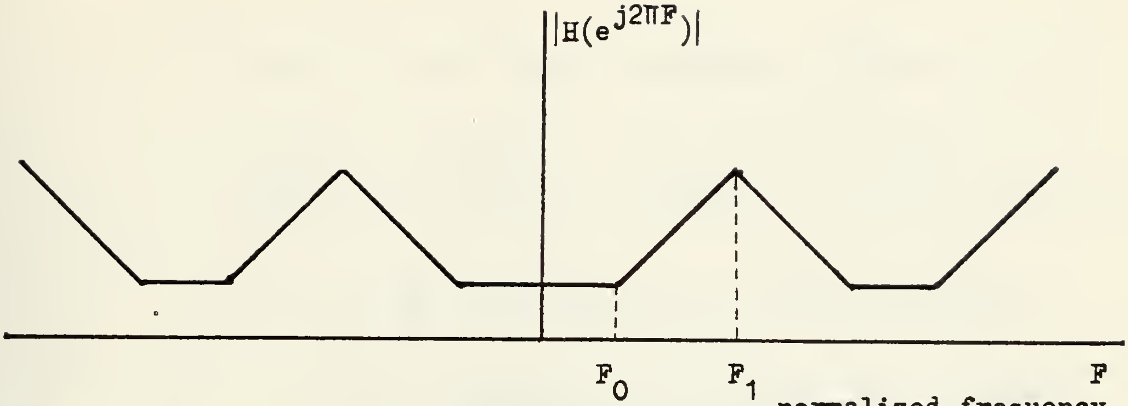


**FIGURE 2.14 Amplitude Frequency Response of Sampled Analog Prewhitening Filter**

The frequency F is normalized with respect to the sampling frequency $F_s$.

The design of a linear phase prewhitening filter consists of the calculation of the impulse response which can be computed using (2-11)

$$h(n) = \frac{1}{2\pi} \int_{-\pi}^{\pi} H(e^{jw})\, e^{jwn}\, dw$$

which becomes, using $\frac{w}{w_s} = F$

$$h(n) = 2 \int_{0}^{F_o} R\, e^{j2\pi nF}\, dF + 2\int_{F_o}^{F_P} [R + A(F-F_o)]e^{j2\pi nF} dF$$

$$h(n) = \qquad U \qquad + \qquad V \qquad (2\text{-}27)$$

Since h(n) is real, one can compute only the real part of U and V.

Case 1: $n \neq 0$ , $F_p = \frac{F_s}{2}$

$$\mathrm{Re}[U] = 2R \int_0^{F_s} \cos(2\pi n F)\,dF = \frac{R}{\pi n} \sin 2\pi n F_o$$

$$\mathrm{Re}[V] = 2R \int_{F_o}^{F_p} \cos(2\pi n F)\,dF + 2A \int_{F_o}^{F_p} (F - F_o) \cos(2\pi n F)\,dF$$

$$= \frac{R}{\pi n} [\sin(2\pi n F_p) - \sin(2\pi n F_o)]$$

$$+ 2A \left[\frac{1}{4\pi^2 n^2} (\cos 2\pi n F_p - \cos 2\pi n F_o)\right.$$

$$\left. + \frac{F_p}{2\pi n} \sin 2\pi n F_p - \frac{F_p}{2\pi n} \sin 2\pi n F_o\right]$$

$$+ \frac{AF_o}{\pi n} [\sin 2\pi n F_o - \sin 2\pi n F_p]$$

$$h(n) = \mathrm{Re}[U] + \mathrm{Re}[V] = \frac{A}{2\pi^2 n^2} [\cos 2\pi n F_p - \cos 2\pi n F_o] \quad (2\text{-}28)$$

Case 2: $n = 0$ , $F_p = F_{s/2}$

With n = 0, (2-27) becomes:

$$h(o) = 2 \int_0^{F_p} R\,dF + 2 \int_{F_o}^{F_p} [R + A(F - F_o)]\,dF$$

$$h(o) = \frac{1}{2F_p} [R + \frac{A}{2F_p} (F_p - F_o)^2] \quad (2\text{-}29)$$

Taking into account the constraint of the linear phase FIR filter:

$$h(n) = h(N - 1 - n)$$

and using (2-28) and (2-29), a computer program is prepared to calculate the impulse response of the filter, a Hamming window function is used to improve the amplitude and phase response of the prewhitening filter.

4. <u>Dewhitening Filter Design Algorithm</u>

In the design of the complementary dewhitening filter, one can use the frequency sampling technique. Using (2-15) and the given impulse response of the prewhitening filter, the frequency samples

$$\{H_p(k)\} \quad , \quad k = 0, 1...., N-1$$

can be computed and stored in the memory of the computer.

Then the frequency samples of dewhitening filter $H_D(k)$ can be computed as:

$$H_D(k) = \frac{1}{H_p(k)} \quad , \quad k = 0, 1,...., N-1$$

Using the inverse discrete Fourier transform given by (2-14), the finite impulse response of the dewhitening filter can be obtained.

Using an appropriate window, such as Hamming window, the frequency response of the dewhitening filter can be improved also.

# III. EXPERIMENTAL EVALUATION OF TAD-12

## A. SYSTEM CONFIGURATION

Reticon Corporation markets a Tapped Analog Delay Device which provides 12 output taps with the following time delay configuration:

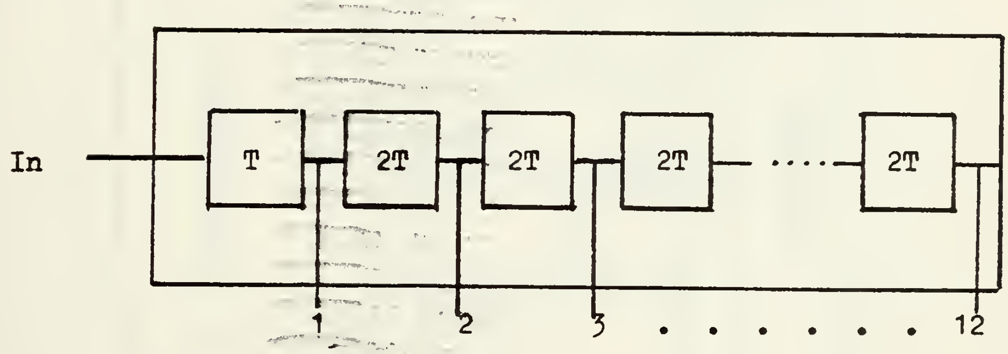


FIGURE 3.1 Equivalent Circuit of TAD-12

The first delay section is delayed by one clock period, the rest have delay time of two clock periods.

The delay lines are structurally organized as shown in Figure 3-2. One delay line contains N capacitive storage elements with two I/O access switches. One access switch connects the storage element to a common input line and the second switch connects it to the common output line. One register and its associated multiplexing switch sequentially time samples the analog input signal onto the "N" capacitive storage elements. Information is read onto the nth element while simultaneously reading out the $n^{th}$ + 1 element.

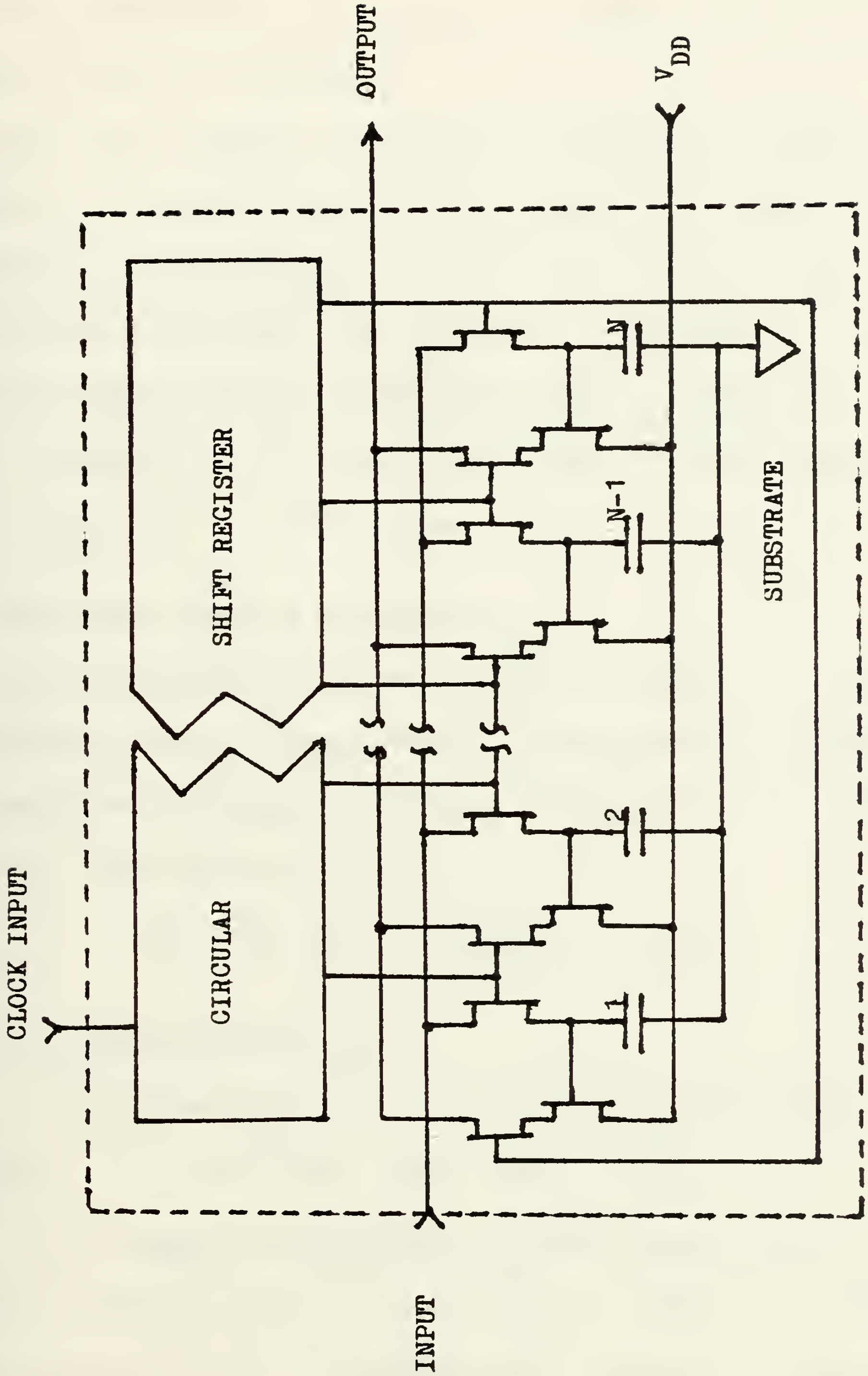


FIGURE 3.2 Organization of a Single Delay Line

Each element has an output buffer amplifier to provide a zero order hold of the sampled signal. This produces a sampled and held output.

The test circuit for TAD-12 is shown in Figure 3-3. It consists of a pulse shaper circuitry and a DMOS flip-flop. Because the tap outputs are at +5 volts bias level, due to the TAD-12 circuitry, the resistor 2 kilo-ohms of the operational amplifier non-inverting input is connected to a +5 volts rather than ground. The output of the summer, therefore, rides on a 5 volts bias level.

## B. FREQUENCY DOMAIN EVALUATION

Using the circuit board shown in Figure 3-3, the frequency dependance, the non-uniformity, the harmonic distortion are evaluated at different sampling frequencies for three different tap resistances:

$$R_k = 10\ K\Omega\ , \quad 100\ K\Omega\ , \quad 1\ M\Omega\ .$$

### 1. Frequency Roll-off

The frequency characteristic of the sampled and hold process is of the $\frac{\sin x}{x}$ shape with $x = \frac{\pi f}{f_s}$ .

At sampling frequency $f_s = 500$ KHz, for $R_{tap} = 10\ K\Omega$, the roll-off is close to the theory. When the tapping resistances $R_{tap}$ is increased, the roll-off is more serious and wriggles around.

Figure 3-4 illustrates the magnitude of the frequency response of Tap #1, Tap #6 and Tap #11 outputs using 10 kilo-ohms resistor. The solid curve represents the theoretical response.

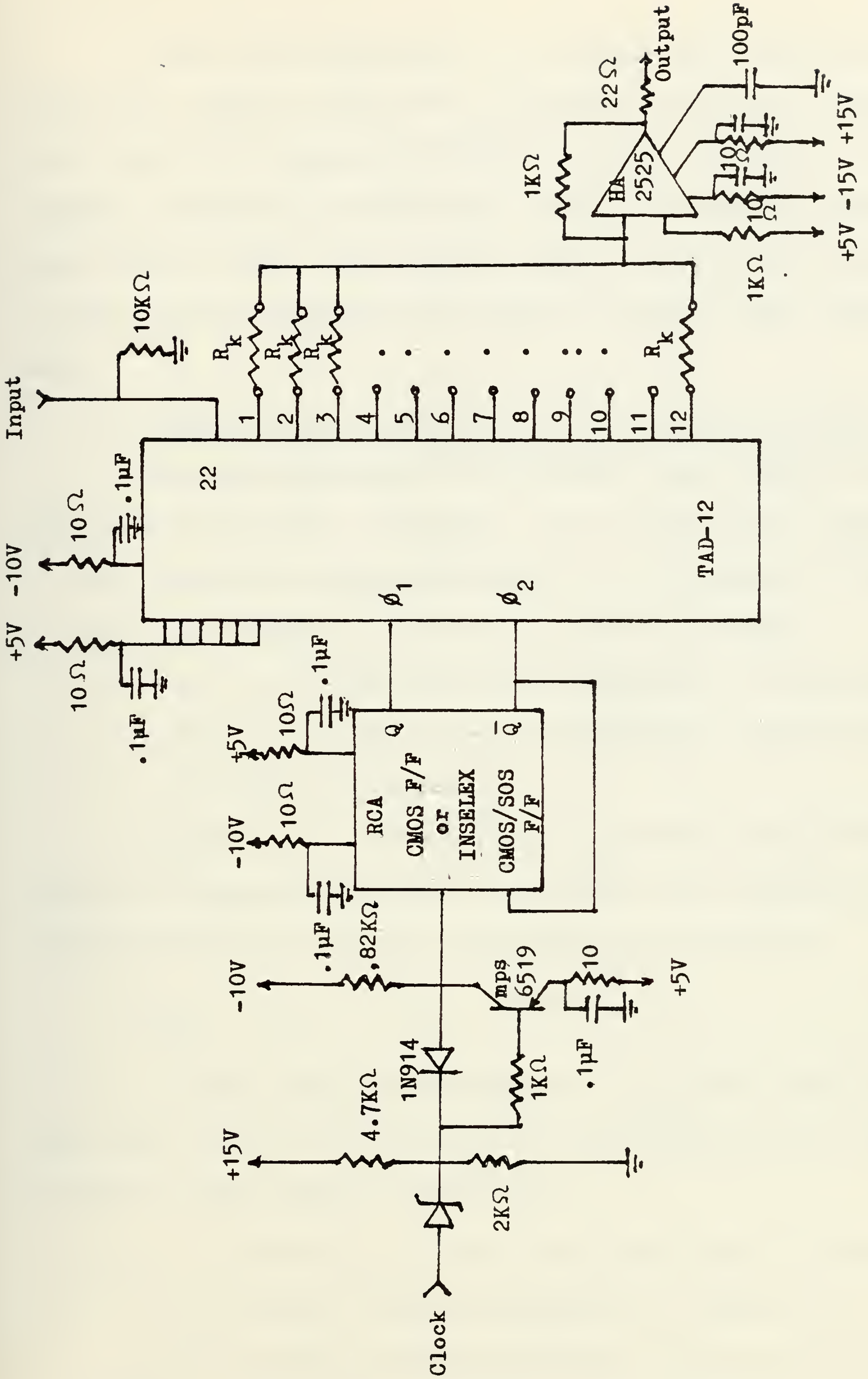


FIGURE 3.3 Test Circuit for Reticon TAD-12 Evaluation

From this experiment it is found that the TAD-12 output has rather complicated frequency variations although they follow the theoretical $\frac{\sin x}{x}$ relation roughly if the tapping resistor is 10 Kilo-ohms and the sampling frequency less than 2.5 MHz. The loading effect is much more pronounced if the tapping resistors are equal or greater than 100 Kilo-ohms.

2. <u>Non-Uniformity (Spatial or Fixed Pattern Noise)</u>

The non-uniformity of different taps outputs varies depending on the tap resistance, $R_k$, the sampling frequency, $f_s$, and the input signal frequency, f. The general result at sampling frequency of 500 KHz is the following:

- For f < 10 KHz, the non-uniformity is within 10%
- For f > 10 KHz, the non-uniformity can deteriorate to 15% - 50% range.

Figures 3-10 through 3-17 illustrate the non-uniformity result of sampling frequency of 500 KHz, for different input signal frequencies and for different tap resistors:

$$R_{tap} = 1\ K\Omega,\ \ 10\ K\Omega,\ \ 100\ K\Omega,\ \ 1\ M\Omega.$$

At high sampling frequencies, using tap resistances less than 100 KΩ, the uniformity of tap output can be improved at higher input signal frequencies.

At $f_s$ = 0.5 MHz, $R_k$ = 10 KΩ and input signal frequencies:

- f < 50 KHz, the non-uniformity is within 10%
- f > 50 KHz, the non-uniformity varies from 13% to 25%.

At $f_s$ = 2.5 MHz, $R_k$ = 100 KΩ and input signal frequencies:

- f < 80 KHz, the non-uniformity is within 10%
- f > 80 KHz, the non-uniformity varies from 11% to 70%

At $f_s$ = 2.5 MHz, $R_k$ = 1 MΩ, and input signal frequencies:

- f < 30 KHz, the non-uniformity is within 20%
- f > 30 KHz, the non-uniformity is greater than 30%.

Figures 3-18 through 3-28 illustrate the non-uniformity data at sampling frequency equal to 2.5 MHz, for different typical tap resistors and for different input signal frequencies.

Figures 3-24 through 3-40 illustrate the pictorial presentation of Reticon TAD-12 performance at different sampling frequencies, using different tap resistances.

3. Temporal Noise Behavior of Different Taps

The temporal noise of different taps is studied at the sampling frequencies higher or equal to 2.5 MHz. It varies, depending on the sampling frequencies and the tap resistances used. However, it should be pointed out that the tap #1 output has little noise at all sampling frequencies and tapping resistors used. It is shown in Figures 3-24, 3-25, 3-26, 3-28, 3-40. The general temporal noise behavior of other taps is shown in Table III.I and Figures 3-24, 3-25, 3-27, 3-35, 3-38.

TABLE III.I Noisiest Tap Outputs

| $R_{tap}$ / $f_s$ | 1 Meg-ohm | 100 Kilo-ohms | 10 Kilo-ohms |
|---|---|---|---|
| 2.5 MHz | Tap #10 | Tap #11 | Tap #12 |
| 3.5 MHz | Tap #10 | Tap #4 | Tap #2 |

The temporal noise of different taps is not serious at low sampling rate (less or equal to 1.25 MHz). Figure 3-41 illustrates the output of tap #1 and #12 at sampling frequency at $f_s$ = 1.25 MHz using 1 Meg-ohm tapping resistors.

4. Harmonic Distortion

The second harmonic distortion data is measured with the input frequency 10 KHz for different input amplitudes at different sampling frequencies:

$$f_s = 500 \text{ KHz}, 1.25 \text{ MHz}, 2.5 \text{ MHz}$$

and using different tap resistors:

$$R_{tap} = 10 \text{ K}\Omega, 100 \text{ K}\Omega, 1 \text{ M}\Omega.$$

The curves for the quantity $20 \log \frac{V \text{ 2nd harmonic}}{V \text{ fundamental}}$ are plotted and shown in Figures 3-42, 3-43, 3-44. The general results of the above measurement are summarized in Table 3.II.

The loading effect on the dynamic range of the TAD-12 is very pronounced at high sampling frequency (2.5 MHz). In order to get the second harmonic amplitude less than 1% of the fundamental, one has to use less than .12 volt rms input voltage if using 1 MΩ tap resistor and less than 2 volts rms input voltage if using 10 KΩ tap resistor.

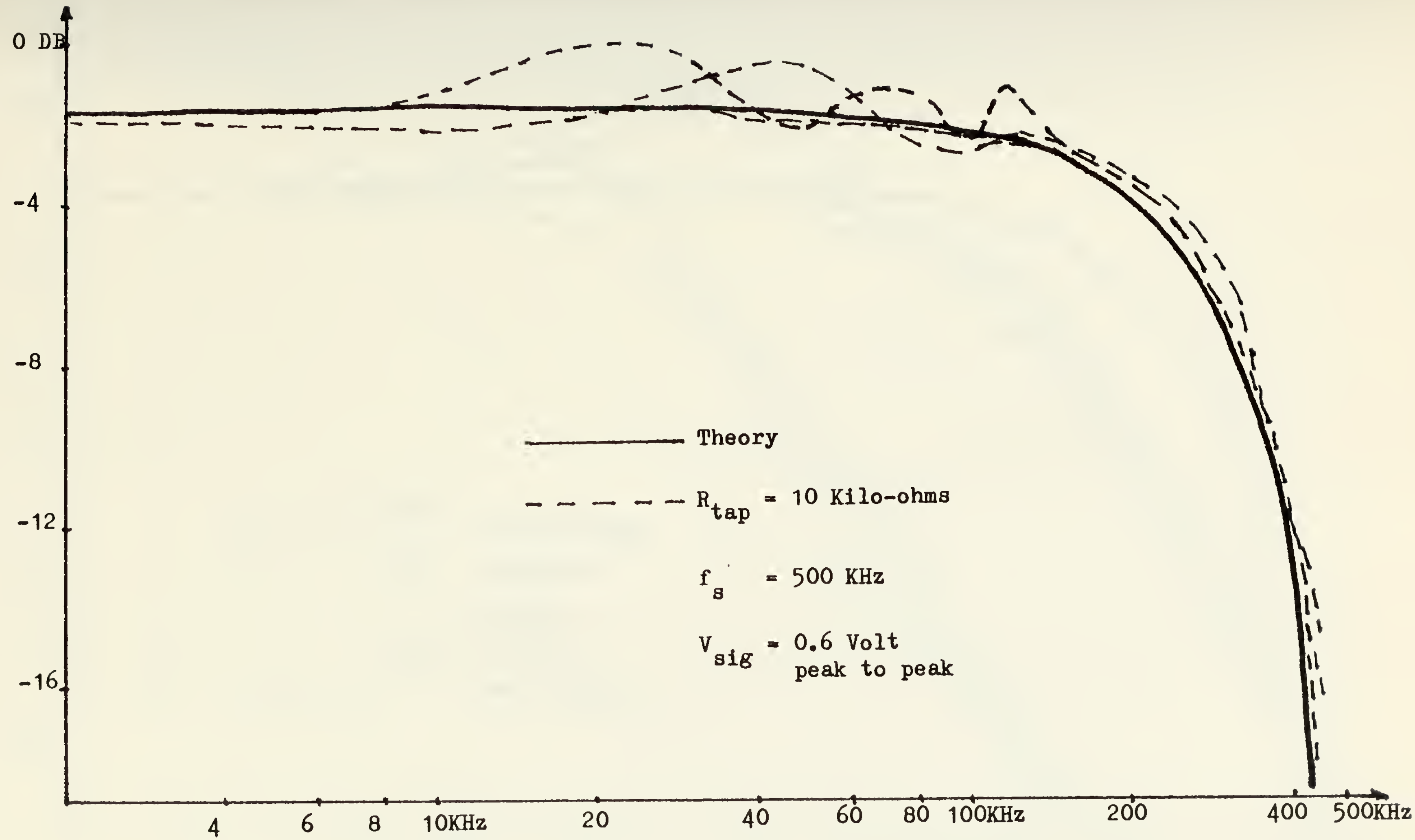


FIGURE 3.4 Amplitude Frequency Response of Reticon TAD-12 Tapped Delay Line.
Tap # 1, 6, 11

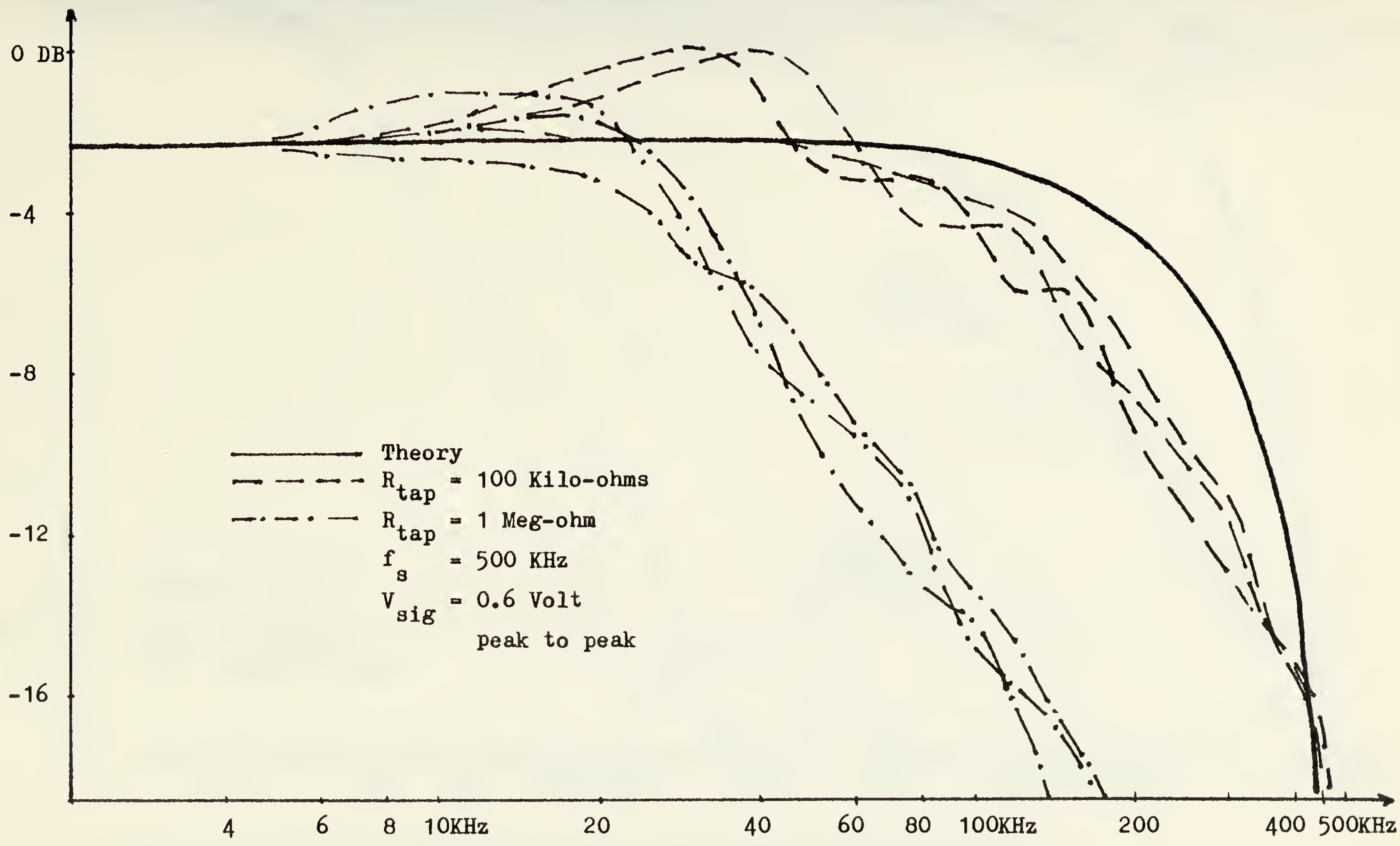


FIGURE 3.5 Amplitude Frequency Response of Reticon TAD - 12 Tapped Delay Line.
Tap # 1, 6, 8

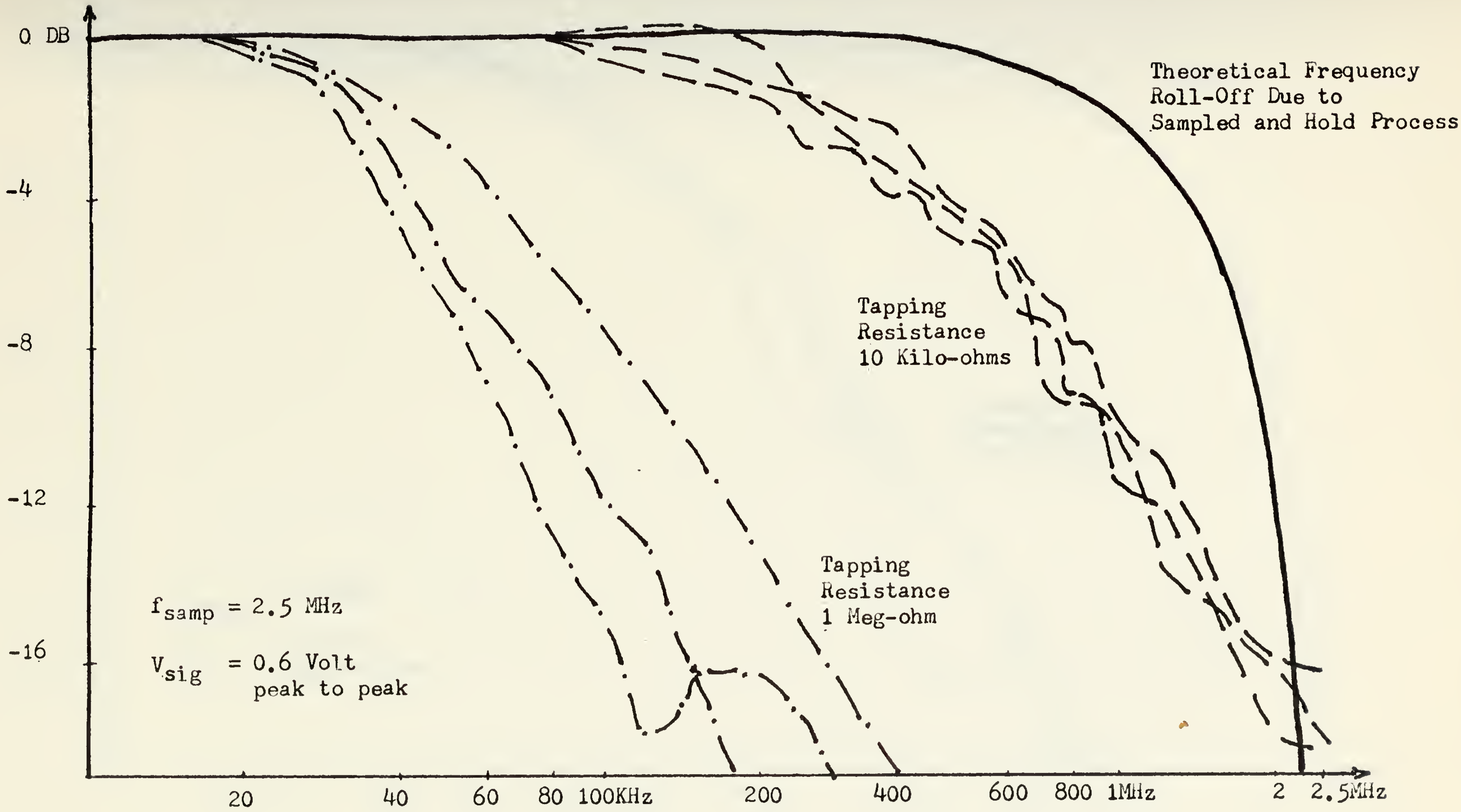


FIGURE 3.6 Frequency Response of Reticon TAD-12 Tapped Delay Line Showing Its Bandwith, Nonuniformities Among Taps and Loading Effect

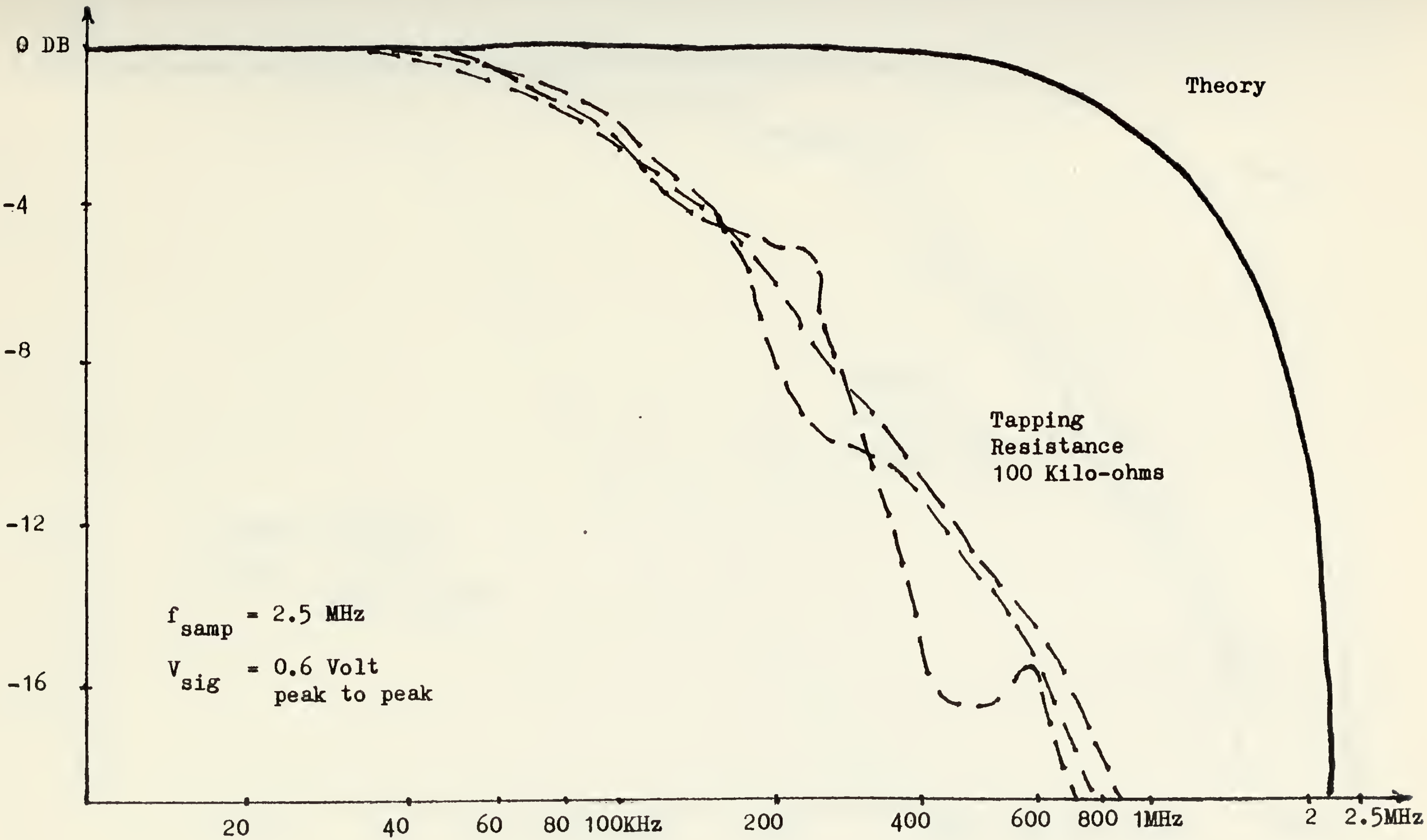


FIGURE 3.7 Amplitude Frequency Response of Reticon TAD-12 Tapped Delay Line .
Tap # 1, #6, #11

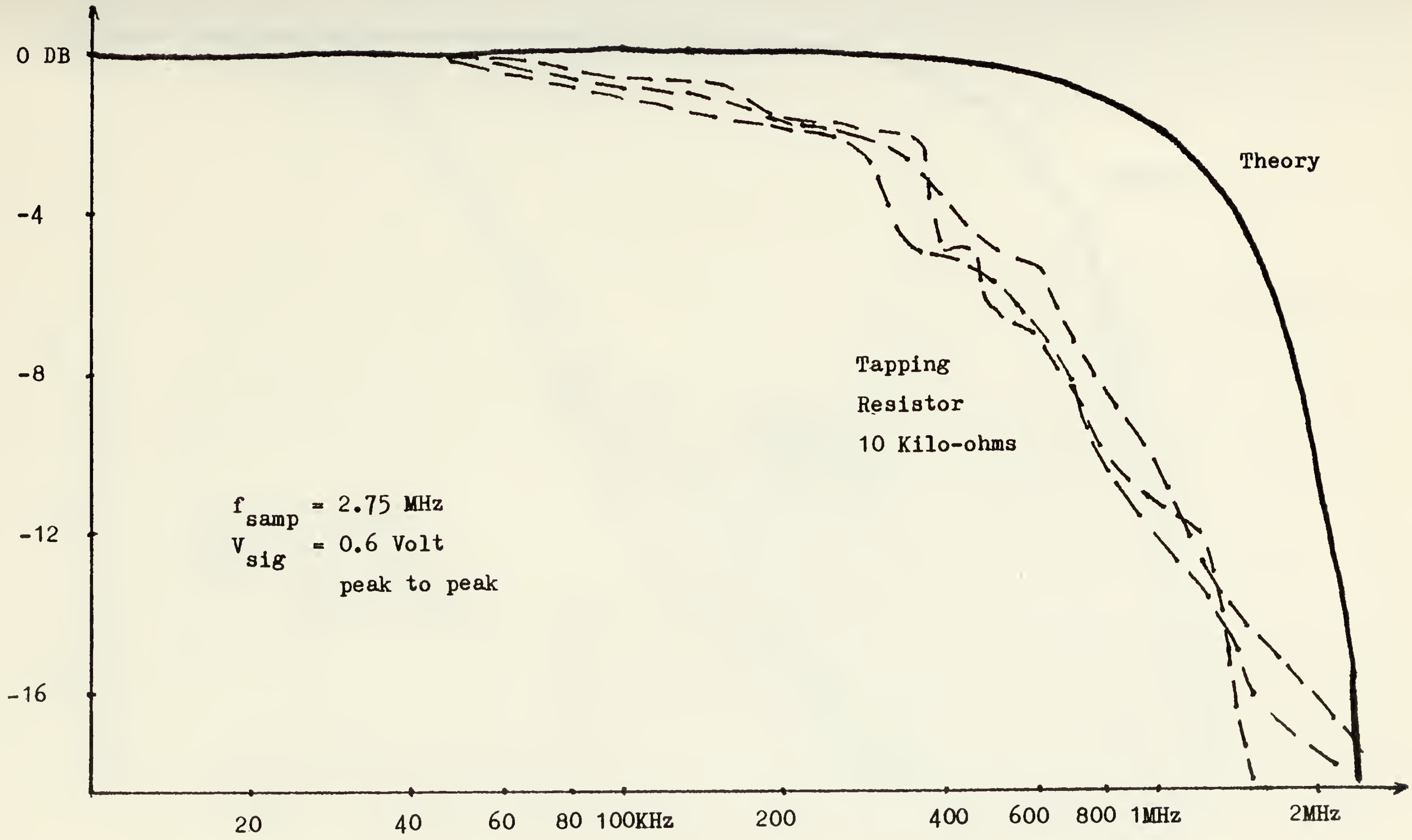


FIGURE 3.8 Amplitude Frequency Response of Reticon TAD-12 Tapped Delay Line.
Tap # 1, 6, 12

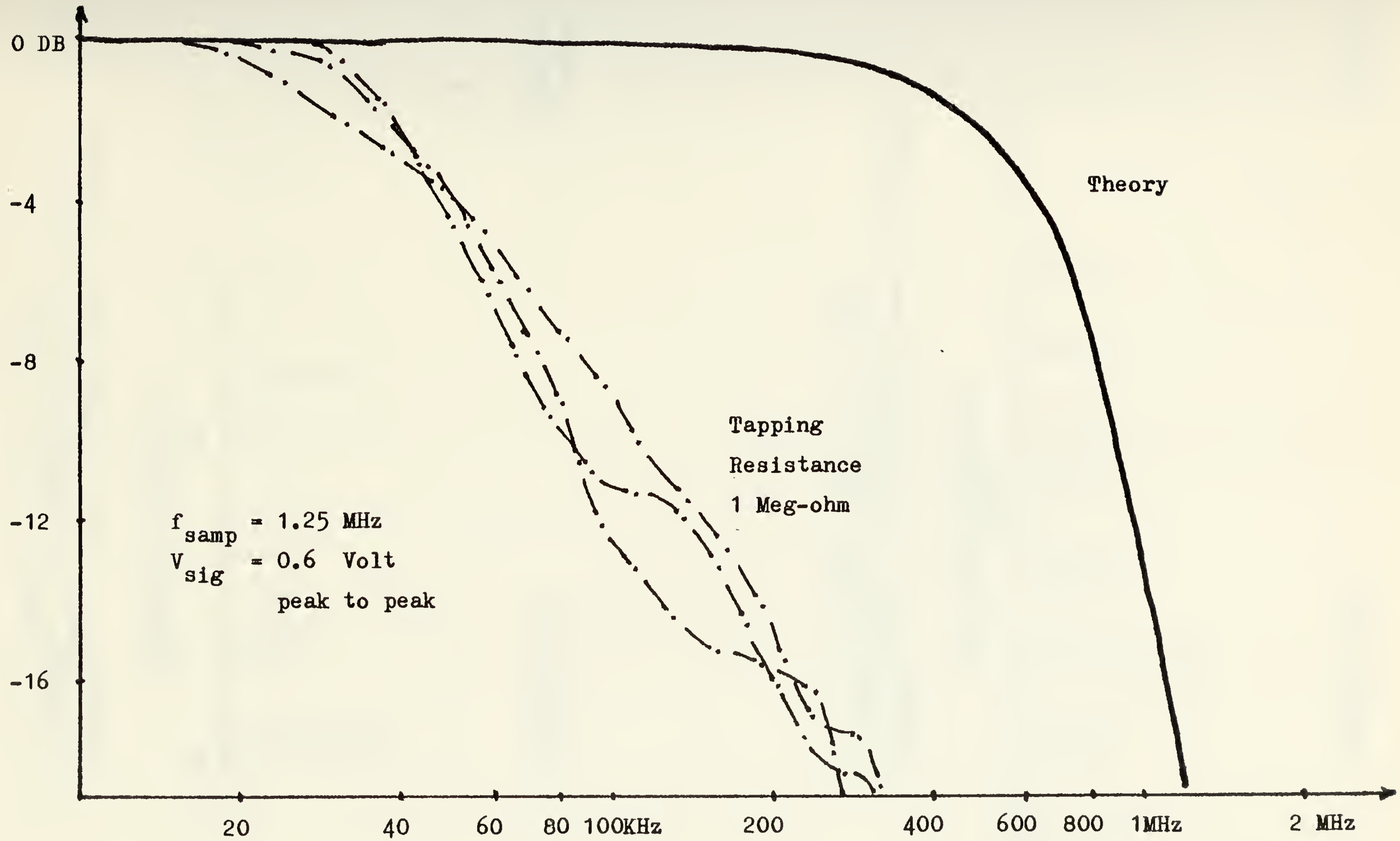


FIGURE 3.9 Amplitude Frequency Response of Reticon TAD-12 Tapped Delay Line.
Tap # 1, 6, 9

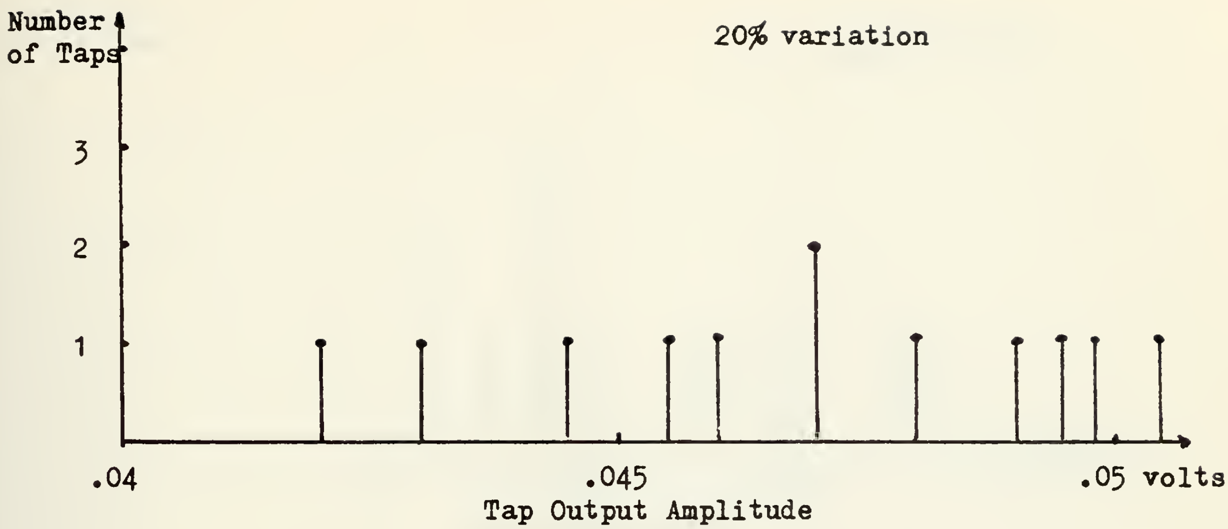


FIGURE 3.10 Non Uniformity Data. $f_{samp}$ = 500 KHz
$R_{tap}$ = 1 Kilo-ohm. $f_{input}$ = 45 KHz

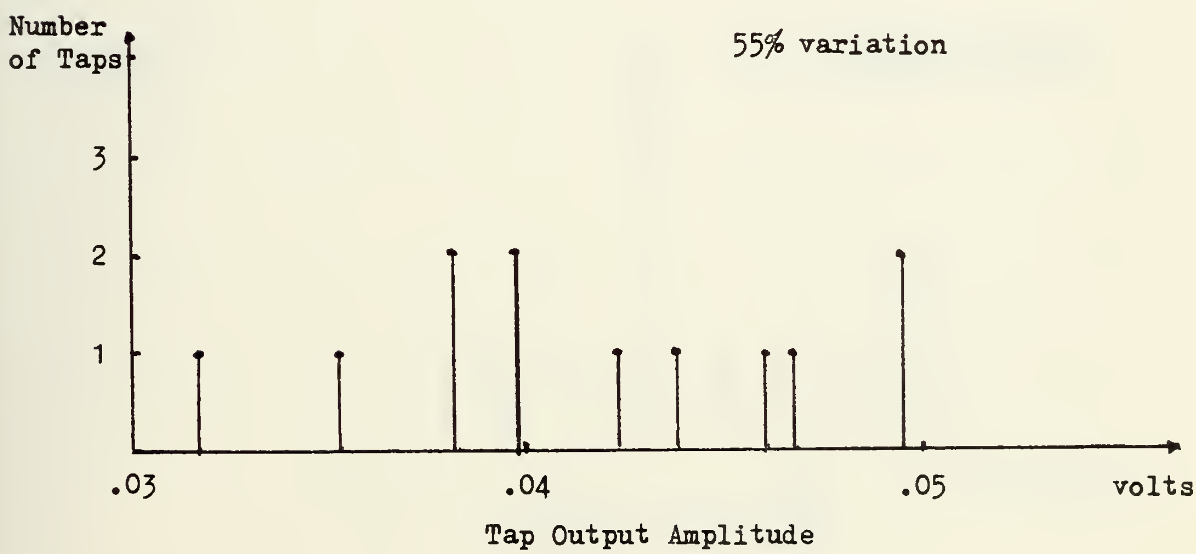


FIGURE 3.11 Non Uniformity Data. $f_{samp}$ = 500 KHz
$R_{tap}$ = 1 Kilo-ohm. $f_{input}$ = 60 KHz

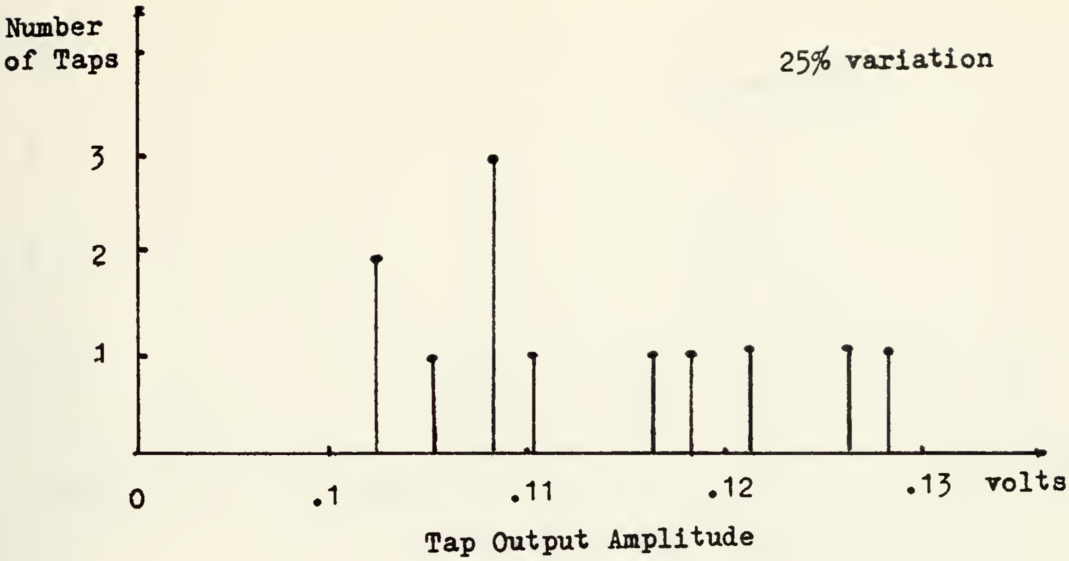


FIGURE 3.12 Non Uniformity Data. $f_{samp} = 500$ KHz
$R_{tap} = 10$ Kilo-ohms. $f_{input} = 50$ KHz

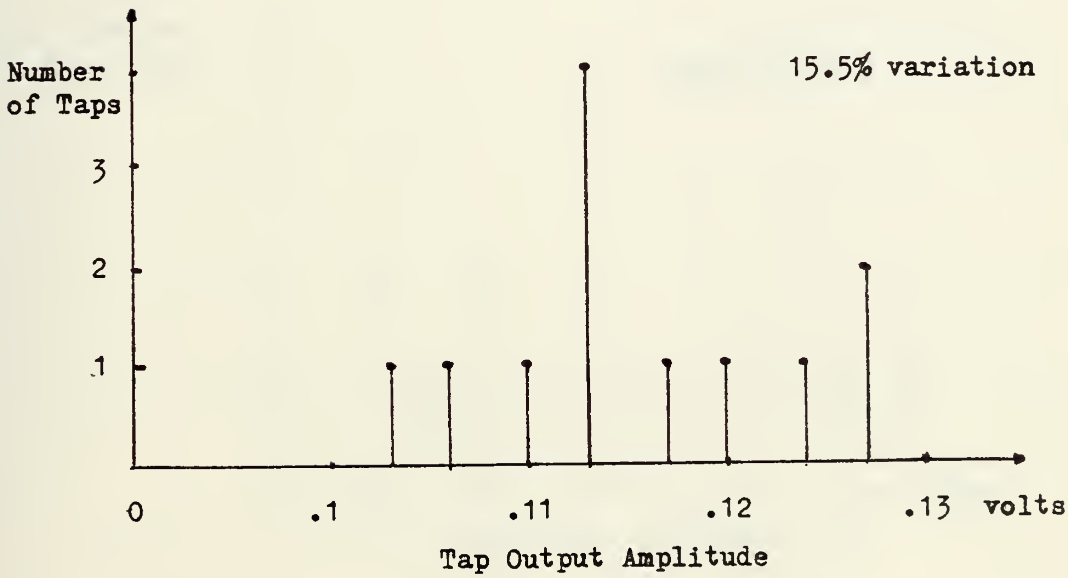


FIGURE 3.13 Non Uniformity Data. $f_{samp} = 500$ KHz
$R_{tap} = 10$ Kilo-ohms. $f_{input} = 100$ KHz

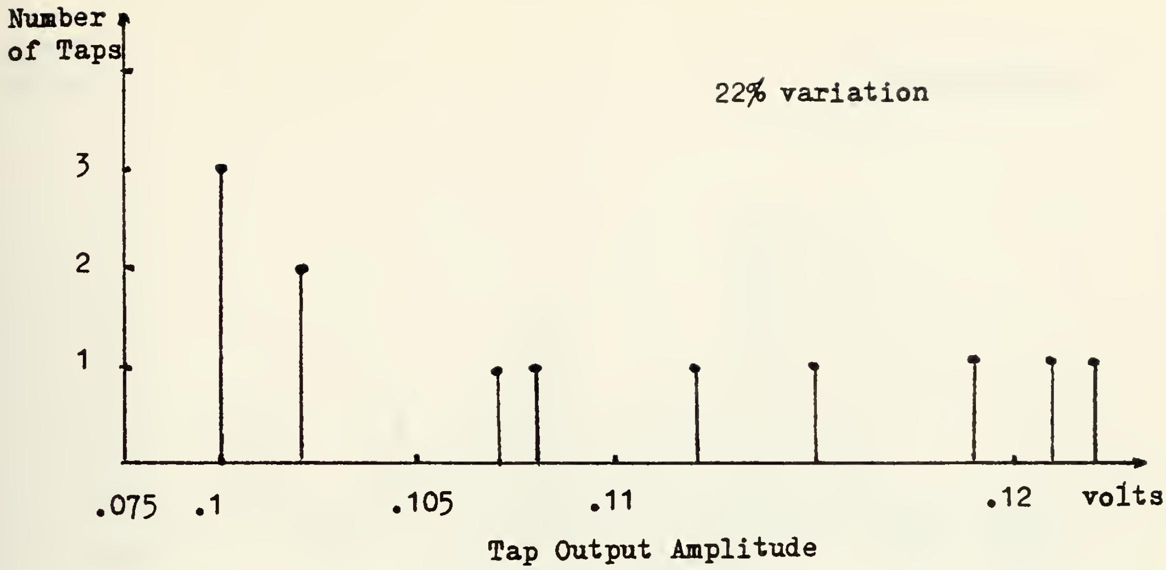


FIGURE 3.14 Non Uniformity Data. $f_{samp}$ = 500 KHz
$R_{tap}$ = 100 Kilo-ohms. $f_{input}$ = 50 KHz

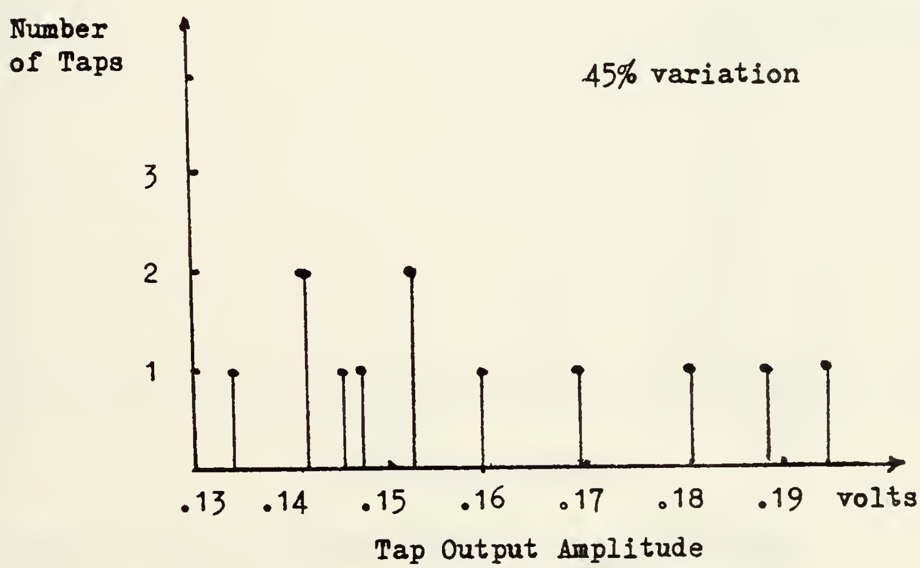


FIGURE 3.15 Non Uniformity Data. $f_{samp}$ = 500 KHz
$R_{tap}$ = 100 Kilo-ohms. $f_{input}$ = 60 KHz

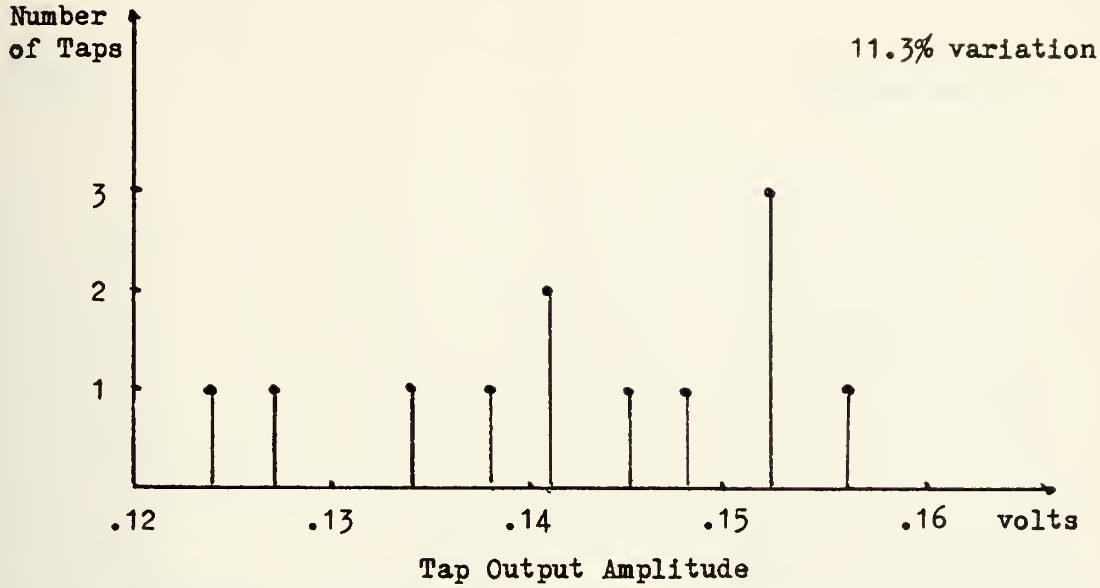


FIGURE 3.16 Non Uniformity Data. $f_{samp}$ = 500 KHz
$R_{tap}$ = 1 Meg-ohm. $f_{input}$ = 30 KHz

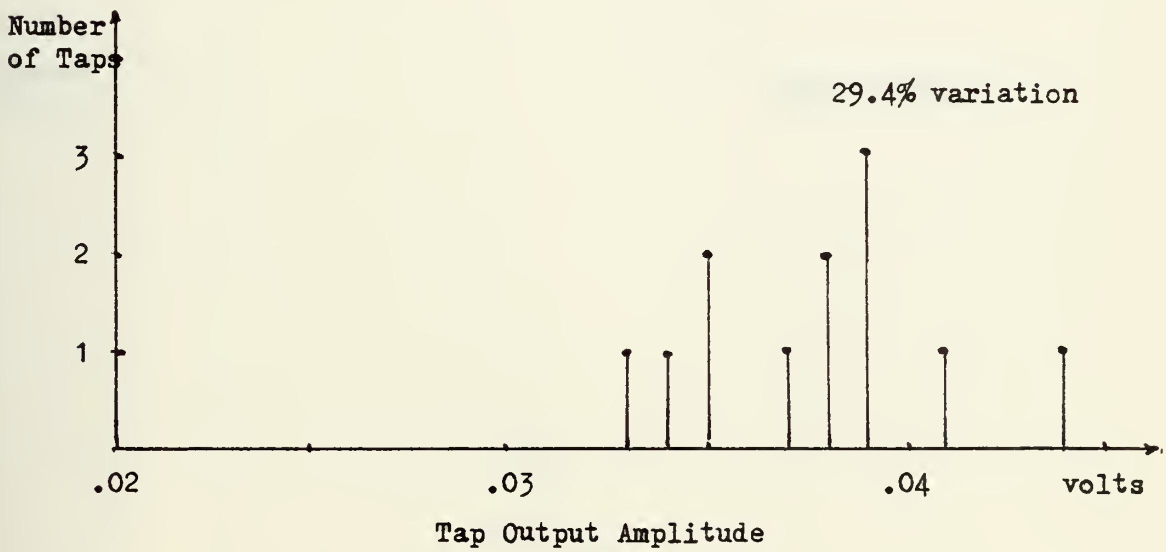


FIGURE 3.17 Non Uniformity Data. $f_{samp}$ = 500 KHz
$R_{tap}$ = 1 Meg-ohm. $f_{input}$ = 120 KHz

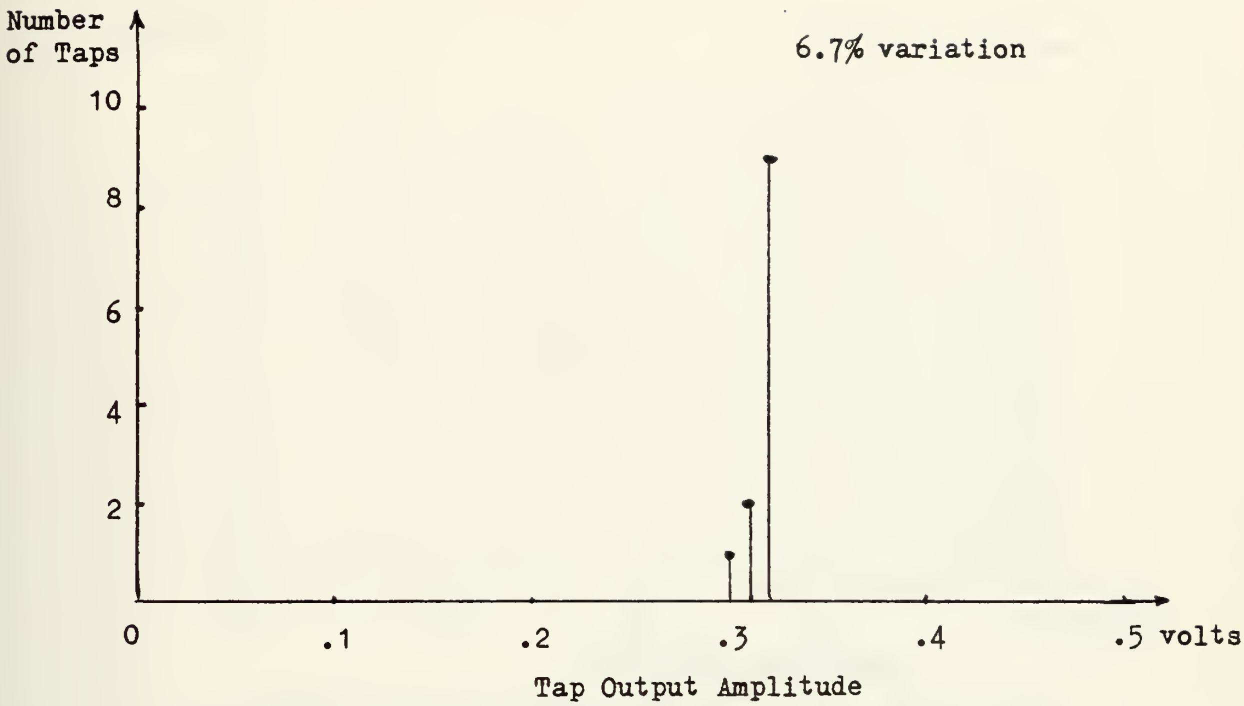


FIGURE 3.18 Non Uniformity Data. $f_{samp}$ = 2.5 MHz
$R_{tap}$ = 10 Kilo-ohms. $f_{input}$ = 50 KHz

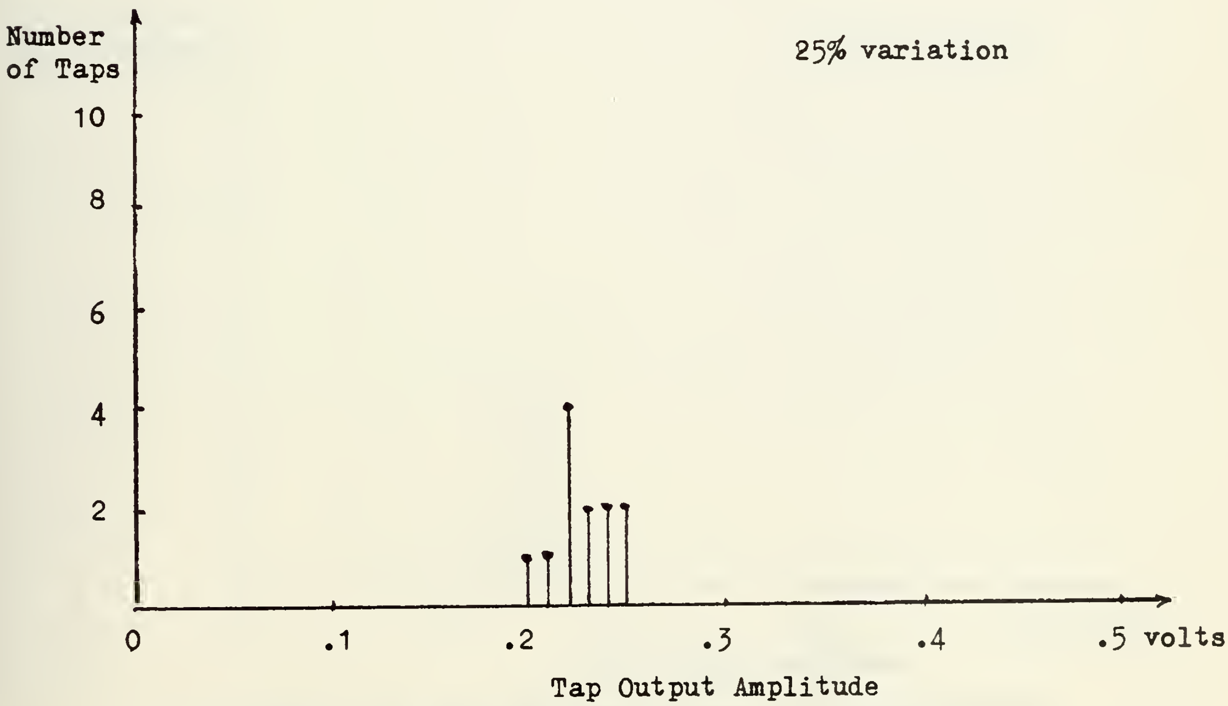


FIGURE 3.19 Non Uniformity Data. $f_{samp}$ = 2.5 MHz.
$R_{tap}$ = 10 Kilo-ohms. $f_{input}$ = 350 KHz

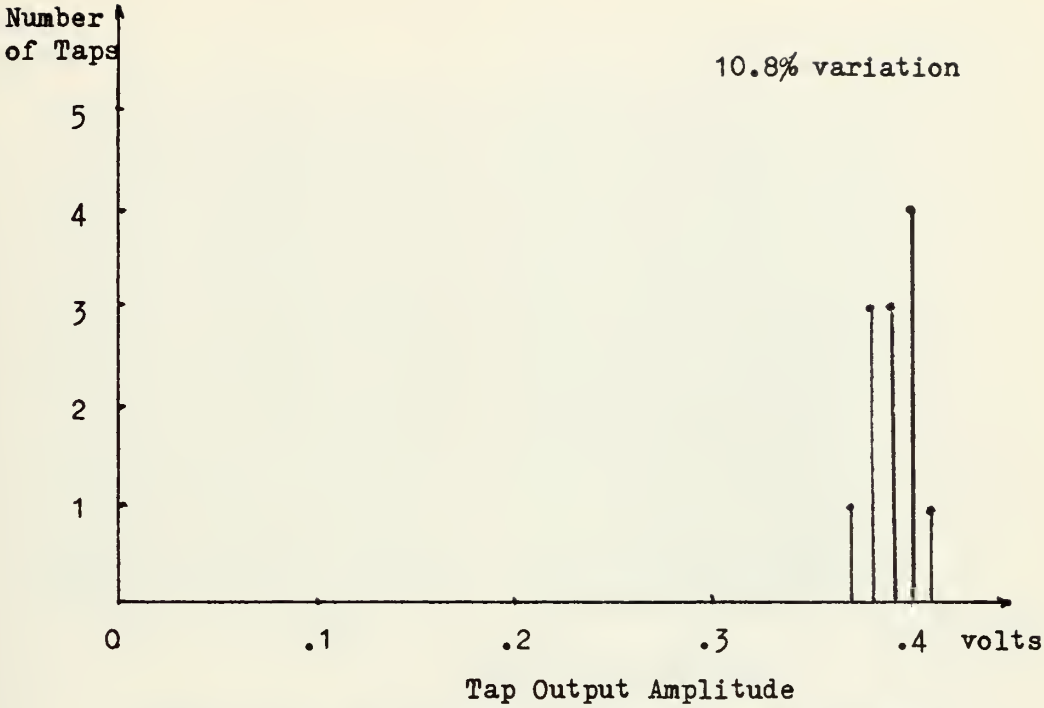


FIGURE 3.20 Non Uniformity Data. $f_{samp} = 2.5$ MHz
$R_{tap} = 100$ Kilo-ohms. $f_{input} = 80$ KHz

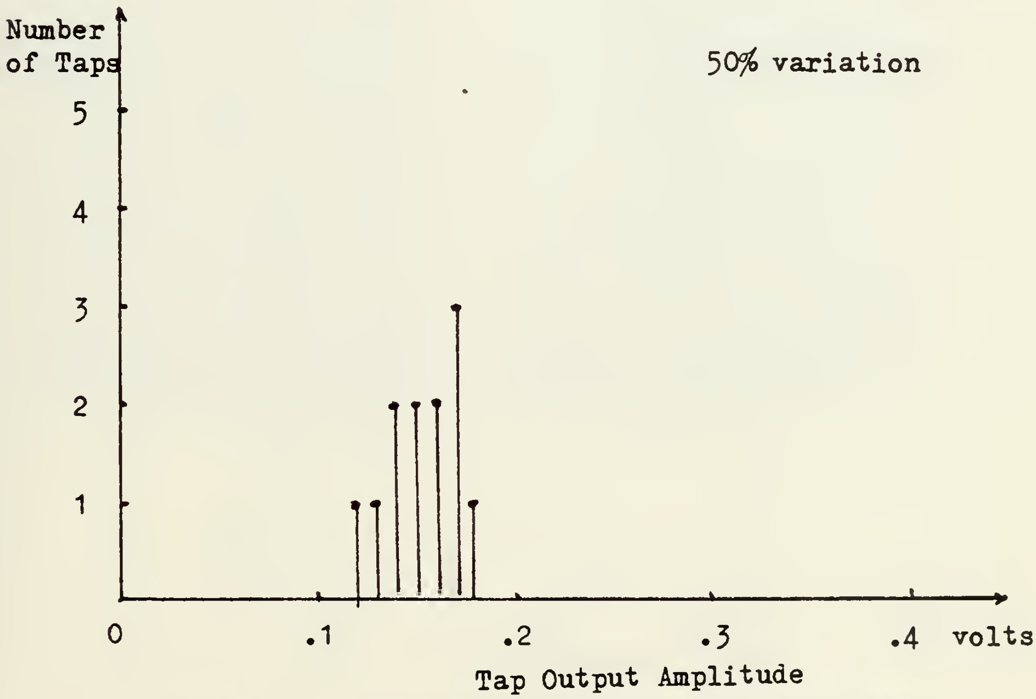


FIGURE 3.21 Non Uniformity Data. $f_{samp} = 2.5$ MHz
$R_{tap} = 100$ Kilo-ohms. $f_{input} = 300$ KHz

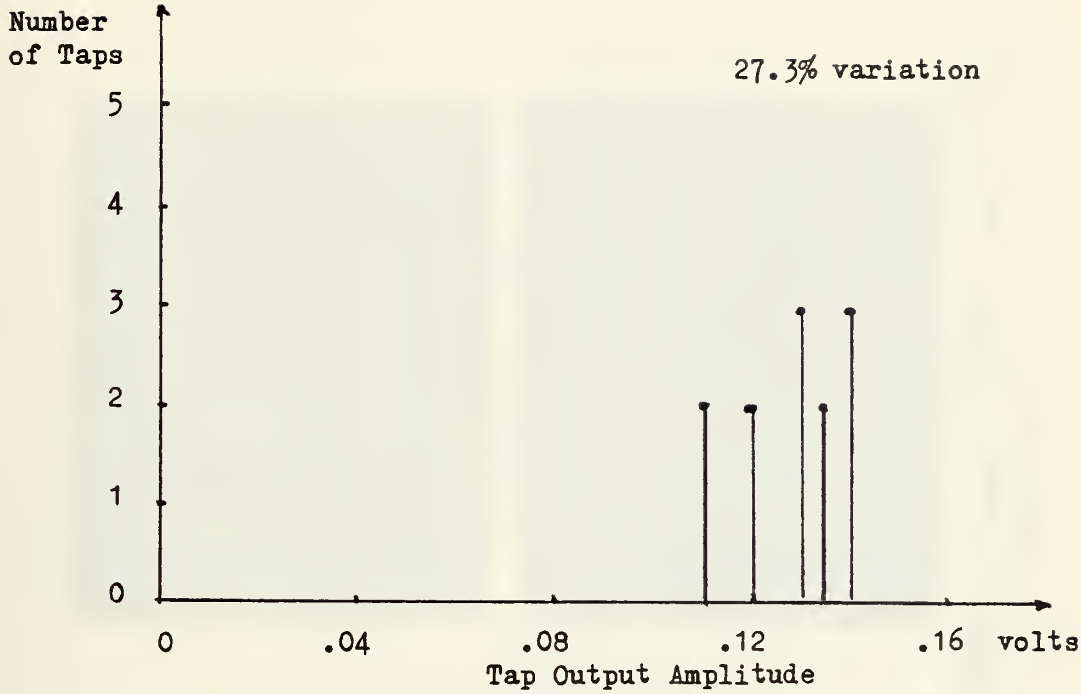


FIGURE 3.22 Non Uniformity Data. $f_{samp} = 2.5$ MHz
$R_{tap} = 1$ Meg-ohm. $f_{input} = 30$ KHz

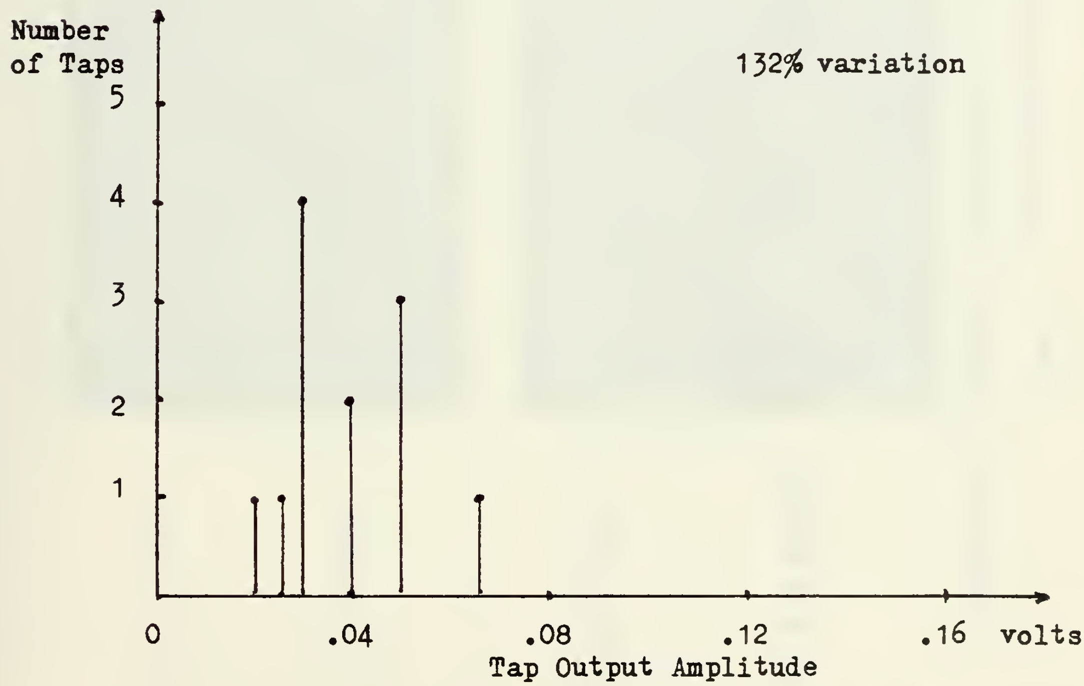


FIGURE 3.23 Non Uniformity Data. $f_{samp} = 2.5$ MHz
$R_{tap} = 1$ Meg-ohm. $f_{input} = 100$ KHz

Input Frequency 30 KHz 100 KHz

Tap #1 Output

Tap #2 Output

Tap #4 Output

Tap #10 Output

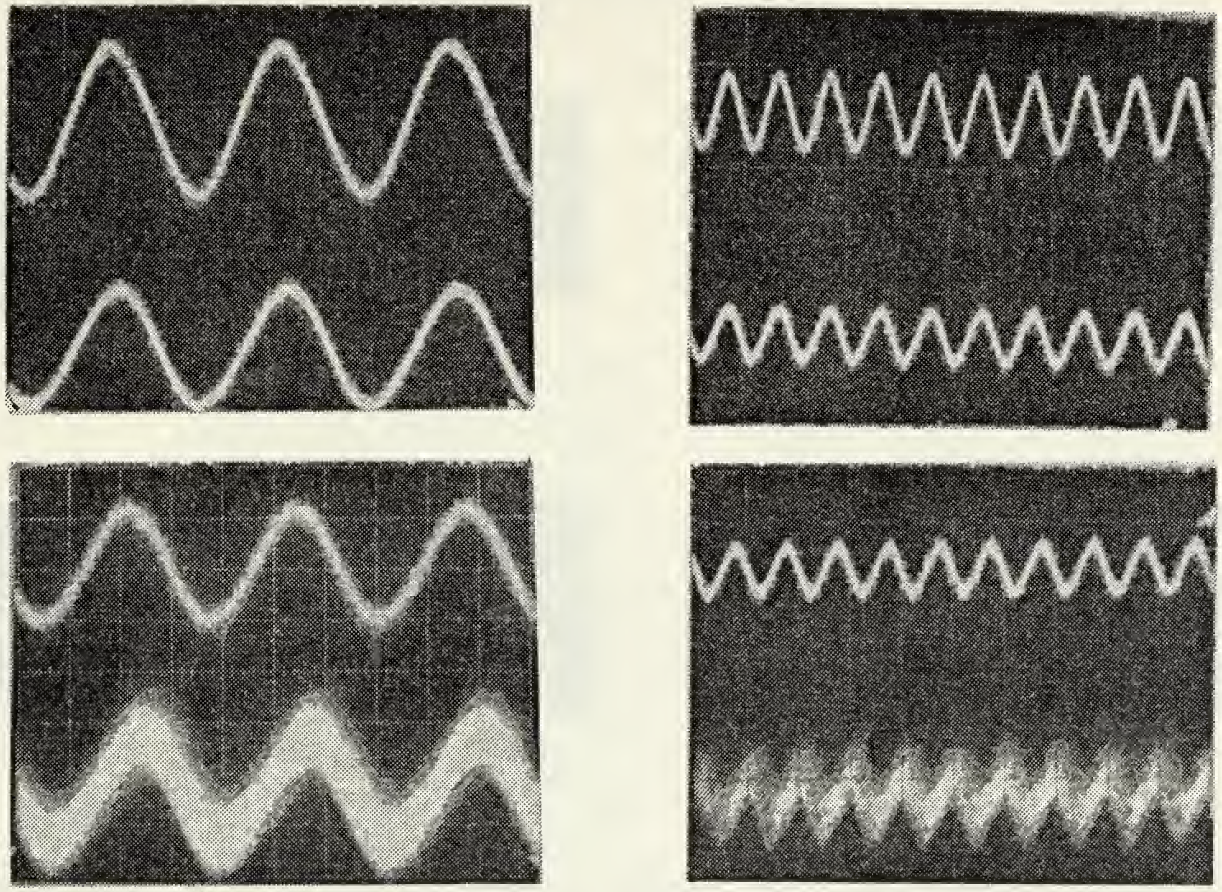

FIGURE 3.24 Pictorial Presentation of TAD-12 Performance. $f_{samp} = 2.5$ MHz. $R_{tap} = 1$ Meg-ohm $V_{input} = .06$ volt peak to peak. Scale: H = 10 microsec./div; V = .05 volt/div

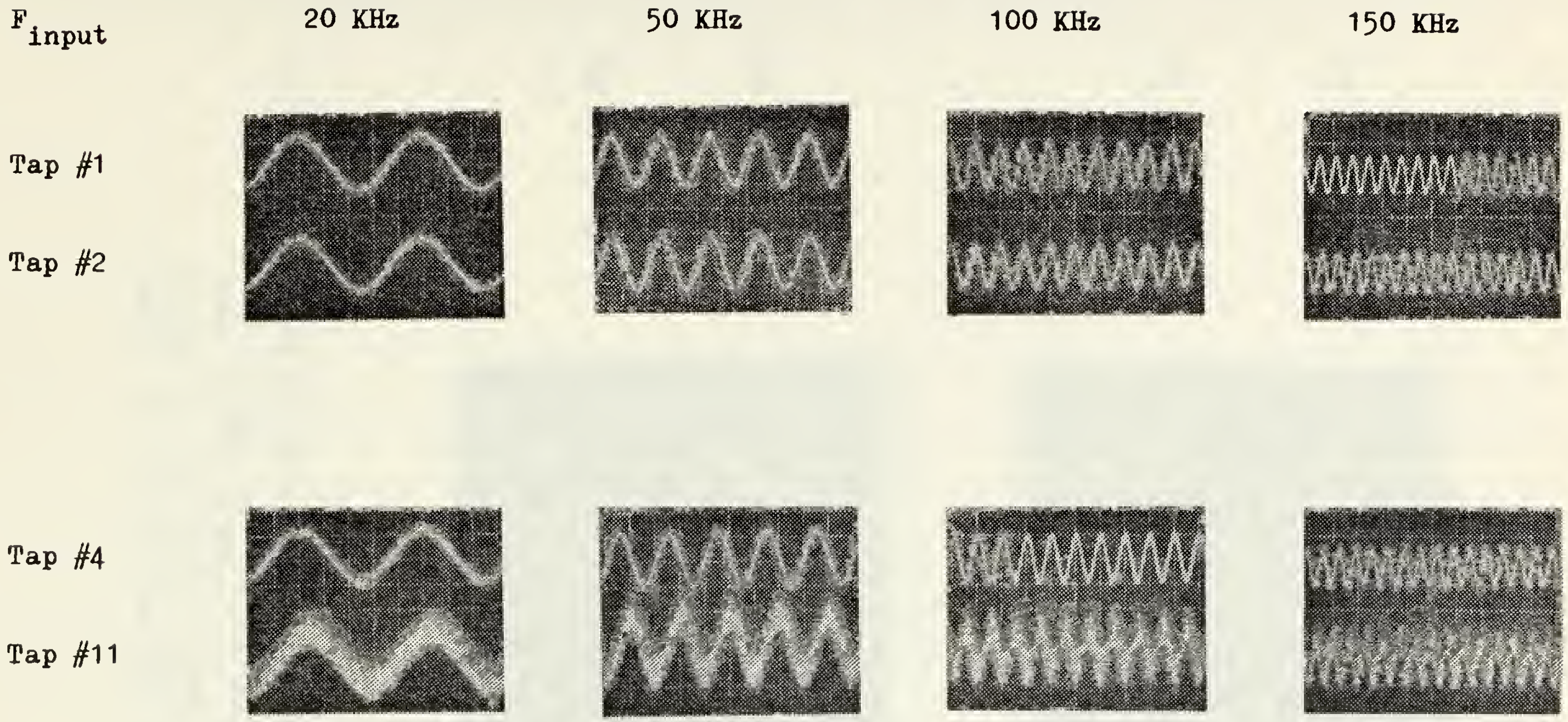


FIGURE 3.25 Pictorial Presentation of Reticon TAD-12 Performance. $f_{samp}$= 2.5 MHz; $R_{tap}$= 100 Kilo-ohms; $V_{input}$= .6 Volt peak to peak(sinusoidal input) . Scale: H=10 microsec./div., V=.2 V/div.

Tap #1 Output

Tap #5 Output

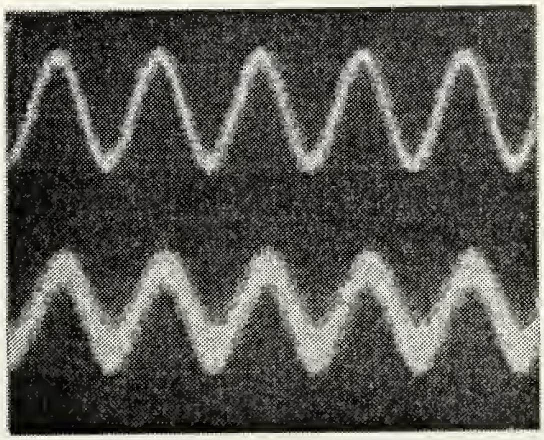

Tap #6 Output

Tap #11 Output

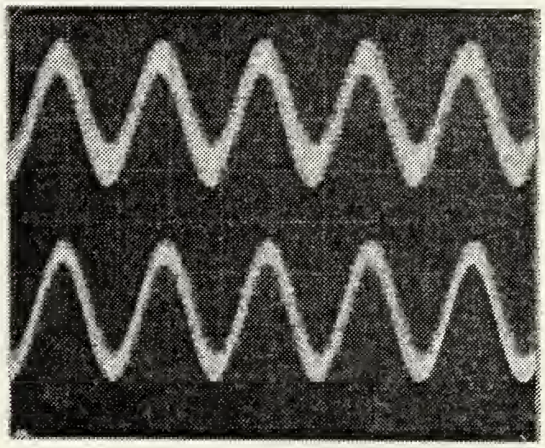

FIGURE 3.26 Pictorial Presentation of TAD-12 Performance.
$f_{samp}$ = 3 MHz; $R_{tap}$ = 100 Kilo-ohms.
$V_{input}$ = .6 volt peak to peak; $f_{input}$ = 50 KHz.
Scale: H = 10 microsec./div, V = .2 volt/div

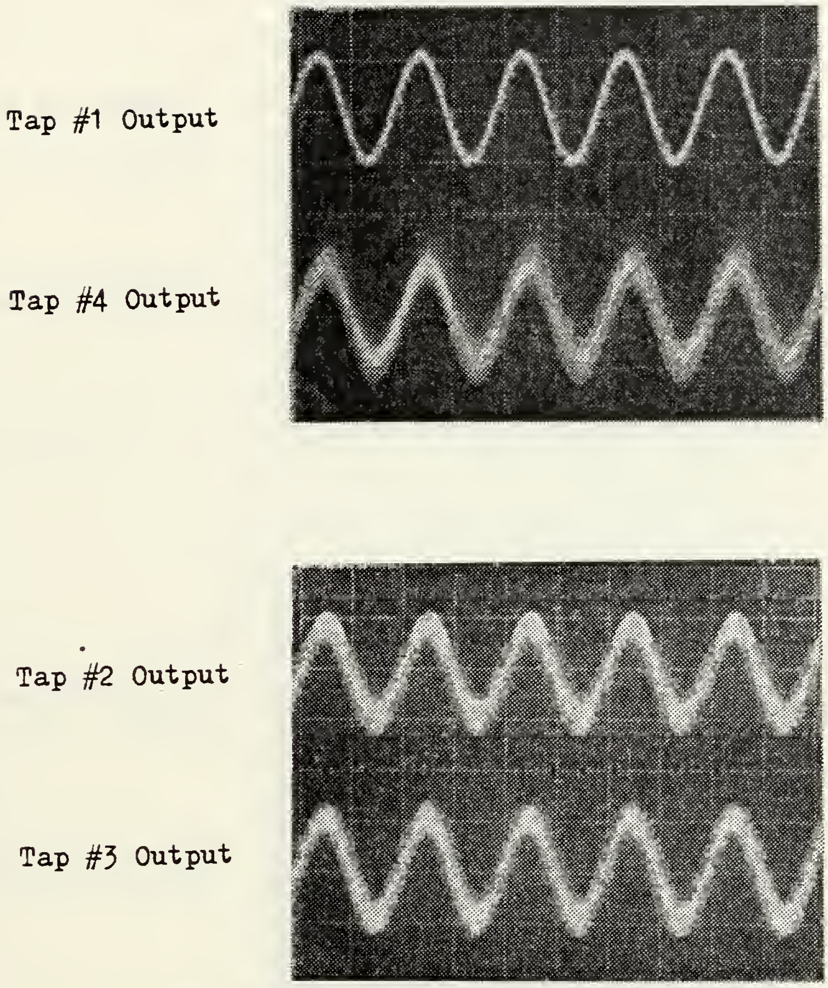


FIGURE 3.27 Pictorial Presentation of Reticon TAD-12 Performance. $f_{samp}$ = 3.5 MHz. $R_{tap}$ = 100 Kilo-ohms $V_{input}$ = .6 Volt peak to peak. $f_{input}$ = 50 KHz. Scale: H = 10 microsec./div; V = .2 Volt/div

Tap #1 Output

Tap #2 Output

Tap #3 Output

Tap #12 Output

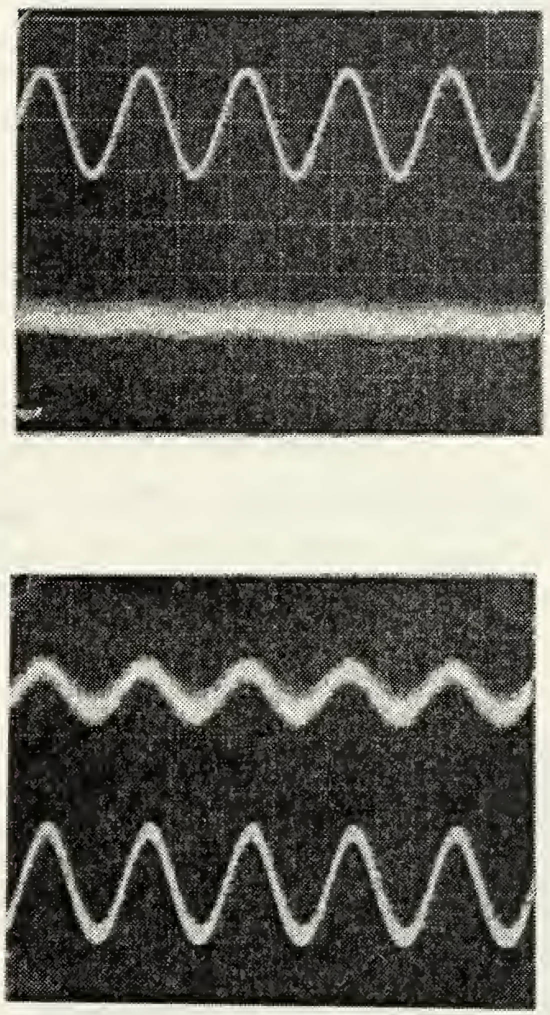

FIGURE 3.28 Pictorial Presentation of Reticon TAD-12. Performance. $f_{samp} = 4$ MHz. $R_{tap} = 100$ Kohms. $V_{input} = .6$ V peak to peak; $f_{input} = 50$ KHz. Scale: H = 10 microsec./div; V = .2 V/div.

Tap #1 Output

Tap #9 Output

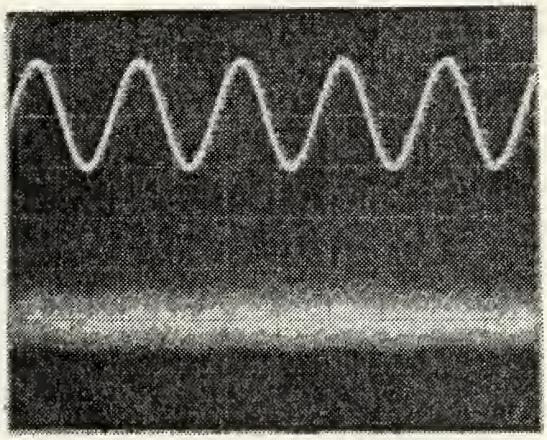

FIGURE 3.29 Reticon TAD-12 Performance.

$f_{samp}$ = 4.5 MHz. $R_{tap}$ = 100 Kilo-ohms.
$V_{input}$ = .6 V peak to peak. $f_{input}$ = 50 KHz.
Scale: H = 10 microsec./div; V = .2 V/div.

Tap #1 Output

Tap #2 Output

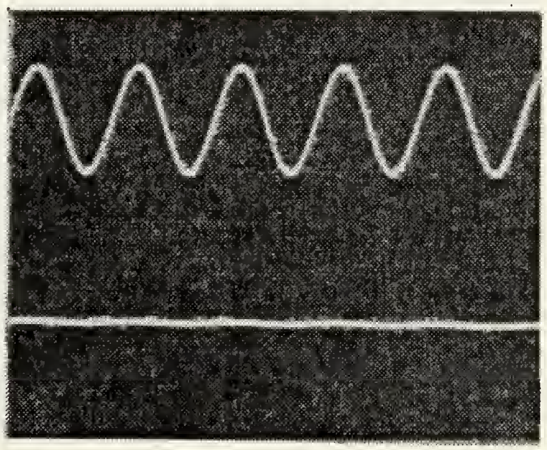

FIGURE 3.30 Reticon TAD-12 Performance.

$f_{samp}$ = 5 MHz. $R_{tap}$ = 100 Kilo-ohms.
$V_{input}$ = .6 V peak to peak. $f_{input}$ = 50 KHz.
Scale: H = 10 microsec./div; V = .2 V/div.

Input

Tap #1 Output

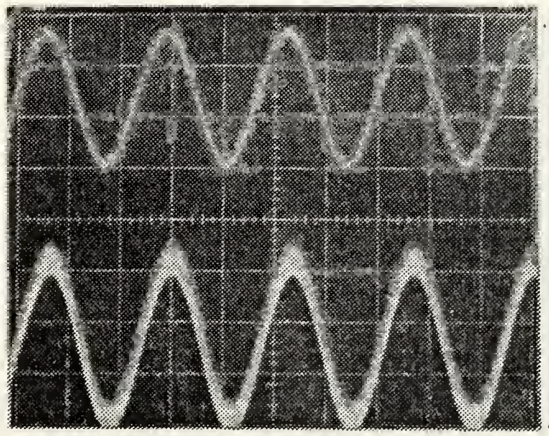

FIGURE 3.31 Reticon TAD-12 Performance.

$f_{samp}$ = 2.5 MHz. $R_{tap}$ = 10 Kilo-ohms.
$V_{input}$ = .6 V peak to peak. $f_{input}$ = 100 KHz.
Upper Scale: H = 5 microsec./div; V = .2 V/div
Lower Scale: H = 5 microsec./div; V = .1 V/div

Input

Tap #1 Output

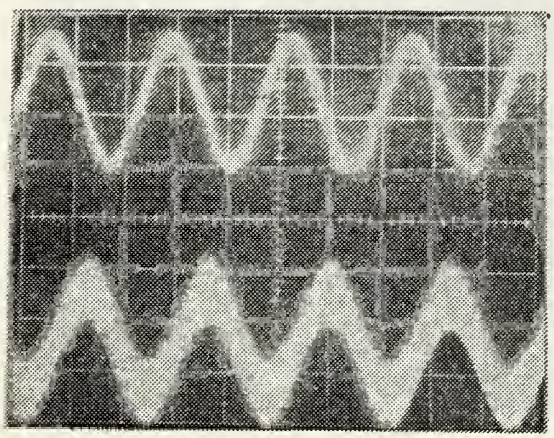

FIGURE 3.32 Reticon TAD-12 Performance

$f_{samp}$ = 2.5 MHz. $R_{tap}$ = 10 Kilo-ohms.
$V_{input}$ = .6 V peak to peak. $f_{input}$ = 1 MHz.
Upper Scale: H = .5 microsec./div; V = .2 V/div
Lower Scale: H = .5 microsec./div; V = .1 V/div

Input

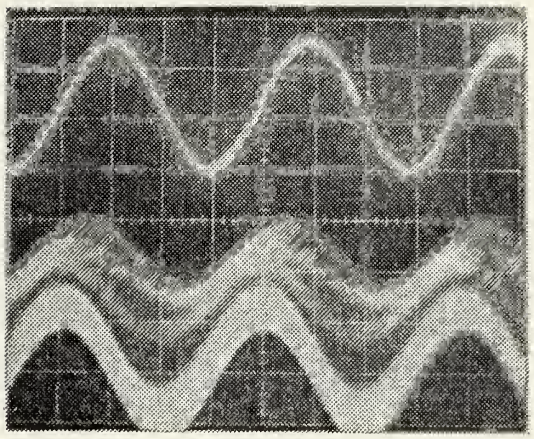

Tap #6 Output

FIGURE 3.33 Reticon TAD-12 Performance.

$f_{samp}$ = 2.5 MHz. $R_{tap}$ = 10 Kilo-ohms.

$V_{input}$ = .6 V peak to peak. $f_{input}$ = 300 KHz.

Upper Scale: H = 1 microsec./div; V = .2 V/div

Lower Scale: H = 1 microsec./div; V = .1 V/div

Input

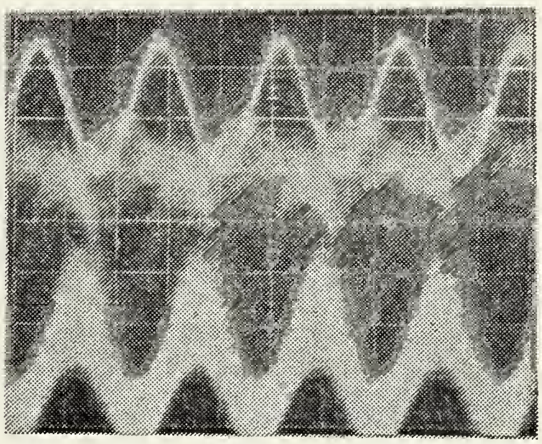

Tap #6 Output

FIGURE 3.34 Reticon TAD-12 Performance.

$f_{samp}$ = 2.5 MHz; $R_{tap}$ = 10 Kilo-ohms.

$V_{input}$ = .6 V peak to peak. $f_{input}$ = 1 MHz

Upper Scale: H = .5 microsec./div; V = .2 V/div

Lower Seale: H = .5 microsec./div; V = .1 V/div

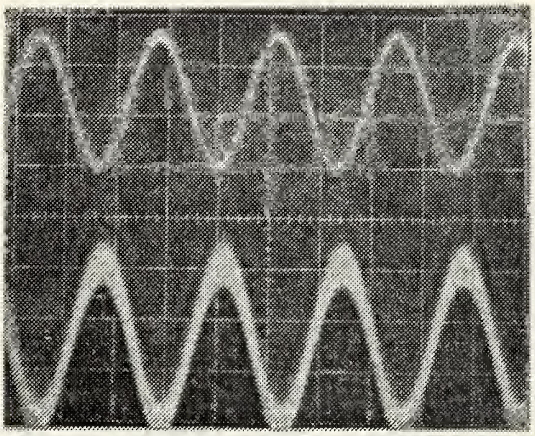


FIGURE 3.35 Reticon TAD-12 Performance.

$f_{samp}$ = 2.5 MHz. $R_{tap}$ = 10 Kilo-ohms.

$V_{input}$ = .6 V peak to peak. $f_{input}$ = 100 KHz

Upper Scale: H = 5 microsec./div; V = .2 V/div

Lower Scale: H = 5 microsec./div; V = .1 V/div

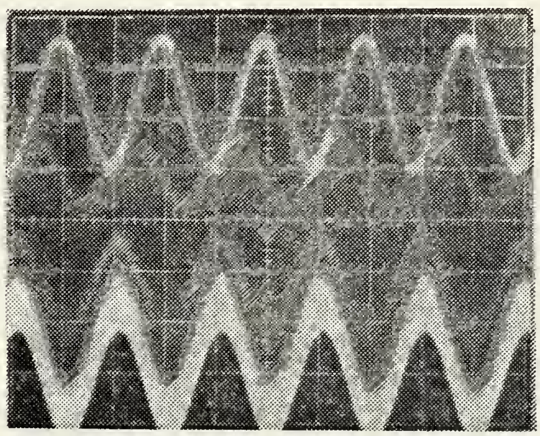


FIGURE 3.36 Reticon TAD-12 Performance.

$f_{samp}$ = 2.5 MHz. $R_{tap}$ = 10 Kilo-ohms.

$V_{input}$ = .6 V peak to peak. $f_{input}$ = 300 KHz

Upper Scale: H = 2 microsec./div; V = .2 V/div

Lower Scale: H = 2 microsec./div; V = .1 V/div

Input

Tap #3 Output

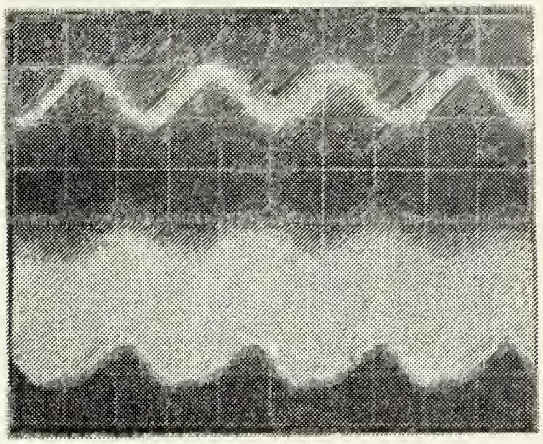

FIGURE 3.37 Reticon TAD-12 Performance.

$f_{samp}$ = 3 MHz. $R_{tap}$ = 10 Kilo-ohms.
$V_{input}$ = .6 V peak to peak; $f_{input}$ = 200 KHz
Upper Scale: H = 2 microsec./div; V = .5 V/div
Lower Scale: H = 2 microsec./div; V = .2 V/div

Input

Tap #2 Output

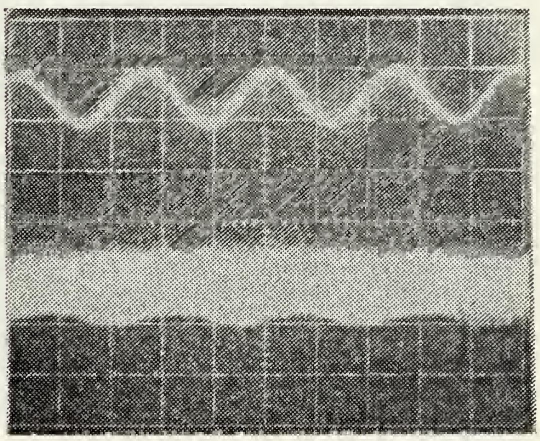

FIGURE 3.38 Reticon TAD-12 Performance.

$f_{samp}$ = 3.5 MHz; $R_{tap}$ = 10 Kilo-ohms.
$V_{input}$ = .6 V peak to peak; $f_{input}$ = 200 KHz
Scale: H = 2 microsec./div; V = .5 V/div

Input

Tap #2 Output

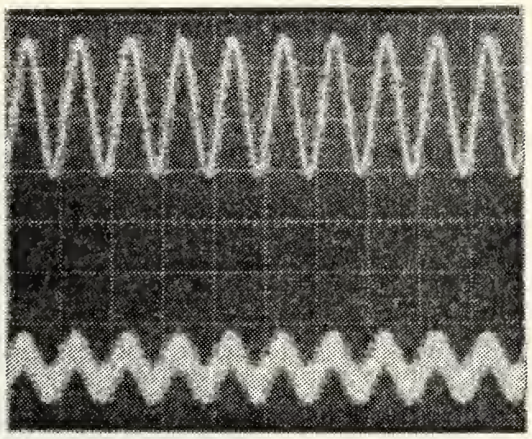

FIGURE 3.39 Reticon TAD-12 Performance.

$f_{samp}$ = 5 MHz. $R_{tap}$ = 10 Kilo-ohms

$V_{input}$ = .6 V peak to peak. $f_{input}$ = 200 KHz

Upper Scale: H = 5 microsec./div; V = .2 V/div

Lower Scale: H = 5 microsec./div; V = .01 V/div

Input

Tap #1 Output

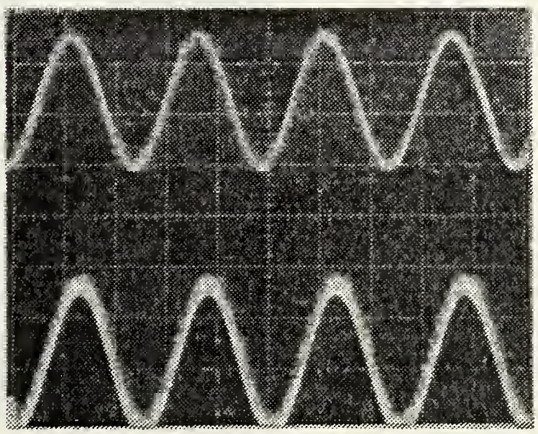

FIGURE 3.40 Reticon TAD-12 Performance.

$f_{samp}$ = 5 MHz. $R_{tap}$ = 10 Kilo-ohms

$V_{input}$ = .6 V peak to peak; $f_{input}$ = 200 KHz

Upper Scale: H = 2 microsec./div; V = .2 V/div

Lower Scale: H = 2 microsec./div; V = .1 V/div

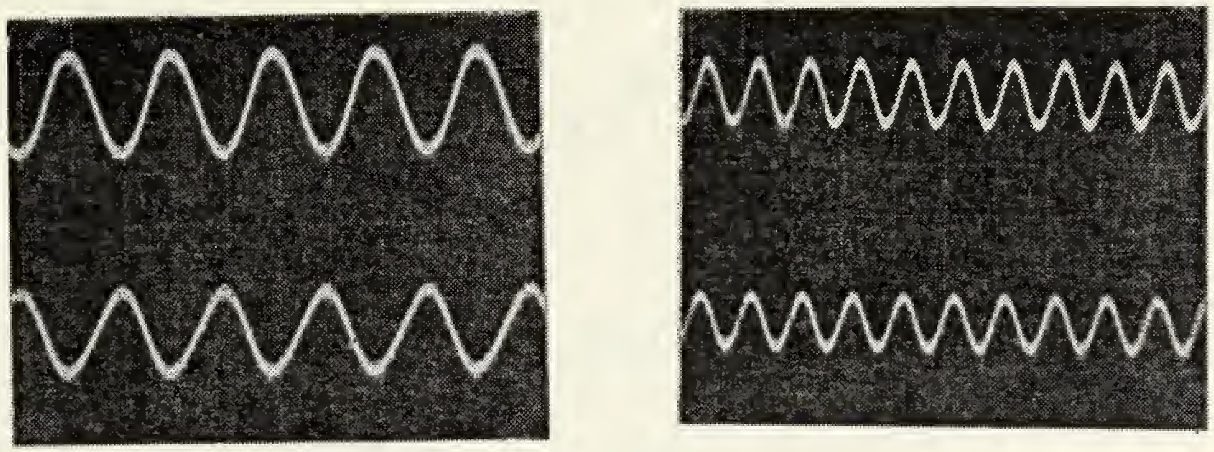


FIGURE 3.41 Reticon TAD-12 Performance. $f_{samp} = 1.25$ MHz. $R_{tap} = 1$ Meg-ohm.
Scale: H = 10 microsec./div; V = .05 Volt/div

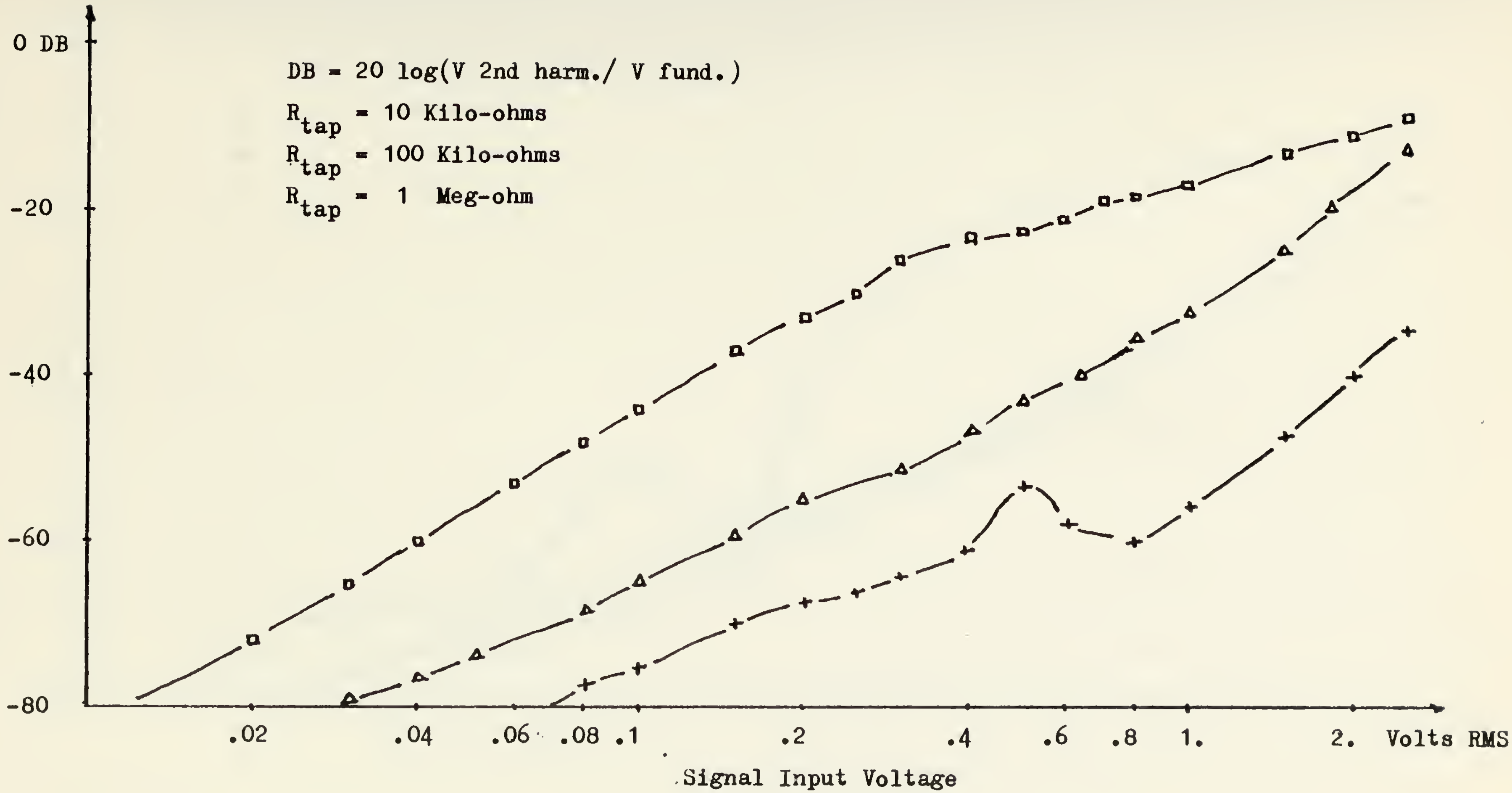


FIGURE 3.42 Second Harmonic Distortion of Different tap outputs. Signal Input Frequency = 10 KHz. $f_{samp}$ = 2.5 MHz.

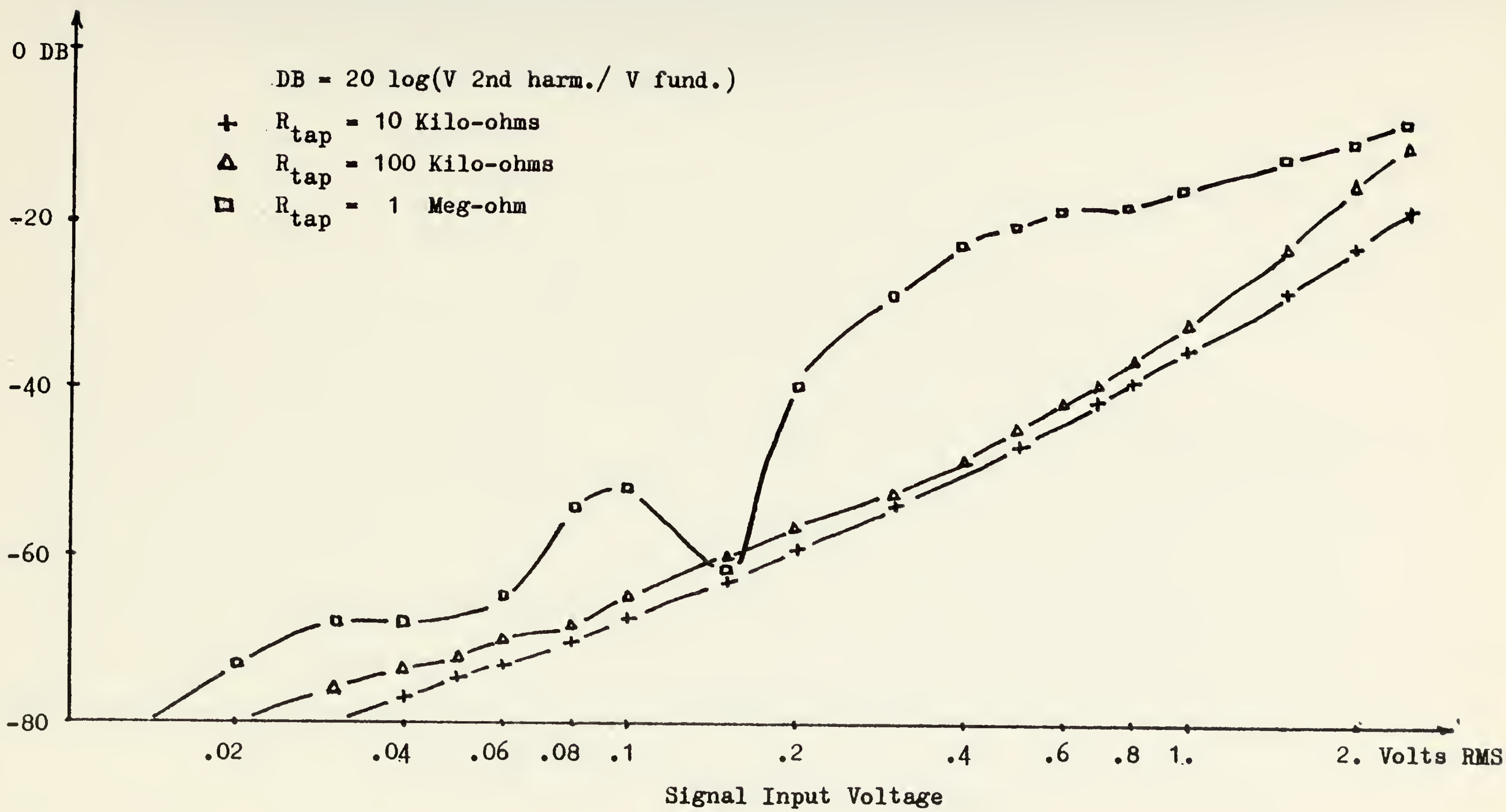


FIGURE 3.43 Second Harmonic Distortion of Different tap outputs. Signal Input Frequency = 10 KHz. $f_{samp}$ = 500 KHz.

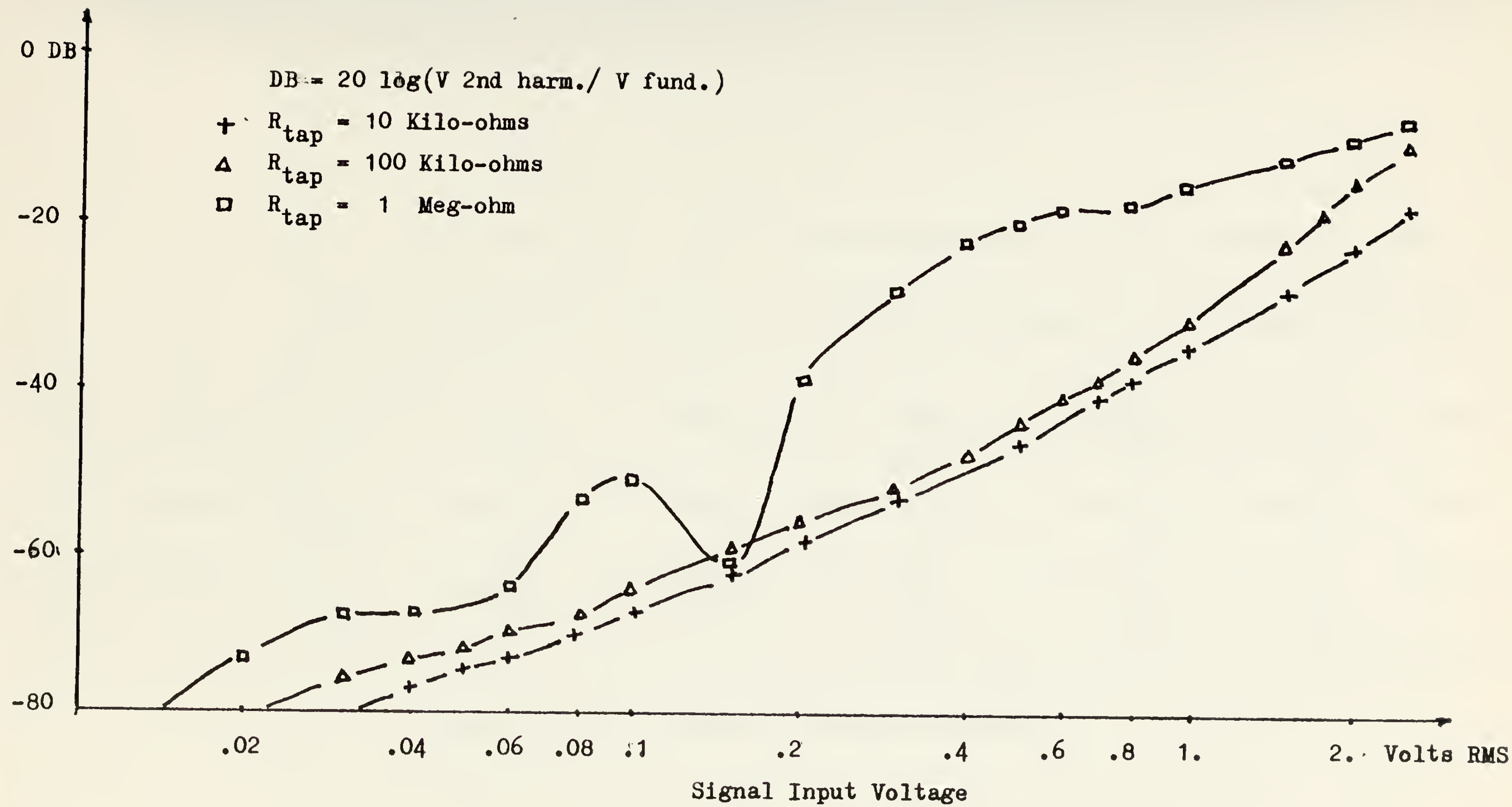


FIGURE 3.44 Second Harmonic Distortion of Different tap outputs. Signal Input Frequency = 10 KHz . $f_{samp}$ = 1.25 MHz .

| | $f_s$ = 500 KHz | | $f_s$ = 1.25 MHz | | $f_s$ = 2.5 MHz | |
|---|---|---|---|---|---|---|
| | 2nd Harmonic Ampl. | | 2nd Harmonic Ampl. | | 2nd Harmonic Ampl. | |
| | < 1% of fund | < 10% of fund | < 1% of fund | < 10% of fund | < 1% of fund | < 10% of fund |
| Tap Resistor 10KΩ | $V_{in}$ < .8 V rms | $V_{in}$ < 2.4 V rms | $V_{in}$ < .95 V rms | $V_{in}$ < 2.9 V rms | $V_{in}$ < 2 V rms | $V_{in}$ < 5 V rms |
| Tap Resistor 10 KΩ | $V_{in}$ < .7 V rms | $V_{in}$ < 1.75 V rms | $V_{in}$ < .66 V rms | $V_{in}$ < 1.85 V rms | $V_{in}$ < .60 V rms | $V_{in}$ <1.8V rms |
| Tap Resistor 1 MΩ | $V_{in}$ < .2 V rms | $V_{in}$ < .52 V rms | $V_{in}$ <.19 V rms | $V_{in}$ < .64 V rms | $V_{in}$ <.12 V rms | $V_{in}$ <.62 V rms |

TABLE III.II Dynamic Range of TAD-12

## C. TIME DOMAIN EVALUATION

The measurement procedure is to use a periodic input pulse. Its period is at least twice the total delay. The width of the pulse must satisfy the condition:

$$\frac{1}{2} \text{ of clock period} \leq \text{width of pulse} < 1 \text{ clock period.}$$

The pulse amplitude should be within the dynamic range. At the output of the summer operational amplifier, one can observe twelve output amplitudes. An analog sample and hold circuit is used to measure each output amplitude.

Figures 3-45 through 3-47 illustrate the impulse response of TAD-12 performance at different sampling frequencies:

$$f_s = 50 \text{ KHz, } 1.25 \text{ MHz, } 2.5 \text{ MHz}$$

and tap resistances:

$$R_{tap} = 10\ \text{K}\Omega,\ 100\ \text{K}\Omega,\ 1\ \text{M}\Omega$$

connected to tap #1, 5, 6.

### 1. Non-Uniformity

The non-uniformity data of tap outputs for the impulse input is shown in Figures 3-48, 3-49, using 10 KΩ tap resistances at different sampling frequencies:

$$f_s = 25 \text{ KHz, } 50 \text{ KHz, } 500 \text{ KHz, } 1.25 \text{ MHz.}$$

The variation of the tap output amplitudes is the following:

- 4.2%, at $f_s$ = 25 KHz
- 1.8%, at $f_s$ = 50 KHz
- 4.1%, at $f_s$ = 500 KHZ
- 10.47%, at $f_s$ = 1.25 MHz.

Figures 3-50, 3-51 illustrate the output of 12 taps using $R_{tap}$ = 10 KΩ at sampling frequencies:

$f_s$ = 50 KHz, 1.25 MHz.

At lower sampling frequency, up to $f_s$ = 1.25 MHz, the non-uniformity of tap output is less than 10%; when the sampling is increased, the uniformity is deteriorated seriously. At $f_s$ = 2.5 MHz, the non-uniformity of different taps is higher than 20%.

The interaction between adjacent taps can also affect the tap uniformity at high sampling frequencies. Figure 3-45 (c), (d), (e), (f) shows these effects. For example, in Figure 3-45 (d) at $f_s$ = 1.25 MHz, the tap #1 output can have an effect on tap #2 before its amplitude reaches the zero value. Another example, in Figure 3-45 (f), at $f_s$ of 2.5 MHz, the effect of tap #1 output can extend to tap #2 and tap #3 before its amplitude goes below the fixed pattern noise.

2. <u>Temporal Noise</u>

The noise of tap outputs can be grouped into two categories:

- fixed pattern noise
- random noise.

The fixed pattern noise is periodic with a period related to the sampling frequency used. At $f_s$ of 50 KHz, this period is about 6.67 microseconds. At $f_s$ of 500 KHz, it is about 80 microseconds, but the number of periods is

constant between tap outputs. For example, there are three periods of fixed pattern noise between tap #1 output and tap #5 output. This is illustrated in Figures 3-45 (a), (c), 3-46 (a), (c), 3-47 (a), (c). The peak to peak amplitude of this noise is about 40 mV for the 10 KΩ load resistors and about 25 mV for the 100 KΩ load.

The random noise varies from one tap to the other. It depends also on the clock frequency and tap resistors. The random noise affects seriously the tap output, except tap #1, at high tap resistor value and high clock frequency. For example, using 10 KΩ resistors, the amplitude of random noise is 40 mV at clock frequency of $f_c$ = 2.5 MHz and is 100 mV at $f_c$ = 5 MHz. This is shown in Figure 3-45 (d), (f). The tap #5 output is deteriorated badly at $f_c$ = 5 MHz for $R_{tap}$ = 100 KΩ and $R_{tap}$ = 1 MΩ in Figures 3-46 (d) and 3-47 (d). However, the noise on tap #1 is very small at any condition. This is illustrated in Figures 3-45 (d), (f), 3-46 (d), (f).

The jitter amplitude observed at the top of tap #1 output in Figure 3-52 equals to 80 microvolts for a signal frequency of 2.83 KHz, $f_c$ = 100 KHz and for $R_{tap}$ = 10 KΩ.

Figure 3-5 shows the magnitude frequency response of Tap #1, Tap #6 and Tap #8 outputs using 100 Kilo-ohms resistors and 1 Meg-ohm resistors. The roll-off starts at about 20 KHz input frequency for the $R_{tap}$ = 1 Meg-ohm curve and at about 60 KHz input frequency for the $R_{tap}$ = 100 Kilo-ohms curves.

When the sampling frequency is increased, the frequency dependence curves are not improved in comparison with the theoretical curve. Figures 3-6 and 3-7 illustrate the magnitude frequency response of different tap outputs at sampling frequency equal to 2.5 MHz using tap resistors:

$R_{tap}$ = 10 Kilo-ohms, 100 Kilo-ohms, 1 Meg-ohm.

With $R_{tap}$ = 10 Kilo-ohms, the frequency roll-off is about 150 KHz. When the signal frequency, f, equals to 200 KHz, the measured curve is 1 db below the theoretical curve. At f = 300 KHz, it is 3 db below the theoretical curve. For the $R_{tap}$ = 1 Meg-ohm curves, the frequency roll-off begins about 30 KHz.

With $R_{tap}$ = 100 Kilo-ohms, the response curve begins to roll off at the input frequency f = 80 KHz. At f = 100 KHz, the response curve is 2 db below the theoretical curve.

Figures 3-8 and 3-9 illustrate respectively the magnitude frequency response of TAD-12 output using 10 Kilo-ohms tap resistors at sampling frequency $f_s$ equal to 2.75 MHz and using 1 Meg-ohm tap resistor at $f_s$ equal to 1.25 MHz.

| $F_{samp}$ | 50 KHz | 1.25 MHz | 2.5 MHz |
|---|---|---|---|
| Input / Output (#1,5,6) | (a) | (c) | (e) |
| Tap#1 / Tap#5 | (b) | (d) | (f) |

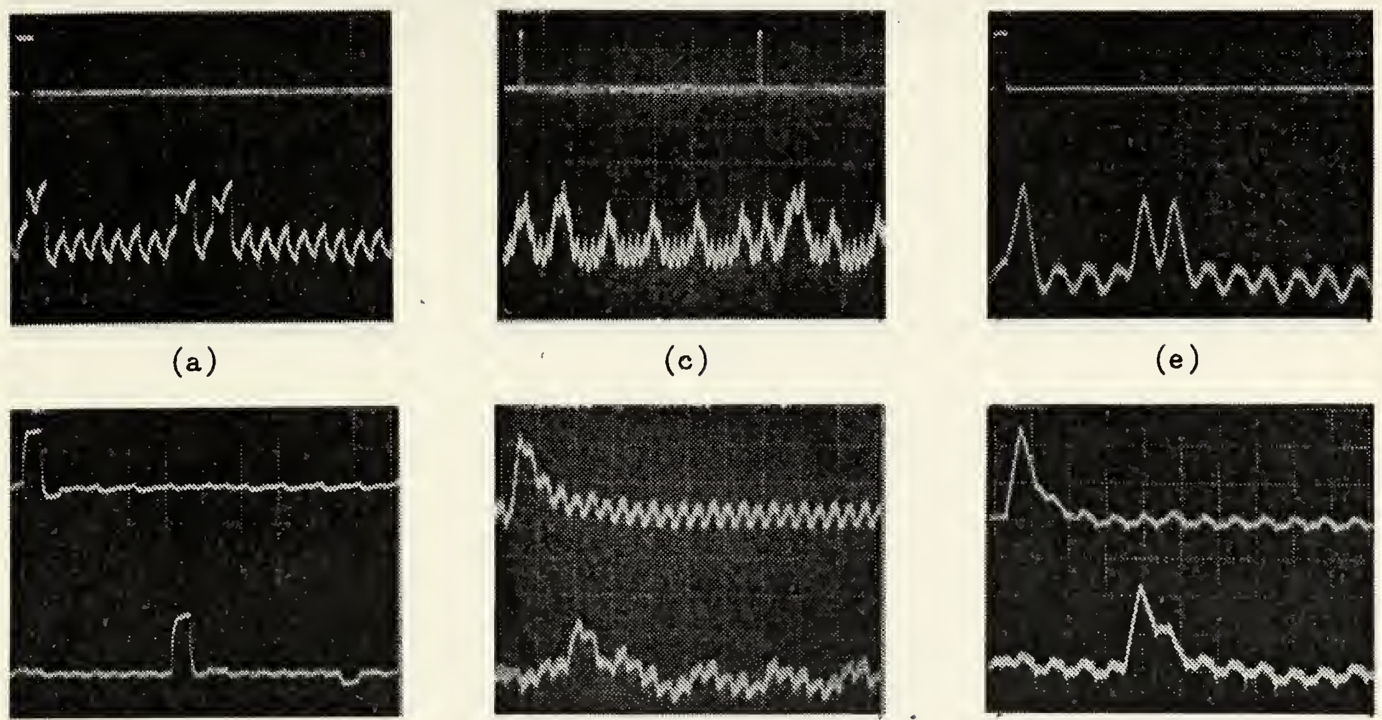

FIGURE 3.45 Pictorial Presentation of TAD-12 Performance in Time Domain. $R_{tap}$= 10 Kilo-ohms.
(a) Upper Scale: H=20 microsec./div. V=1 V/div.; Lower Scale: H=20 microsec./div V=.05 V/div
(b) Scale: H=20 microsec./div. V=.5 V/div.; (c) Upper Scale: H=1 microsec./div.;
Lower Scale: H=1 microsec./div. V=.02 V/div.; (d) Scale: H=1 microsec./div. V=.1 V/div.
(e) Upper Scale: H=2 microsec./div. V=1 V/div., Lower Scale: H=2 microsec./div. V=.02 V/div.
(f) Upper Scale: H=10 microsec./div. V=.05 V/div., Lower Scale: H=10 microsec./div. V=.1V/div

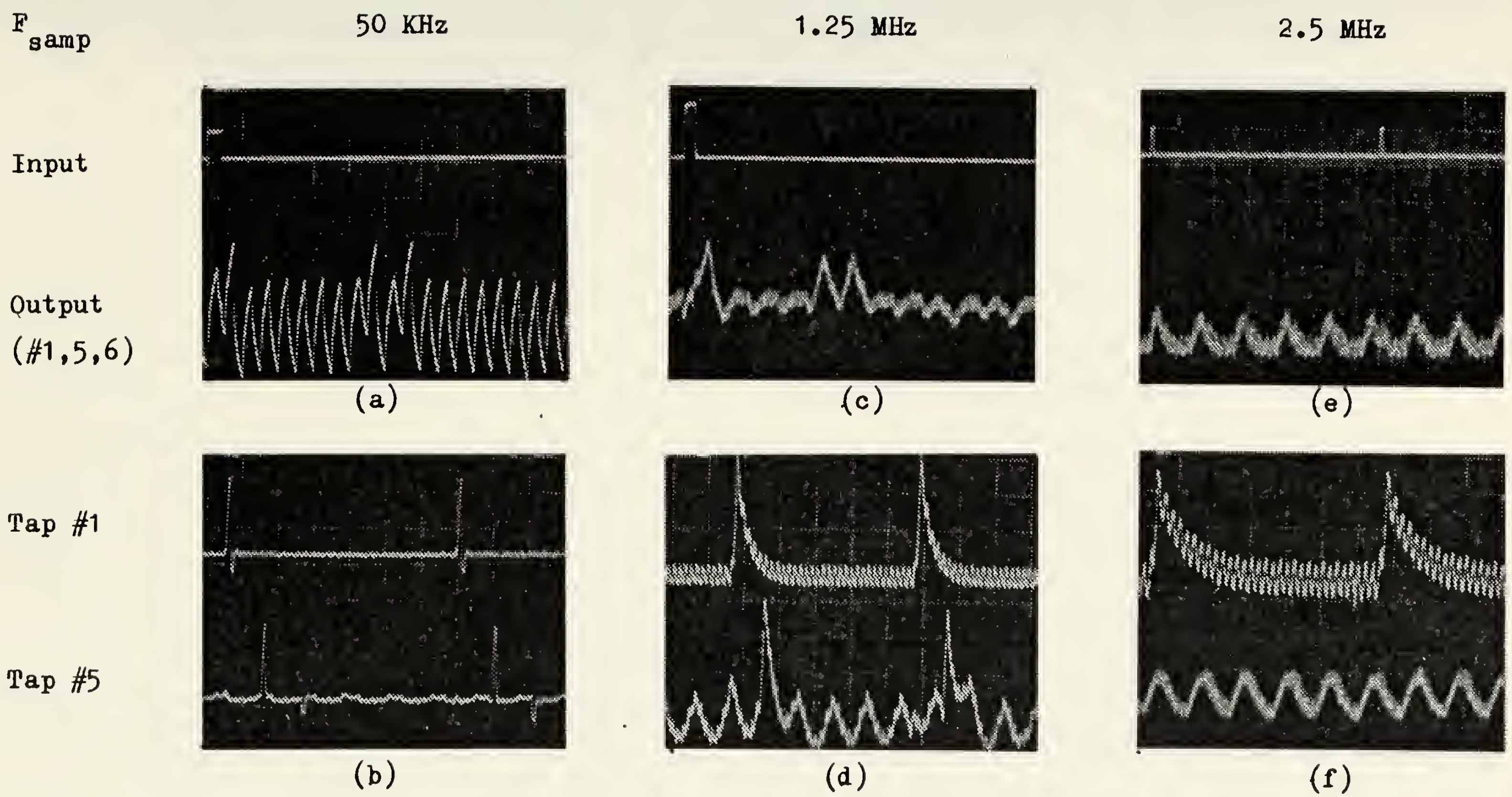


FIGURE 3.46 Pictorial Presentation of TAD-12 Performance in Time Domain. $R_{tap}$= 100 Kilo-ohms. (a) Upper Scale: H=20 microsec./div. V=2 V/div., Lower Scale: H=20 microsec./div. V=.1 V/div. (b) Scale: H=10 microsec./div. V=.5 V/div.; (c) Upper Scale: H=1 microsec./div. V=1 V/div., Lower Scale: H=1 microsec./div. V=.05 V/div.; (d) Scale: H=5 microsec./div. V=.02 V/div.; (e) Upper Scale: H=2 microsec./div. V=2 V/div., Lower Scale: H=2 microsec./div. V=.01 V/div.; (f) Scale: H=2 microsec./div. V=.1 V/div.

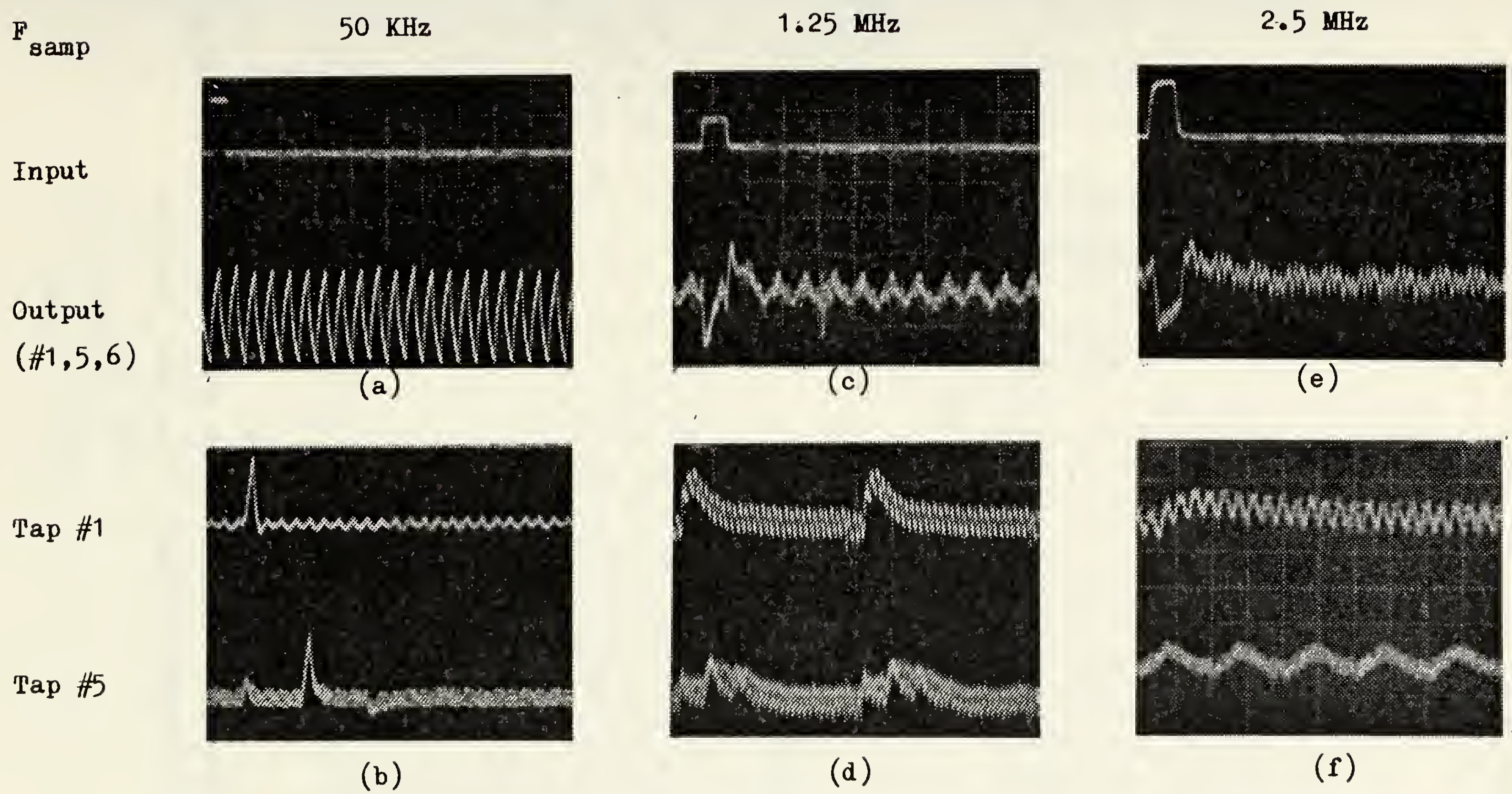


FIGURE 3.47 Pictorial Presentation of TAD-12 Performance in Time Domain. $R_{tap}$=1 Meg-ohm.
(a) Upper Scale: H=20 microsec./div. V=1 V/div., Lower Scale: H=20 microsec./div. V=.01 V/div.
(b) Scale: H=50 microsec./div. V=.1 V/div.; (c) Upper Scale: H=.5 microsec./div. V=2 V/div., Lower Scale: H=.5 microsec./div. V=.002 V/div.; (d) Scale: H=5 microsec./div. V=.01 V/div.;
(e) Upper Scale: H=.2 microsec./div. V=1 V/div., Lower Scale: H=.2 microsec./div. V=.002 V/div.;
(f) Upper Scale: H=10 microsec./div. V=.01 V/div., Lower Scale: H=10 microsec./div. V=.02 V/div.

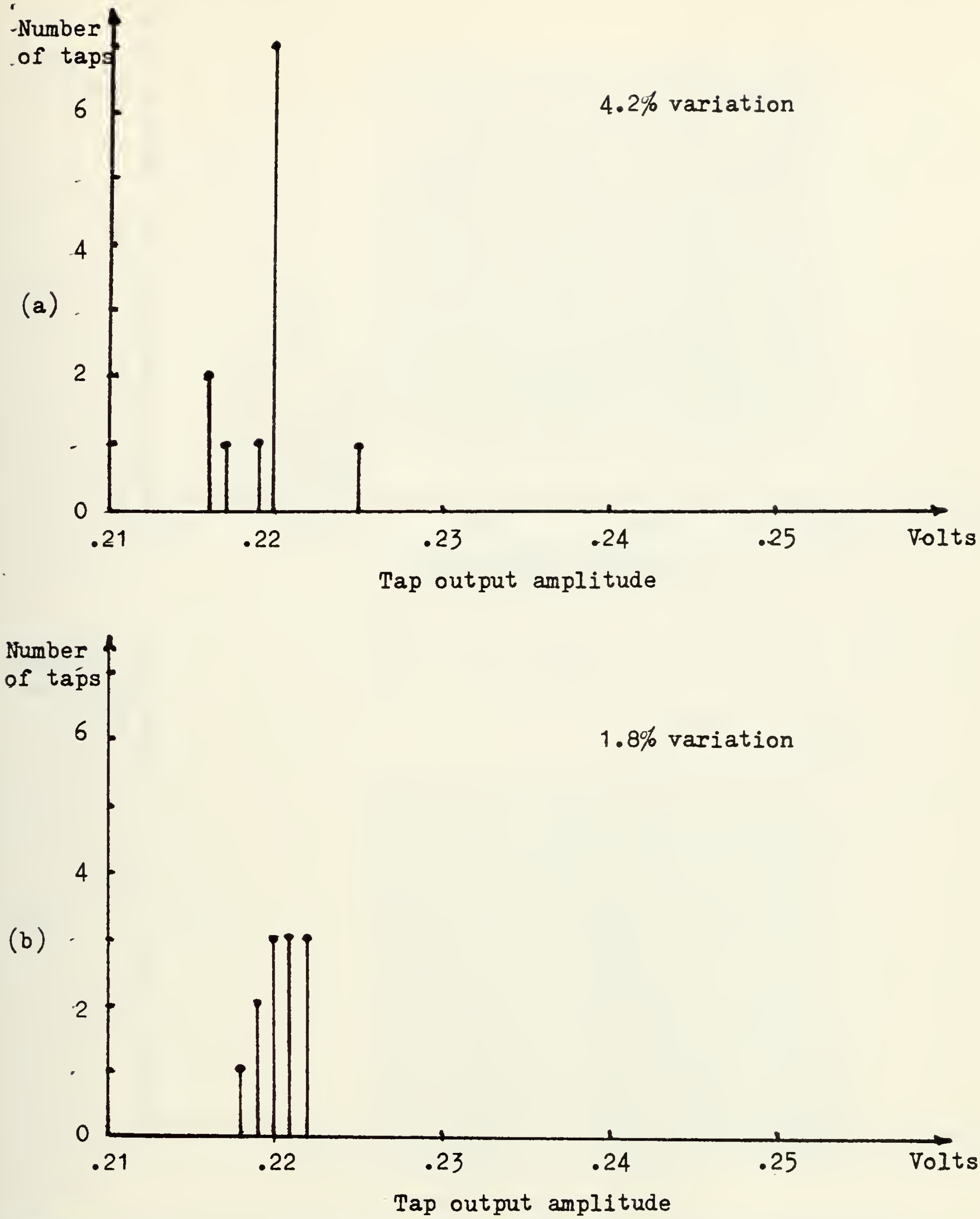


FIGURE 3.48 Non Uniformity Data. Input Pulse: Amplitude=1 Volt, Width=.2 microsec.. Tapping Resistor=10 Kilo-ohms

(a) $F_{samp}$ = 25 KHz

(b) $F_{samp}$ = 50 KHz

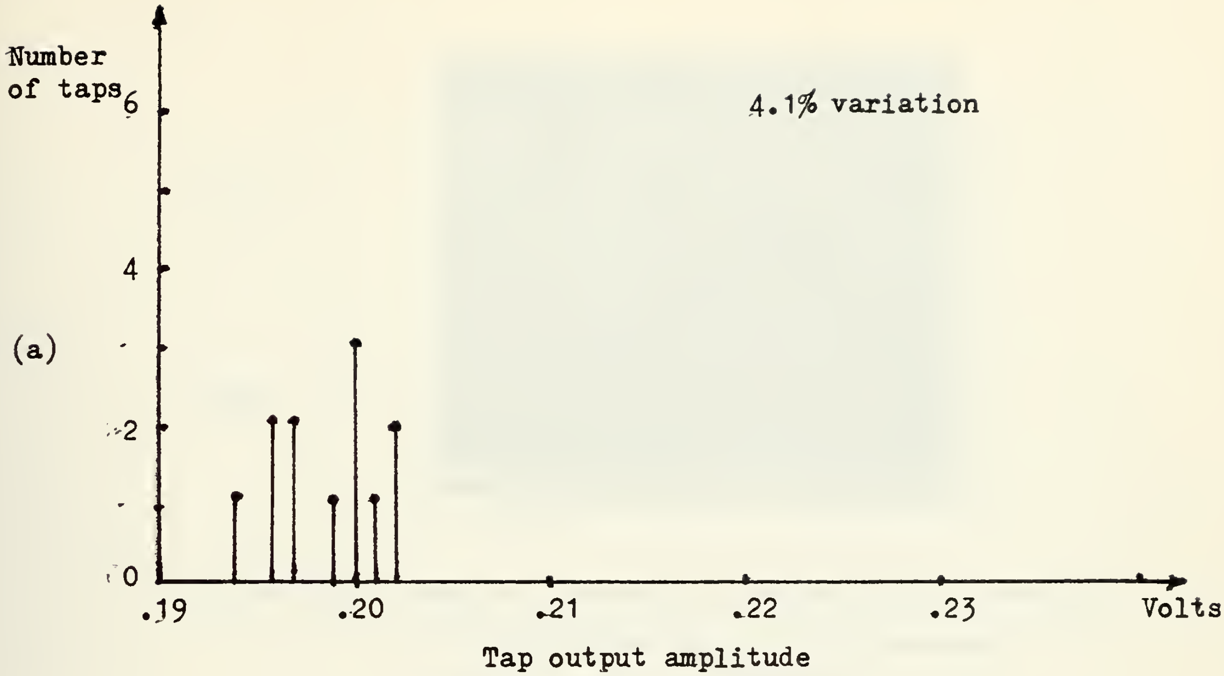


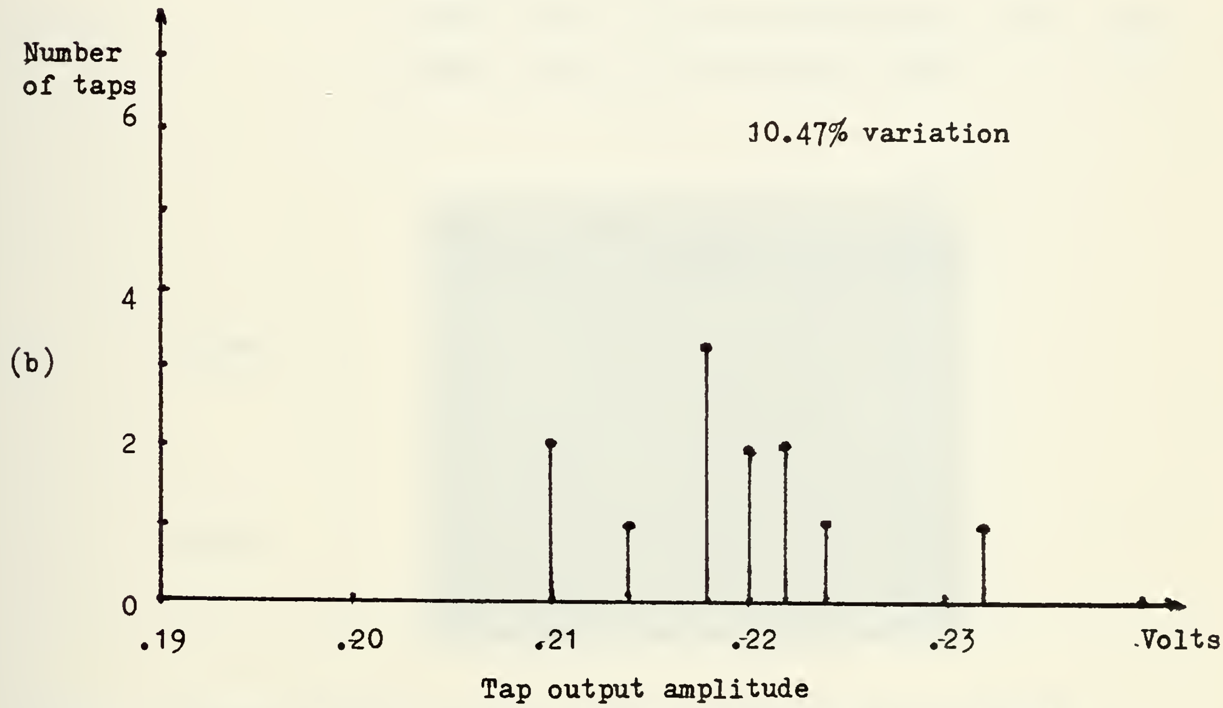


FIGURE 3.49 Non Uniformity Data. Tapping Resistors=10 Kilo-ohms

(a) Input Pulse: Amplitude=1.1 Volt, Width=.6 microsec. $F_{samp}$=500 KHz

(b) Input Pulse: Amplitude=1.1 Volt, Width=.3 microsec. $F_{samp}$=1.25 MHz

Output

Input

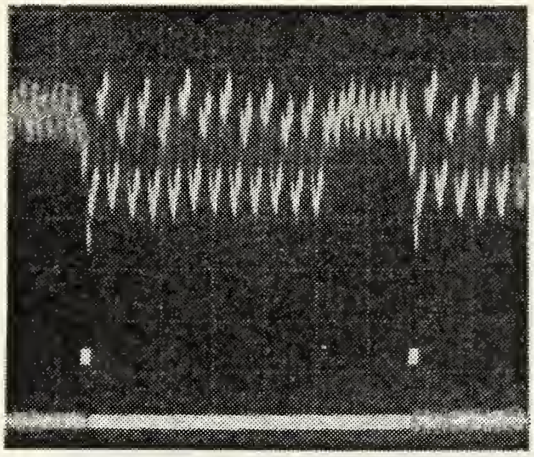

FIGURE 3.50 Impulse Response of Reticon TAD-12 showing 12 Tap Outputs. $R_{tap}$ = 10 Kilo-ohms. Sampling Frequency = 50 KHz. Upper Scale: H = 50 microsec./div; V= .5 V/div Lower Scale: H = 50 microsec./div; V = 1 V/div

Output

Input

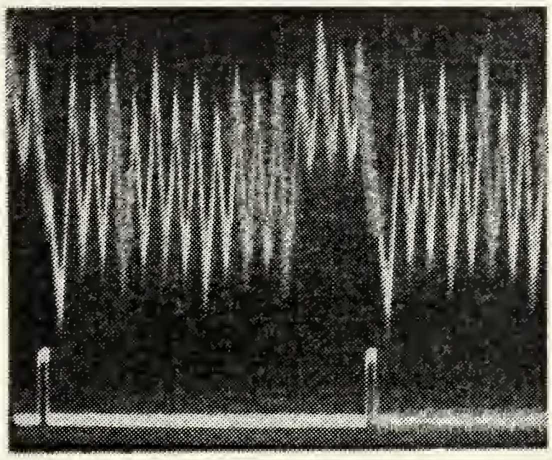

FIGURE 3.51 Impulse Response of Reticon TAD-12 Showing 12 Tap Outputs. $R_{tap}$ = 10 Kilo-ohms. Sampling Frequency = 1.25 MHz. Upper Scale: H = 2 microsec./div; V = .2 V/div Lower Scale: H = 2 microsec.div/; V = 1 V/div

Output

Tap #1 Jittering Waveform

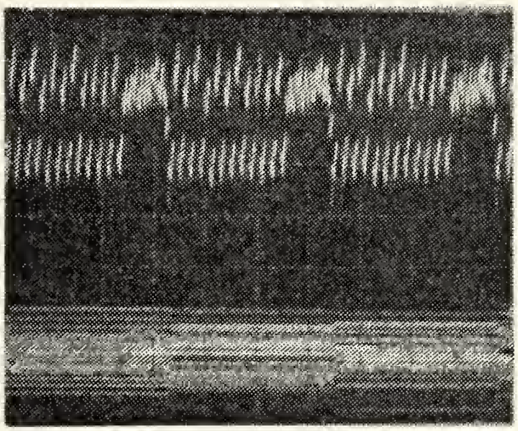

FIGURE 3.52 Upper Trace: Impulse Response of 12 Tap Outputs
Scale: H = .1 msec./div; V = .05 V/div
Lower Trace: Jittering Waveform of Tap #1
Scale: H = .1 msec./div; V = .02 V/div
Sampling Frequency = 50 KHz
Tapping Resistance = 10 Kilo-ohms.

## IV. INVESTIGATION OF FILTER I - PREWHITENING FILTER

### A. THEORY

Based on the design algorithm described in II.D.1, a computer program shown in Appendix A is written to give the impulse response of the prewhitening filter for the required frequency characteristics. Using this program, a prewhitening filter is designed for the following conditions:

$f_o = 2.1$ KHz $\qquad f_p = 1/2\ f_s = 625$ KHz

$R = 0.1$ $\qquad$ Slope $A = 1$

Length of filter: $M = 11$ taps

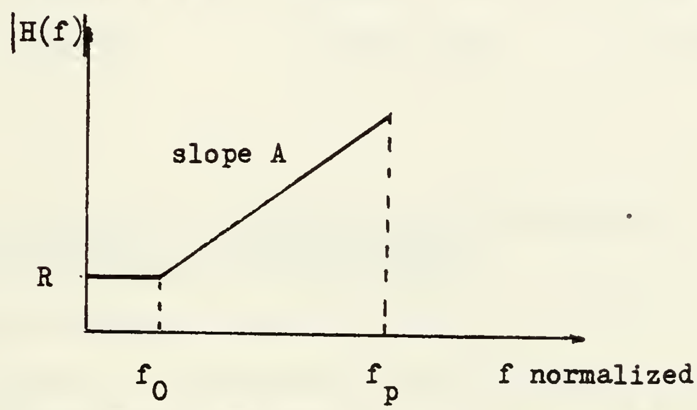


The tapping coefficients improved by Hamming window are listed in Table IV.I.

The magnitude frequency response of the theoretical prewhitening filter is shown in Figure 4-1. It is plotted in linear scale on Y-axis versus normalized frequencies, $f/f_s$ on X-axis.

TABLE IV.I Theoretical Tapping Coefficients & Resistors

| k | $A_k$ | $R_k$ (Kilo-ohms) | $A_k$ Measured |
|---|---|---|---|
| -5 | -0.00091 | -16478.516 | 0.02564 |
| -4 | 0.0 | open | 0.15385 |
| -3 | -0.01219 | -1225.517 | 0.05128 |
| -2 | 0.0 | open | 0.0 |
| -1 | -0.21407 | -65.005 | -0.23076 |
| 0 | 1. | 10. | 1. |
| 1 | -0.21427 | -65.005 | -0.19231 |
| 2 | 0.0 | open | 0.02564 |
| 3 | -0.01219 | -1225.517 | 0.02564 |
| 4 | 0.0 | open | 0.02566 |
| 5 | -0.00091 | -16478.516 | -0.07692 |

## B. EXPERIMENT

### 1. Tapping Resistors According to Theoretical Design with $R_{min} \simeq 10$ Kilo-ohms

A minimum value of 10 Kilo-ohms is set for the tapping resistances. Appendix F indicates the following expression for $R_k$,

$$R_k = (10\,K + r)\left(\frac{A_{max}}{|A_k|}\right) - r$$

where r is the internal output resistance. For the TAD-12, r is about 5 Kilo-ohms. The tapping resistors corresponding to the designed prewhitening filter are given in Table IV.1 and used to implement the filter using the 11 taps of

Reticon TAD-12. Since their theoretical coefficients $A_k$ for k higher than 5 have negligible values, the implementation of the filter on a longer delay line, number of taps higher than 11, is not necessary.

The measured impulse response of this filter is illustrated in Figure 4-2 at three different sampling frequencies:

$$f_s = 50 \text{ KHz}, 500 \text{ KHz}, 1.25 \text{ MHz}$$

The pulse inputs used have the amplitude and width listed in Table IV.II.

TABLE IV.II <u>Pulse Inputs</u>

| $f_s$ | Amplitude | Width |
|---|---|---|
| 50 KHz | 1.5 V | 8 microsec. |
| 500 KHz | 1.5 V | .8 microsec. |
| 1.25 MHz | 1.5 V | .3 microsec. |

Using the sample and hold circuit, the impulse response, $A_k$ is measured and the result is listed in Table IV.1. The $A_k$ measured and the theoretical $A_k$ are quite different for some taps. The maximum deviation occurs between tap #7 and #8 outputs. Its peak amplitude is about 30% of the output at tap #6.

The theoretical magnitude frequency response and measured response curves for three different sampling frequencies are plotted on Figure 4-3. The response curves for $f_s$ of 1.25 MHz and 500 KHz show some wiggling shape due probably to the non-uniformity of tap output and the clock

noise which cause the unsymmetrical tapping coefficients. The response curve for $f_s$ equal to 50 KHz is rather satisfactory if it is multiplied by a factor of 1.07.

2. Tapping Resistors Adjusted to Yield Better Impulse Response. $R_{min}$ = 10 Kilo-ohms

Since only three taps have strong contribution to the filter, the adjustment is done only on the taps #5, #6, #7 by using the sample and hold circuit. The other taps are left open. The tapping resistors used are listed in Table IV.III.

TABLE IV.III. Tapping Resistors

| k | $A_k$ | $R_k$ (Kilo-ohms) $f_s$ = 50 KHz | $f_s$ = 500 KHz | $f_s$ = 1.25 MHz |
|---|---|---|---|---|
| -1 | -0.21427 | 28 | 50 | 52 |
| 0 | 1. | 10 | 10 | 10 |
| 1 | -0.21427 | 28 | 35 | 100 |

The amplitude and width of inputs pulse are listed in Table IV.II.

The impulse response of this filter is illustrated in Figure 4-4, at three different sampling frequencies.

The theoretical and measured curves of prewhitening filter magnitude frequency response are shown in Figure 4-5. The response curves for $f_s$ equal to 50 KHz, 500 KHz and 1.25 MHz still show some wiggling. The gain of these curves are lower than the last curves in Figure 4-3. If these three curves are multiplied by a factor of 1.22, they are somewhat satisfactory in comparison with the theoretical curve.

3. <u>Tapping Resistors Adjusted to Yield Better Impulse Response. $R_{min}$ = 50 ohms</u>

A minimum value of 50 ohms is set for the tap #6. The taps #5 and #7 are adjusted by using sample and hold circuit, to yield better impulse response. The other taps are left open. The tapping resistors used are listed in Table IV.IV.

TABLE IV.IV. Tapping Resistors

| k | $A_k$ | $R_k$ (Kilo-ohms) $f_s$ = 50 KHz | $f_s$ = 500 KHz | $f_s$ = 1.25 MHz |
|---|---|---|---|---|
| -1 | -0.21427 | 4.8 | 2.8 | 3.8 |
| 0 | 1. | 0.05 | 0.05 | 0.05 |
| 1 | -0.21427 | 2.8 | 1.8 | 11.5 |

The pulse inputs used have the amplitudes and widths listed in Table IV.II.

Figure 4-6 illustrates the impulse response of the filter at sampling frequencies:

$$f_s = 50 \text{ KHz}, 500 \text{ KHz}, 1.25 \text{ MHz}$$

The theoretical and measured curves of prewhitening filter magnitude frequency response are shown in Figure 4-7. The wiggling of the three measured curves is much reduced in comparison with the previous curves. If the experimental curve $f_s$ = 1.25 MHz is multiplied by a factor of 1.2 and curves $f_s$ = 50 KHz, 500 KHz multiplied by a factor of 1.35, the agreement is somewhat satisfactory.

4. Tapping Resistors Obtained by Experimental Cut & Try Based on Frequency Response Adjustment

The procedure consists of the use of a chirped waveform from DC to 1 MHz as the input of the filter, and adjust the displayed frequency response to get the minimum wiggling by adjusting the tapping resistances. The result obtained is shown in Figure 4-9. The wiggling of the three response curves is much reduced. Raising these curves by a factor of 1.27 can improve the agreement between the theoretical and measured curves.

The impulse response corresponding to these curves is unsymmetrical and has the values listed in Table IV.V.

TABLE IV.V Tapping Coefficients

| k | $A_k$ | $R_k$ (Kilo-ohms) |
|---|---|---|
| -1 | -0.1694 | 24.812 |
| 0 | 1. | .05 |
| 1 | -1 | .05 |

The amplitude and width of pulse inputs used are listed in Table IV.II.

FIGURE 4.1 Theoretical Amplitude Frequency Response of Prewhitening Filter. Length = 11. Hamming window.
X - Scale = .1 units/inch for normalized frequency
Y - Scale = .2 units/inch for Amplitude frequency response.

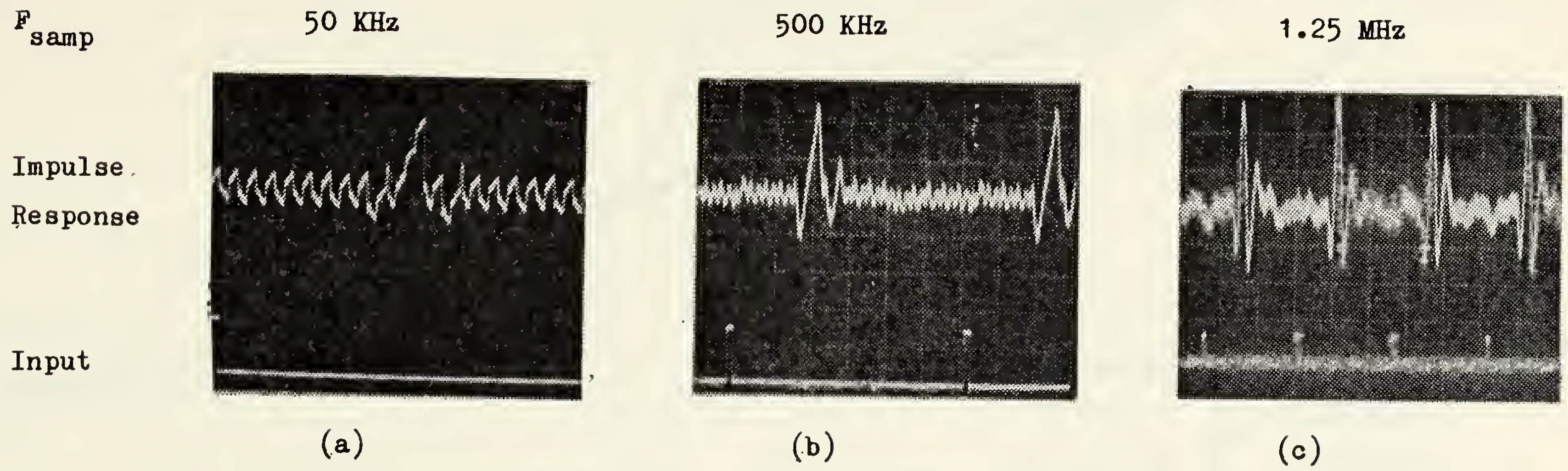


FIGURE 4.2 Impulse Response of Prewhitening Filter with Tapping Resistors According to Theoretical Design. $R_{min}$ = 10 Kilo-ohms.

(a) Upper Scale: H=20 microsec./div. V=.05 V/div.; Lower Scale: H=20 microsec./div. V=1 V/div

(b) Upper Scale: H=5 microsec./div. V=.02 V/div.; Lower Scale: H=5 microsec./div. V=1 V/div

(c) Upper Scale: H=.3 microsec./div. V=1.5 V/div.; Lower Scale: H=5 microsec./div. V=2 V/div

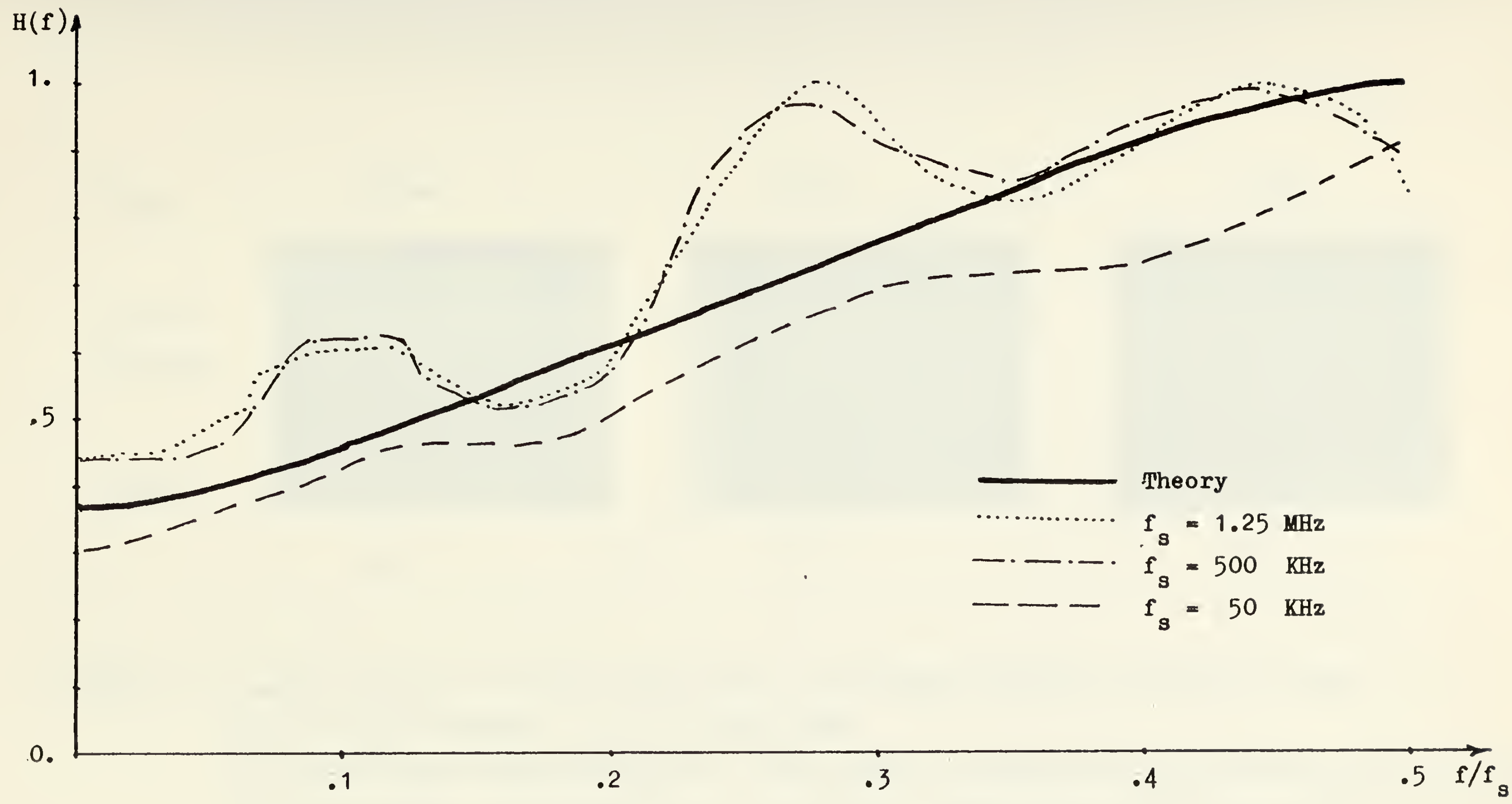


FIGURE 4.3 Prewhitening Filter Magnitude Frequency Response.
Tapping Resistors According to Theoretical Design. $R_{min}$ = 10 Kilo-ohms

| $F_{samp}$ | 50 KHz | 500 KHz | 1.25 MHz |
| --- | --- | --- | --- |

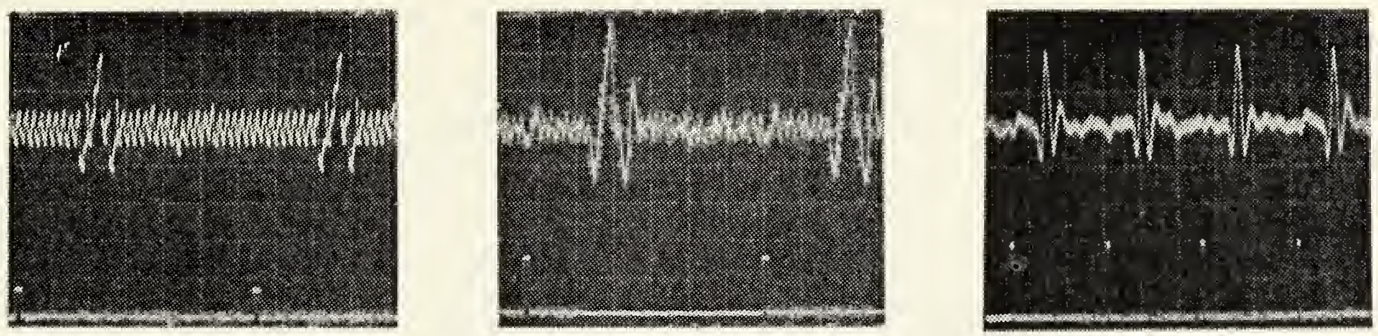


(a) (b) (c)

FIGURE 4.4 Impulse Response of Prewhitening Filter with Tapping Resistors Adjusted to Yield Better Impulse Response. $R_{min}$= 10 Kilo-ohms.

(a) Upper Scale: H=50 microsec./div. V=.05 V/div.; Lower Scale: H=50 microsec./div, V=2 V/div

(b) Upper Scale: H=5 microsec./div. V=.02 V/div.; Lower Scale: H=5 microsec./div. V=1 V/div

(c) Upper Scale: H=5 microsec./div. V=.02 V/div.; Lower Scale: H=5 microsec./div. V=1 V/div

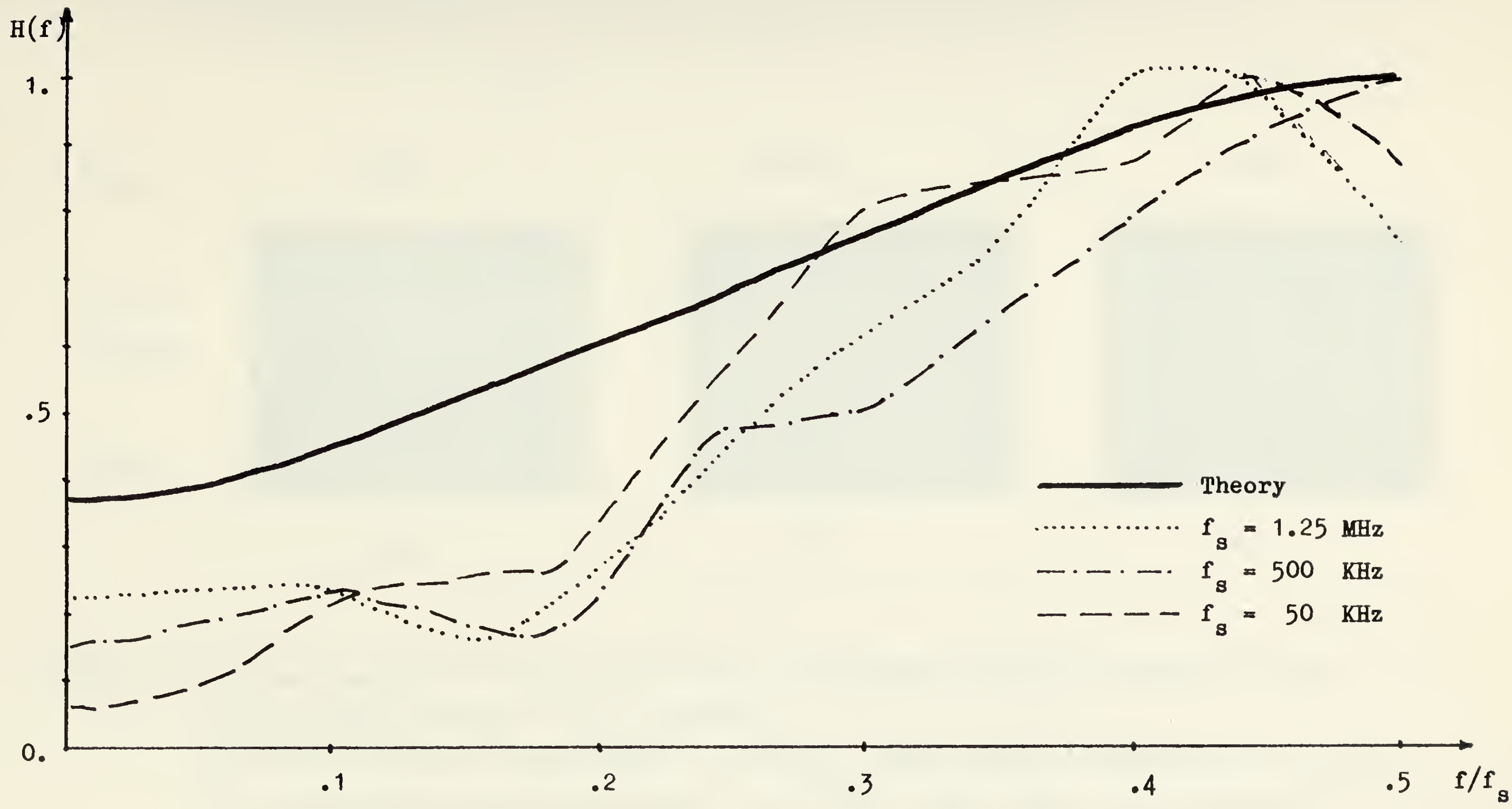


FIGURE 4.5 Prewhitening Filter Magnitude Frequency Response.
Tapping Resistors Adjusted to Yield Better Impulse Response. $R_{min}$ = 10 Kilo-ohms

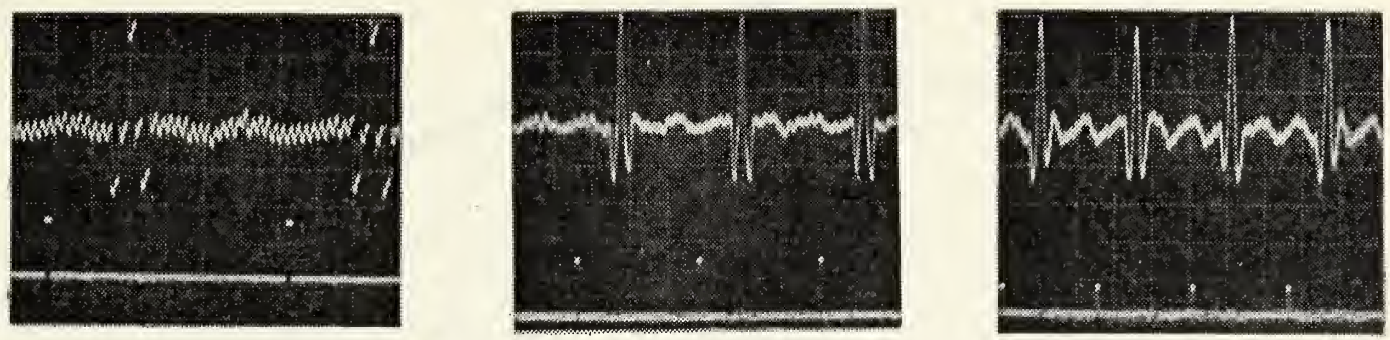


FIGURE 4.6 Impulse Response of Prewhitening Filter with Tapping Resistors Adjusted to Yield Better Impulse Response. $R_{min}$ = 50 ohms.

(a) Upper Scale: H=.1 msec./div. V=.1 V/div.; Lower Scale: H=.1msec./div. V=1 V/div

(b) Upper Scale: H=10 microsec./div. V=.1 V/div.; Lower Scale: H=10 microsec./div. V=2 V/div

(c) Upper Scale: H=5 microsec./div. V=.5 V/div.; Lower Scale: H=5 microsec./div. V=2 V/div

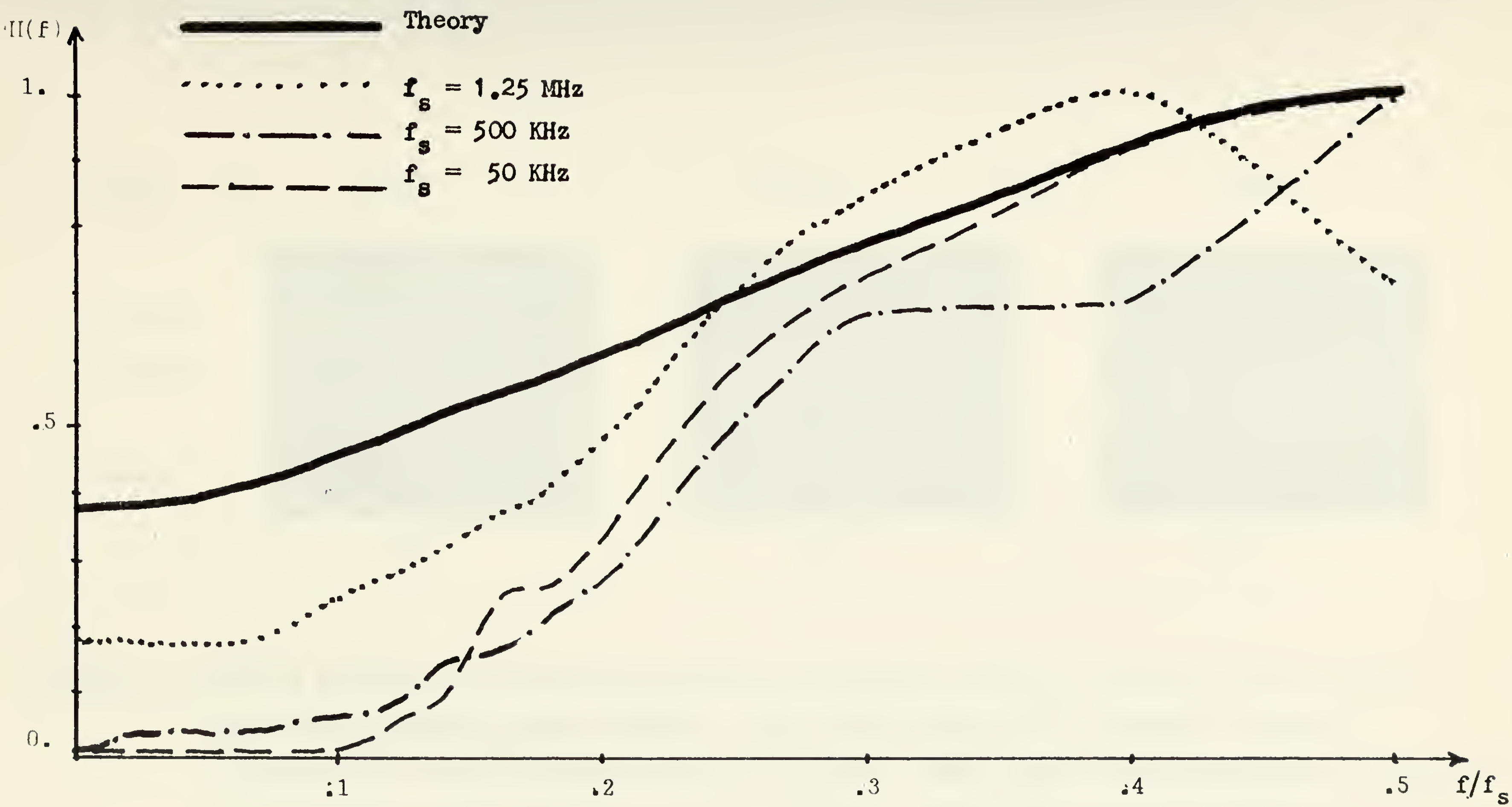


FIGURE 4-7 Prewhitening Filter Magnitude Frequency Response.

Tapping Resistors Adjusted to Yield Better Impulse Response. $R_{min}$ = 50 ohms

$F_{samp}$ 50 KHz 500 KHz 1.25 MHz

Impulse Response

Input

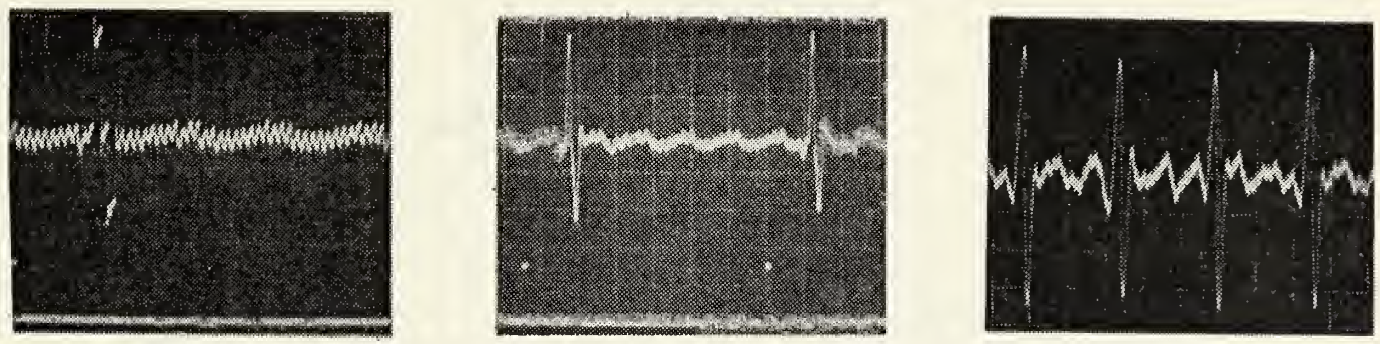

(a) (b) (c)

FIGURE 4.8 Impulse Response of Prewhitening Filter with Tapping Resistors obtained by cut and try based upon Frequency Domain Response. Input Pulse: Ampl.=1.5 V, Width=.3 microsec.

(a) Upper Scale: H=50 microsec./div. V=.1 V/div.; Lower Scale: H=10 microsec./div. V=1 V/div

(b) Upper Scale: H=10 microsec./div. V=.1 V/div.; Lower Scale: H=10 microsec./div. V=1 V/div

(c) Scale: H=5 microsec./div. V=.1 V/div.

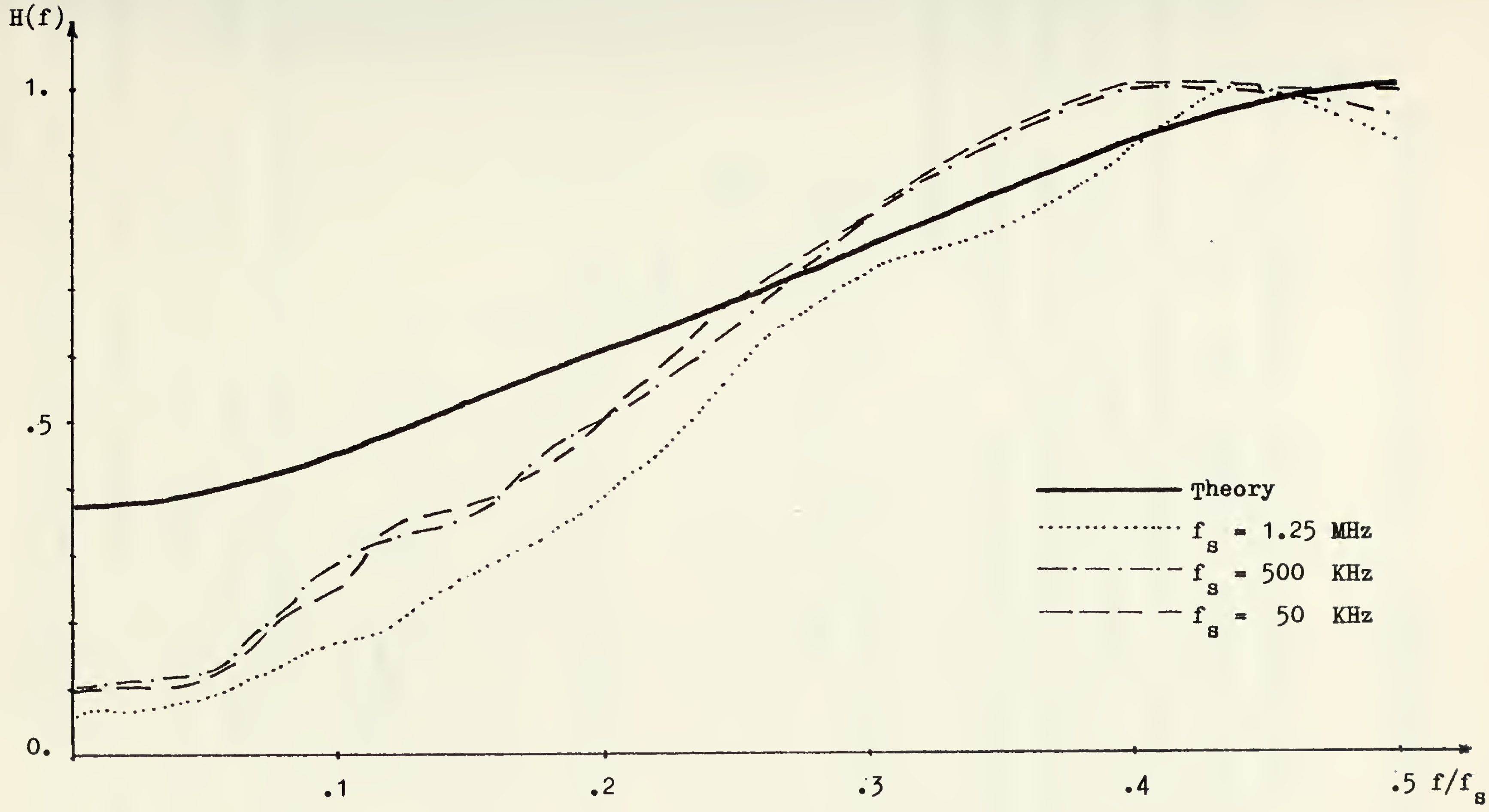


FIGURE 4.9 Prewhitening Filter Magnitude Frequency Response.
Tapping Resistors Obtained by Cut and Try Based on Frequency Domain Response.

# V. INVESTIGATION OF FILTER II - DEWHITENING FILTER

## A. THEORY

The design algorithm of the dewhitening filter is described in II.D.2. The computer program in Appendix B is used to calculate the impulse response of the filter from the given frequency response. A dewhitening filter is designed, based on the impulse response of the prewhitening filter of paragraph IV.A. The frequency characteristics are the following:

$f_o = 2.1$ KHz $\qquad f_p = \frac{1}{2} f_s = 625$ KHz

Length of filter $M = 11$ taps

$\frac{1}{R} = 10$

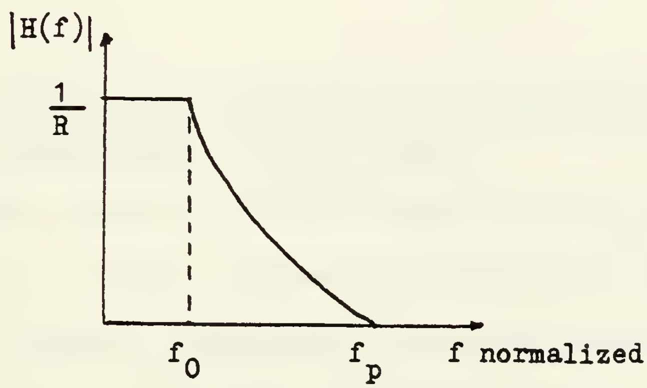


The tapping coefficients are improved by a Hamming window and by a factor of 1.13 and are listed in Table V.I.

The magnitude frequency response of the theoretical prewhitening filter is shown in Figure 5.1. It is plotted in linear scale on Y-axis versus normalized frequencies, $f/f_s$ on X-axis.

TABLE V.I. Theoretical Tapping Coefficients & Resistors

| k | $A_k$ theor. | $R_k$ (Kilo-ohms) with $R_{min}$ = K ohms | $R_k$ (Kilo-ohms) with $R_{min}$ = 50 ohms |
|---|---|---|---|
| -5 | 0.00113 | 13269.336 | 4464.026 |
| -4 | 0.00632 | 2368.417 | 794.050 |
| -3 | 0.01156 | 1292.577 | 431.851 |
| -2 | 0.04846 | 304.661 | 99.252 |
| -1 | 0.19681 | 71.215 | 20.659 |
| 0 | 1. | 10. | .05 |
| 1 | 0.19681 | 71.215 | 20.659 |
| 2 | 0.04844 | 304.661 | 99.252 |
| 3 | 0.01156 | 1292.577 | 431.851 |
| 4 | 0.00632 | 2368.417 | 794.050 |
| 5 | 0.00113 | 13269.336 | 4464.026 |

## B. EXPERIMENT

### 1. Tapping Resistors According to Theoretical Design with $R_{min}$ = 10 Kilo-ohms

A minimum value of 10 Kilo-ohms is set for the tapping resistors. Using the expression of $R_k$ given in Appendix F, the tapping resistances are calculated and listed in Table V.I in the third column. They are used to implement the dewhitening filter using 11 taps of Reticon TAD-12.

The impulse response of this filter is illustrated in Figure 5-2 at three different sampling frequencies:

$$f_s = 50 \text{ KHz}, 500 \text{ KHz}, 1.25 \text{ MHz}.$$

TABLE V.II Theoretical & Measured Coefficients

| k | $A_k$ theor. | $A_k$ Measured $f_s$ = 50 KHz | $f_s$ = 500 KHz | $f_s$ = 1.25 MHz |
|---|---|---|---|---|
| -5 | 0.00113 | 0.16216 | 0.10869 | 0.11667 |
| -4 | 0.00632 | 0.16216 | 0.17391 | 0.20830 |
| -3 | 0.01156 | 0.16216 | 0.15217 | 0.25 |
| -2 | 0.04844 | 0.2027 | 0.19565 | 0.2708 |
| -1 | 0.19681 | 0.39119 | 0.41304 | 0.41667 |
| 0 | 1. | 1. | 1. | 1. |
| 1 | 0.19681 | 0.39189 | 0.39130 | 0.41667 |
| 2 | 0.04844 | 0.18918 | 0.13043 | 0.0 |
| 3 | 0.01156 | 0.16216 | 0.13043 | 0.16667 |
| 4 | 0.00632 | 0.17567 | 0.13043 | 0.16667 |
| 5 | 0.00113 | 0.16216 | 0.10869 | 0.16667 |

The impulse inputs are noted in Table IV.II for different sampling frequencies. The tapping coefficients are measured with the sample and hold circuit and the results are listed in Table V.II. The theoretical and measured $A_k$ are quite different for some taps due to the fixed pattern noise and non-uniformity of tap outputs. The maximum noise amplitude is observed before the tap #1 output and has amplitude of about 30% of $A_0$.

The theoretical magnitude frequency response and measured response for three different sampling frequencies are plotted in Figure 5-3. The response curves for $f_s$ of 500 KHz and 1.25 MHz are somewhat in agreement with the

theoretical curve. Their difference is about 12% for f less than 0.2 $f_s$ and it becomes worse than 40% for input signal frequency higher than 0.25 $f_s$. For $f_s$ of 50 KHz, the result is quite satisfactory.

2. <u>Tapping Resistors Adjusted to Yield Better Impulse Response. $R_{min}$ = 10 Kilo-ohms</u>

Since the coefficients, $A_k$ for k greater than 3, have negligible values in comparison with the noise, the adjustment is done only on seven tap outputs. The adjustment is quite delicate for the tap outputs which are greater than or equal to 5, because of the interaction between them. Experimental tap resistances are listed in Table V.III. A slight modification has to be done on the values of some tap resistors in order to get better impulse responses for different sampling frequencies. The sample and hold circuit is used to make the adjustment.

The amplitude and width of inputs pulse used are listed in Table IV.II.

The impulse response of this filter is illustrated in Figure 5-4 at three different sampling frequencies. The maximum noise occurs near tap #1 output; its peak amplitude is about 19% of $A_o$.

The theoretical and measured curves of dewhitening filter magnitude frequency response are shown in Figure 5-5. The wiggling of the response curves is reduced in comparison with the curves in Figure 5-3, but the difference between the theoretical and measured curves ($f_s$ = 1.25 MHz and 500 KHz)

is still high, greater than 30%, for the input signal frequency f higher than 0.25 $f_s$. At low sampling frequency, 50 KHz, the result is quite satisfactory.

TABLE V.III. Adjusted Coefficients & Resistors

| k | $A_k$ $f_s$=50 KHz | $f_s$=500 KHz | $f_s$=1.25MHz | $R_k$ $f_s$=50 KHz | $f_s$=500 KHz | $f_s$=1.25MHz |
|---|---|---|---|---|---|---|
| -5 | 0.09836 | 0.02083 | 0.125 | 13269. | 13269. | 13269. |
| -4 | 0.10655 | 0.02083 | 0.1 | 2368. | 2368. | 2368. |
| -3 | 0.10655 | 0.04167 | 0.075 | 1292.5 | 1292.5 | 1292.5 |
| -2 | 0.09836 | 0.0625 | 0.075 | 300. | 300. | 300. |
| -1 | 0.18852 | 0.20833 | 0.175 | 110. | 109. | 110. |
| 0 | 1. | 1. | 1. | 5. | 9.5 | 5. |
| 1 | 0.18852 | 0.20833 | 0.2 | 110 | 110. | 110. |
| 2 | 0.09836 | 0.0625 | 0.1 | 311. | 311. | 320. |
| 3 | 0.10655 | 0.02083 | 0.075 | 1292.5 | 1295.5 | 1292.5 |
| 4 | 0.11675 | 0.02083 | 0.075 | 2368. | 2368. | 2368. |
| 5 | 0.10655 | 0.02083 | 0.075 | 13269. | 13269. | 13269. |

### 3. Tapping Resistors According to Theoretical Design. $R_{min}$ = 50 ohms.

A minimum value of 50 ohms is set for the tap #6. Using the formula described in Appendix F, one can calculate the theoretical tapping resistances whose values are listed in the fourth column of Table V.I.

The input pulses have the amplitude and width listed in Table IV.II. Figure 5-6 illustrates the impulse response

of the filter at sampling frequencies:

$$f_s = 50 \text{ KHz}, 500 \text{ KHz}, 1.25 \text{ MHz}$$

The measured coefficients $A_k$ are listed in Table V.IV:

TABLE V.IV. Measured Coefficients ($R_{min}$ = 50 ohms)

| k | $A_k$ $f_s$=50 KHz | $f_s$=500 KHz | $f_s$=1.25 MHz |
|---|---|---|---|
| -5 | 0.11111 | 0.06667 | 0.22826 |
| -4 | 0.11111 | 0.06667 | 0.08695 |
| -3 | 0.11111 | 0.06667 | 0.09782 |
| -2 | 0.16667 | 0.13333 | 0.15217 |
| -1 | 0.27778 | 0.26667 | 0.34782 |
| 0 | 1. | 1. | 1. |
| 1 | 0.22223 | 0.26667 | 0.48913 |
| 2 | 0.13888 | 0.13333 | 0.20652 |
| 3 | 0.11111 | 0.06667 | 0.13043 |
| 4 | 0.11111 | 0.06667 | 0.04347 |
| 5 | 0.11111 | 0.06667 | 0.07608 |

The maximum peak amplitude of noise measured is about 13% of $A_o$ for $f_s$ equal to 1.25 MHz and 500 KHz and 19% of $A_o$ for $f_s$ equal to 100 KHz.

The theoretical and measured curves of dewhitening filter magnitude frequency response are shown in Figure 5-7. The response curve for $f_s$ equal to 50 KHz is similar to the theoretical one. The curves $f_s$ equal to 1.25 MHz and 500 KHz have some wiggling effect for input frequencies higher than .29 $f_s$.

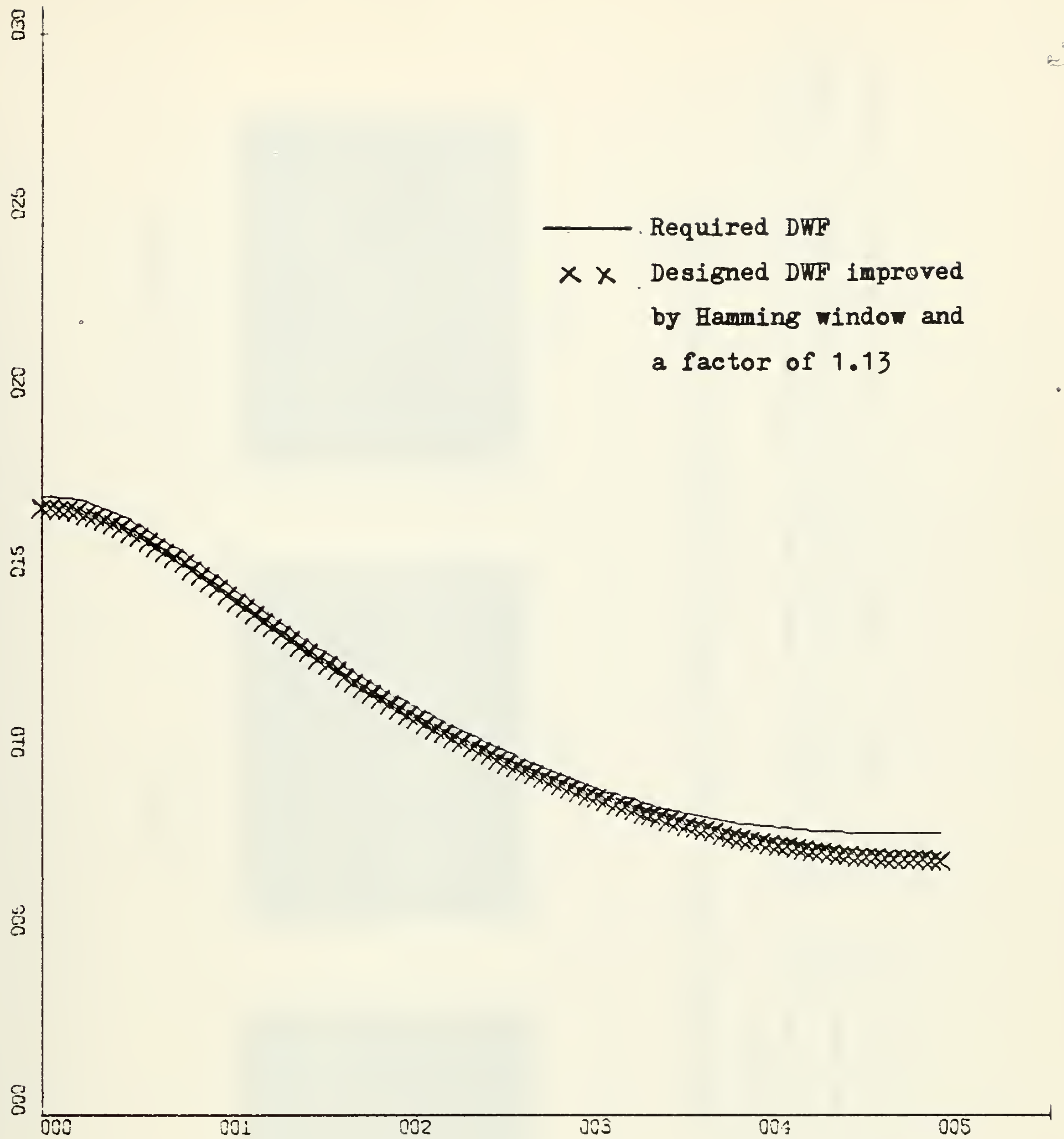


FIGURE 5.1 Amplitude Frequency Response of Dewhitening Filter.
Length = 11 / Hamming window
X - Scale = .1 units/inch for normalized frequency
Y - Scale = .5 units/inch for amplitude frequency response.

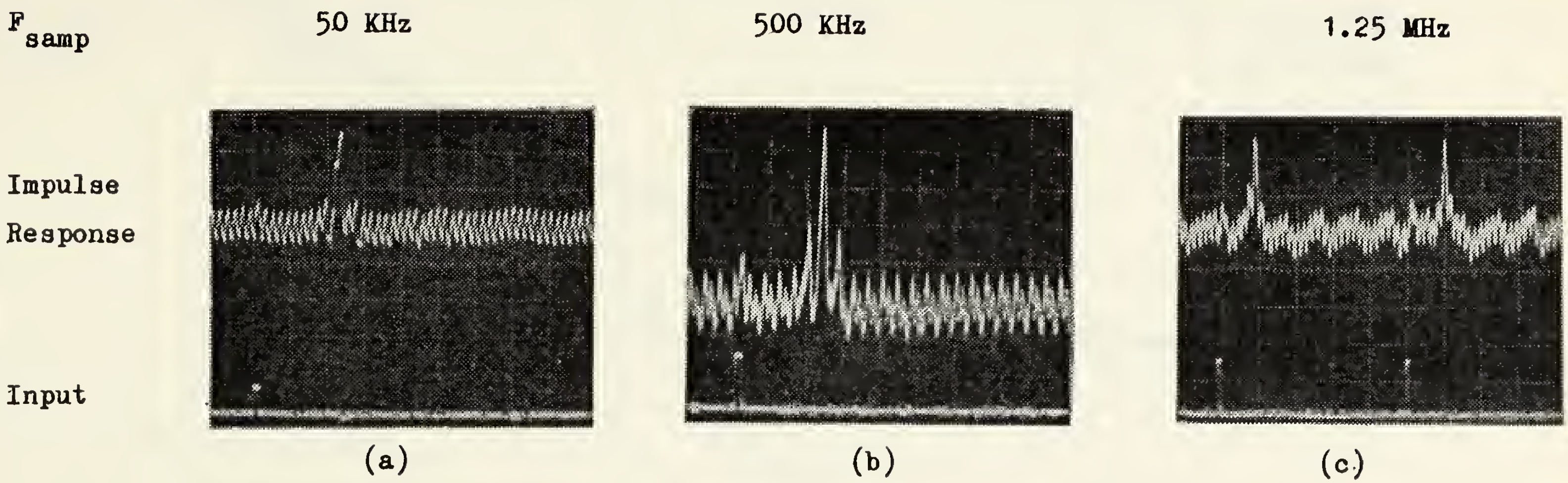


FIGURE 5.2 Impulse Response of Dewhitening Filter. Tapping Resistors According to Theoretical Design. $R_{min}$ = 10 Kilo-ohms.

(a) Upper Scale:H=50 microsec./div. V=.05 V/div.; Lower Scale: H=50 microsec./div. V=1 V/div

(b) Upper Scale: H=5 microsec./div. V=.01 V/div.; Lower Scale: H=5 microsec./div. V=1 V/div

(c) Upper Scale: H=5 microsec./div. V=.01 V/div.; Lower Scale: H=5 microsec./div. V=1 V/div

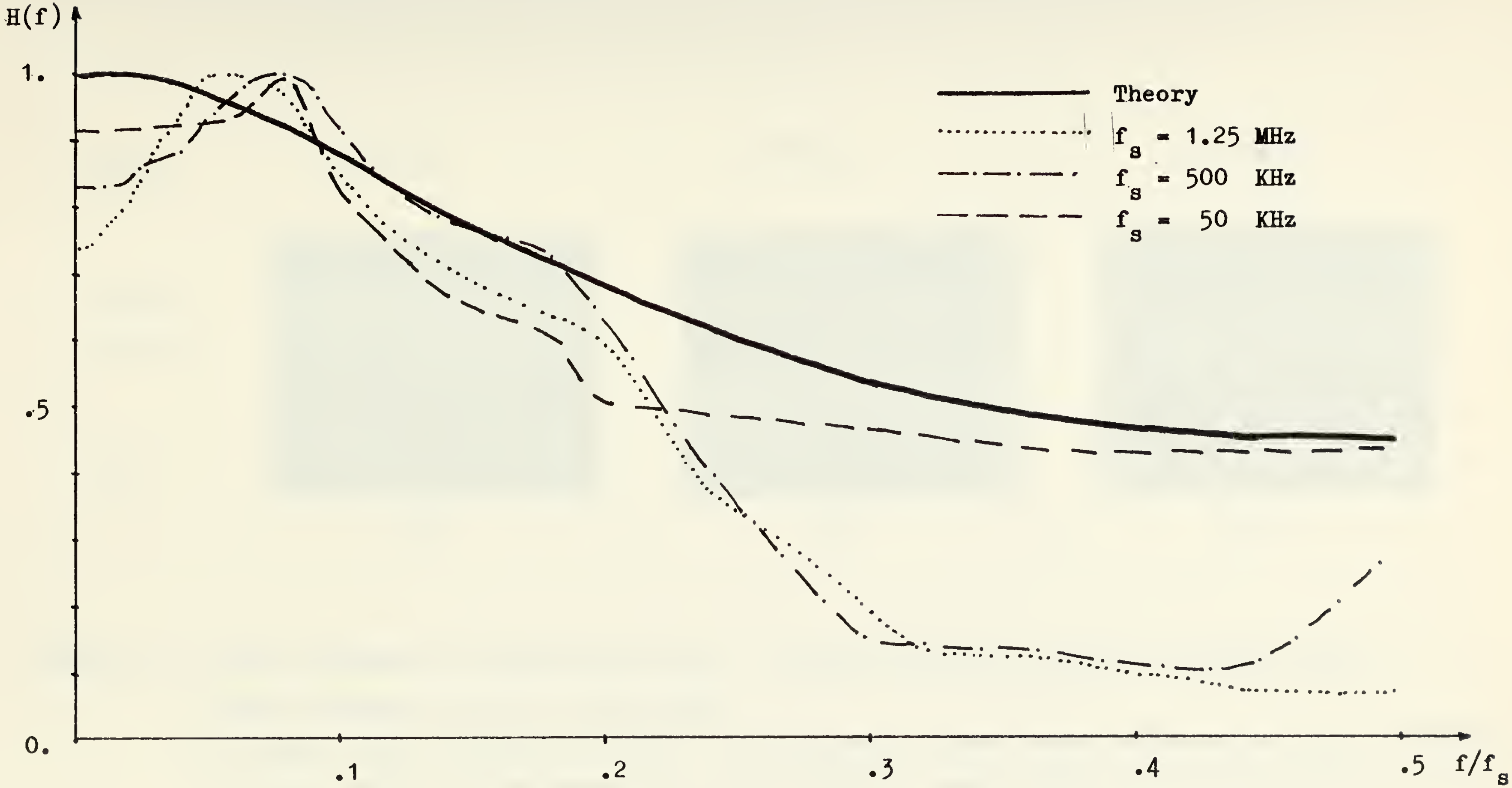


FIGURE 5.3 Dewhitening Filter Frequency Response.
Tapping Resistors According to Design. $R_{min}$ = 10 Kilo-ohms

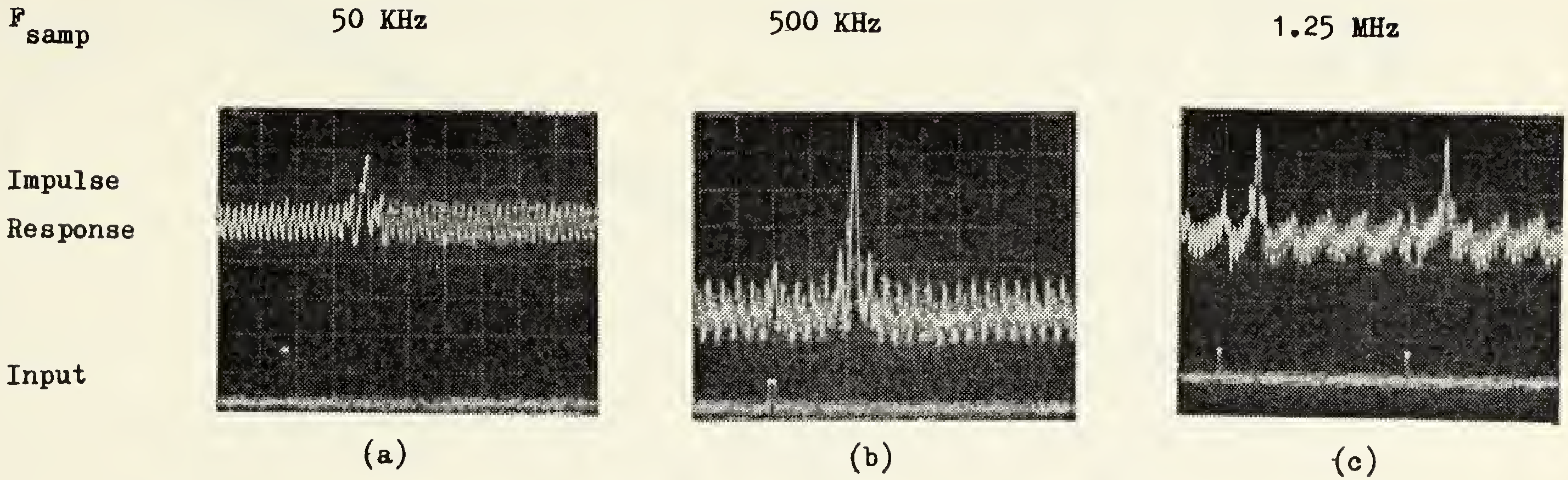


FIGURE 5.4 Impulse Response of Dewhitening Filter. Tapping Resistors Adjusted to Yield Better Impulse Response. $R_{min}$ = 10 Kilo-ohms.

(a) Upper Scale: H=50 microsec./div. V=.05 V/div.; Lower Scale: H=5 microsec./div. V=2 V/div

(b) Upper Scale: H=5 microsec./div. V=.01 V/div.; Lower Scale: H=5 microsec./div. V=2 V/div

(c) Upper Scale: H=5 microsec./div. V=.01 V/div.; Lower Scale: H=5 microsec./div. V=2 V/div

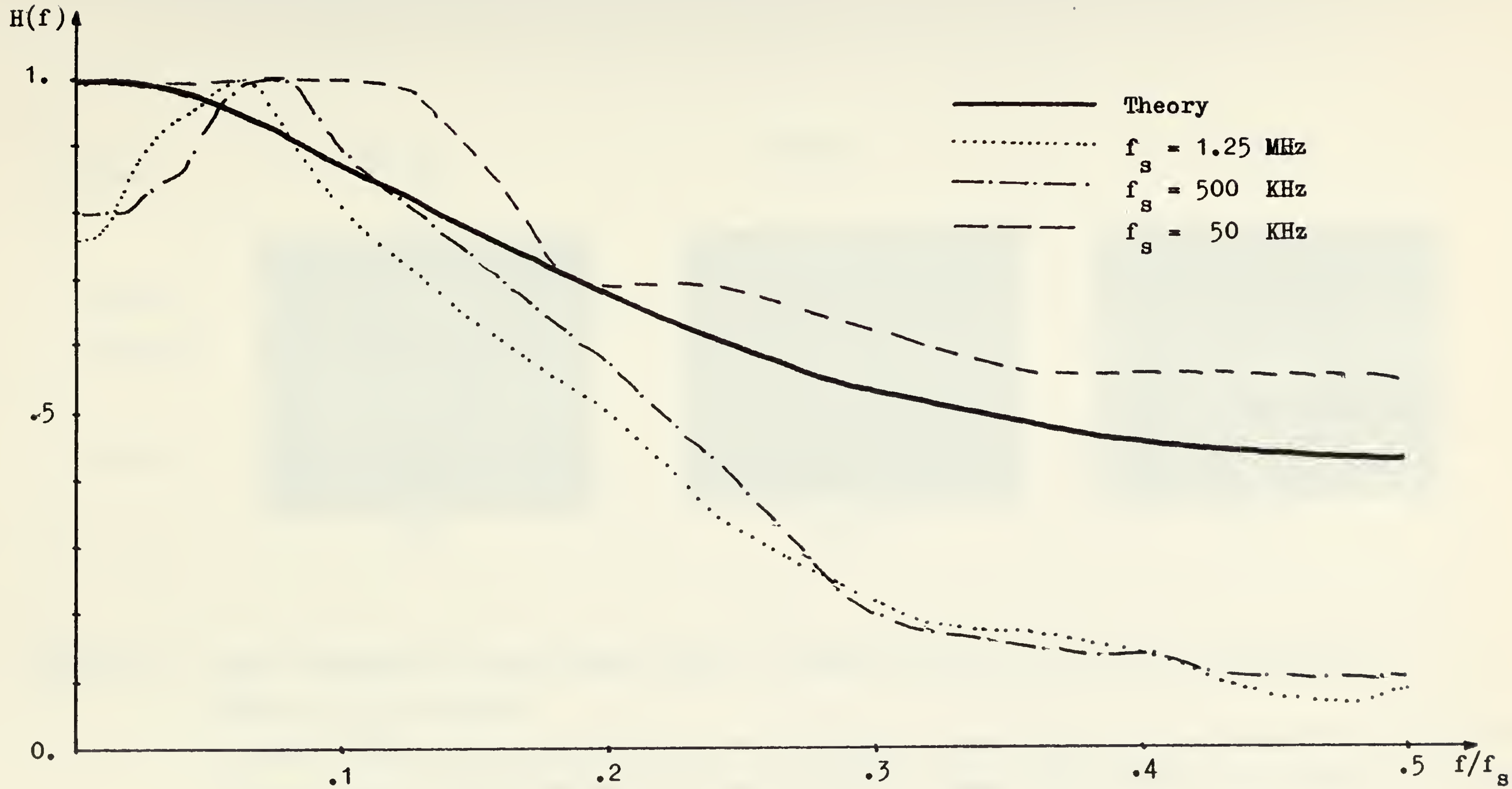


FIGURE 5.5 Dewhitening Filter Magnitude Frequency Response.
Tapping Resistors Adjusted to Yield Better Impulse Response . $R_{min}$ = 10 Kilo-ohms

$F_{samp}$ 50 KHz 500 KHz 1.25 MHz

Impulse Response

Input

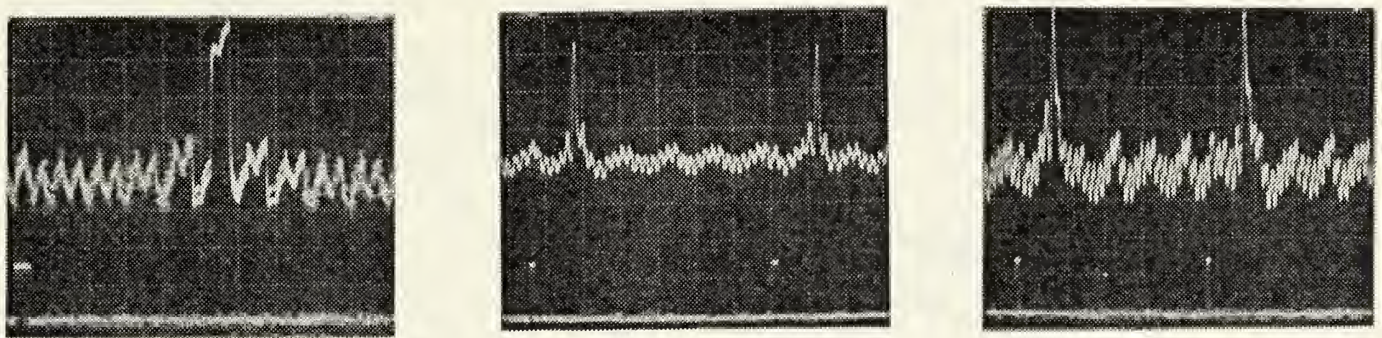

(a) (b) (c)

FIGURE 5.6 Impulse Response of Dewhitening Filter. Tapping Resistors According to Theoretical Design. $R_{min} = 50$ ohms.

(a) Upper Scale: H=20 microsec./div. V=.05 V/div.; Lower Scale: H=10 microsec./div. V=1 V/div

(b) Upper Scale: H=10 microsec./div. V=.05 V/div.; Lower Scale: H=10 microsec./div. V=1 V/div

(c) Upper Scale: H=5 microsec./div. V=.02 V/div.; Lower Scale: H=5 microsec./div. V=1 V/div

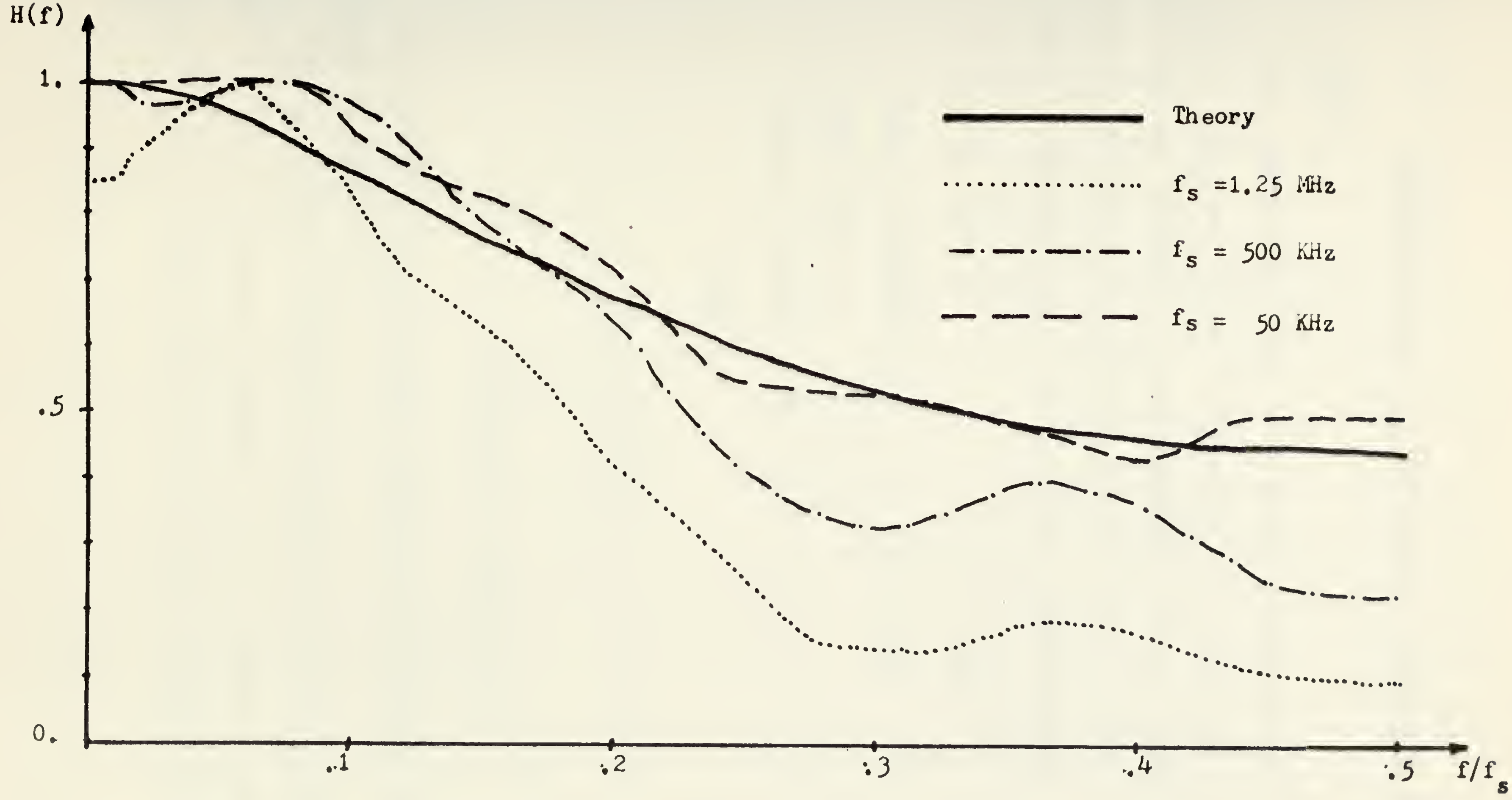


FIGURE 5-7 Dewhitening Filter Magnitude Frequency Response.

Tapping Resistors According to Theoretical Design. $R_{min}$ = 50 ohms

# VI. INVESTIGATION OF FILTER III - BANDPASS FILTER

## A. THEORY

Based upon the design algorithm described in II.D.3, a computer program shown in Appendix C is written to calculate the impulse response of the bandpass filter based on the required frequency response. Using this program, a bandpass filter is designed for the following conditions:

$f_1 = .1996$ $\qquad$ $f_2 = .2004$

Center frequency $f_o = .2$ $\qquad$ $Q = 250$

Amplitude $\qquad A = 1.$

Number of taps $\qquad M = 11.$

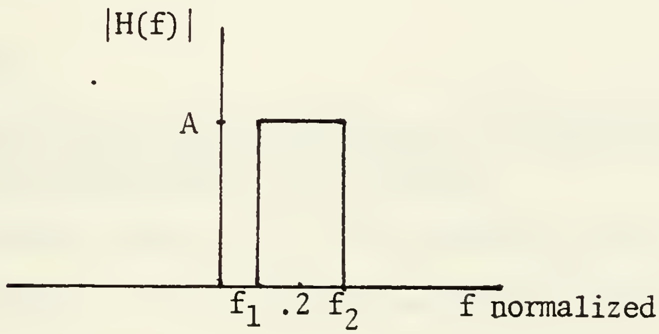


The tapping coefficients improved by Hamming window are listed in Table VI.I.

The magnitude frequency response of the theoretical bandpass filter is shown in Figure 6-1, in linear scale, and in Figure 6-2, in logarithmic scale versus normalized frequencies, $f/f_s$.

TABLE VI.I. Theoretical Coefficients and Resistors

| k | $A_k$ | $R_k(R_{min}=10\ k)$ | $R_k(R_{min}=.05\ k)$ |
|---|---|---|---|
| -5 | 0.09863 | 147.083 | 46.201 |
| -4 | 0.07378 | 198.307 | 63.447 |
| -3 | -0.38389 | 34.074 | 8.155 |
| -2 | -0.59148 | 20.360 | 3.538 |
| -1 | 0.28647 | 47.362 | 12.628 |
| 0 | 1. | 10. | .05 |
| 1 | 0.28647 | 47.362 | 12.628 |
| 2 | -0.59148 | 20.360 | 3.538 |
| 3 | -0.38389 | 34.074 | 8.155 |
| 4 | 0.07378 | 198.307 | 63.447 |
| 5 | 0.09863 | 147.083 | 46.201 |

## B. EXPERIMENT

### 1. Tapping Resistors According to Theoretical Design with $R_{min}$ = 10 K ohms.

A minimum value of 10 Kilo-ohms is set for the tapping resistors. The expression of $R_k$ given in Appendix F is used to calculate the tapping resistances. These values are listed in Table VI.I in the third column and are used to implement the bandpass filter using the 11 taps of Reticon TAD-12.

The impulse response of this filter is illustrated in Figure 6-3 at three different sampling frequencies:

$$f_s = 50\text{ KHz, } 500\text{ KHz, } 1.25\text{ MHz}$$

TABLE VI.II. Theoretical & Measured Coefficients

| k | $A_k$ Theor. | $A_k$ Measured $f_s$=50 KHz | $f_s$=500 KHz | $f_s$=1.25 MHz |
|---|---|---|---|---|
| -5 | 0.09863 | 0.34444 | 0.30508 | 0.34483 |
| -4 | 0.07378 | 0.33333 | 0.209339 | 0.06896 |
| -3 | -0.38389 | -0.5 | -0.66102 | -0.86306 |
| -2 | -0.59148 | -0.6 | -0.66102 | -0.51724 |
| -1 | 0.28647 | 0.48888 | 0.49152 | 0.72413 |
| 0 | 1. | 1. | 1. | 0.86206 |
| 1 | 0.28647 | 0.44444 | 0.54237 | 0.4 |
| 2 | -0.59148 | -0.65555 | -0.76271 | -1. |
| 3 | -0.38389 | -0.48888 | -0.71186 | -0.34482 |
| 4 | 0.07378 | 0.31111 | 0.13559 | 0.51724 |
| 5 | 0.09863 | 0.26666 | 0.13559 | 0.24138 |

The input pulses used are listed in Table IV.II for different sampling frequencies. The tapping coefficients measured with the sample and hold circuit are shown in Table VI.II. The theoretical and measured $A_k$ are quite different for some taps due to the fixed pattern noise and the non-uniformity of the tap outputs. The maximum noise observed occurs between tap #3 and #4 outputs. Its peak amplitude is about 30% of $A_o$.

The theoretical magnitude frequency response and measured response curves for three different sampling frequencies are plotted in Figure 6-4. The main lobes of measured response curves are rather similar to the theoretical one.

But there are some differences at the side lobes which have their peak magnitudes as follows:

- 15% of maximum amplitude for $f_s$ = 50 KHz
- 35% of maximum amplitude for $f_s$ = 500 KHz
- 51% of maximum amplitude for $f_s$ = 1.25 MHz.

There are also some wiggles for input frequencies less than .15 $f_s$.

2. Tapping Resistors Adjusted to Yield Better Impulse Response, $R_{min}$ = 10 Kilo-ohms

Since for k greater than 3, the coefficients $A_k$ have negligible values in comparison with the noise, the adjustment is done only on 7 tap outputs. Obtaining the exact values of the theoretical design is very delicate because of the interaction between tap outputs. The adjusted coefficients and the corresponding tap resistances are listed in Table VI.III. Some modification has to be done on the values of some tap resistors in order to get better impulse response for different sampling frequencies.

The amplitude and width of input pulses are listed in Table IV.II.

The impulse response of this filter is illustrated in Figure 6-5 at three different typical sampling frequencies. The maximum noise observed has its peak amplitude about 19% of $A_0$.

The theoretical and measured curves of bandpass filter magnitude frequency response are shown in Figure 6-6. The wiggling of the frequency response at input frequencies less

than .15 $f_s$ is much reduced for $f_s$ = 50 KHz, but the side lobe is still high at 15% of the maximum amplitude. For $f_s$ = 1.25 MHz and $f_s$ = 500 KHz, the peak amplitudes of side lobes are increased to 29% of maximum amplitude.

TABLE VI.III. Adjusted Coefficients & Resistors ($R_{min} \simeq$ 10 k)

| k | $A_k$ | | | $R_k$ (Kilo-ohms) | | |
|---|---|---|---|---|---|---|
| | $f_s$=50KHz | $f_s$=500KHz | $f_s$=1.25MHz | $f_s$=50KHZ | $f_s$=500KHz | $f_s$=1.25MHz |
| -5 | .07246 | .01587 | .07317 | 147. | 147. | 147. |
| -4 | .08695 | .04762 | .04878 | 198. | 198. | 198. |
| -3 | -.20289 | -.55555 | -.34146 | 48.07 | 40. | 60.11 |
| -2 | -.62318 | -.62492 | -.53658 | 23. | 20. | 16. |
| -1 | .28985 | .30156 | .26829 | 47. | 75. | 210. |
| 0 | 1. | 1. | 1. | 8. | 8. | 6. |
| 1 | .28985 | .30156 | .26829 | 47. | 75. | 9.8 |
| 2 | -.62318 | -.63492 | -.53658 | 23. | 24.8 | 8.5 |
| 3 | -.20289 | -.55555 | -.34146 | 48.07 | 40. | 23. |
| 4 | .08695 | .04762 | .07317 | 198. | 198. | 198. |
| 5 | .07246 | .01587 | -.04878 | 147. | 147. | 147. |

### 3. Tapping Resistors According to Theoretical Design. $R_{min}$ = 50 ohms

A minimum value of 50 ohms is set for the tapping resistance. Using the formula described in Appendix F, the tapping resistances are calculated and have the values listed in Table VI.I, fourth column.

The pulse inputs used have the amplitude and width listed in Table IV.II. Figure 6-7 illustrates the impulse

the impulse response of the filter at sampling frequencies:

$$f_s = 50 \text{ KHz}, 500 \text{ KHz}, 1.25 \text{ MHZ}$$

The measured coefficients $A_k$ are listed in Table VI.IV.

TABLE VI.IV. Measured Coefficients ($R_{min}$ = 50 ohms)

| k | $A_k$ $f_s$=50 KHz | $f_s$=500 KHz | $f_s$=1.25 MHz |
|---|---|---|---|
| -5 | .03211 | .03137 | .82810 |
| -4 | .05504 | .07058 | .82062 |
| -3 | -.37155 | -.27451 | .76083 |
| -2 | -.58256 | -.40392 | .74439 |
| -1 | .24312 | .22745 | .84603 |
| 0 | 1. | 1. | 1. |
| 1 | .24312 | .24314 | .84603 |
| 2 | -.58256 | -.34509 | .73243 |
| 3 | -.37155 | -.38823 | .73094 |
| 4 | .05504 | .04313 | .83408 |
| 5 | .05504 | .09803 | .81464 |

The maximum peak amplitude of noise measured is about 18% of $A_o$.

The theoretical and measured curves of bandpass filter magnitude frequency response are shown in Figure 6-8. The wiggling effect of the response curves are strongly diminished in comparison with previous curves in Figures 6-4 & 6-6. The amplitudes of side lobes are also reduced and have the following values:

- 7.5% of maximum amplitude for $f_s$ = 50 KHz
- 11% of maximum amplitudes for $f_s$ = 500 KHz
- 12.5% of maximum amplitude for $f_s$ = 1.25 MHz.

4. <u>Tapping Resistor Adjusted to Yield Better Impulse Response. $R_{min}$ = 50 ohms</u>

a. Driving Circuit Using RCA/CMOS Flip-Flop

A minimum value of 50 ohms is set for tap #6. The tap outputs are adjusted by sample and hold circuit to yield better impulse response. The tapping coefficients and resistances adjusted are listed in Table VI.V.

TABLE VI.V. <u>Adjusted Tapping Coefficients & Resistors</u>

| k | $A_k$ | | | $R_k$ (Kilo-ohms) | | |
|---|---|---|---|---|---|---|
| | $f_s$=50KHz | $f_s$=500KHz | $f_s$=1.25 MHz | $f_s$=50KHz | $f_s$=500KHz | $f_s$=1.25 MHz |
| -5 | .16733 | .08532 | .01234 | 46.2 | 46.2 | 46.2 |
| -4 | .06374 | .07508 | .03086 | 63.45 | 63.45 | 63.45 |
| -3 | -.37450 | -.33673 | -.25308 | 6.25 | 4.05 | 4.05 |
| -2 | -.60557 | -.59183 | -.59876 | 1.2 | 1.2 | .5 |
| -1 | .28287 | .23849 | .22222 | 23.023 | 25.023 | 10. |
| 0 | 1. | 1. | 1. | .05 | .05 | .05 |
| 1 | .28287 | .23849 | .23457 | 6.1 | 6.1 | 4.1 |
| 2 | -.60557 | -.59183 | -.59876 | 1.083 | 1.083 | 1.08 |
| 3 | -.37450 | -.33673 | -.23457 | 4.083 | 4.55 | 1.083 |
| 4 | .06374 | .07508 | .04321 | 63.45 | 63.45 | 63.45 |
| 5 | .16733 | .08532 | .02469 | 46.2 | 46.2 | 46.2 |

The input pulse used have the amplitudes and widths listed in Table IV.II. Figure 6-9 illustrates the impulse response of

the filter at three different typical sampling frequencies. The maximum noise has its peak amplitude about 15% of $A_o$.

The theoretical and measured curves of bandpass filter magnitude frequency response are shown in Figure 6-10. The wiggling does not appear at the main lobe but the amplitudes of the side lobes are still high:

- 15% of maximum amplitude for $f_s$ = 500 KHz
- 10% of maximum amplitude for $f_s$ = 500 KHz & 1.25 MHz

b. Driving Circuit Using INSELEX CMOS/SOS Flip-Flop

A new circuit with faster flip-flop is made and a minimum value of 50 ohms is set for tapping resistance. The adjustment is done for $f_s$ equal to 500 KHz; the coefficients and resistances obtained are used also for $f_s$ of 50 KHz and 1.25 MHz. Table VI.VI lists these coefficients and resistances.

TABLE VI.VI Adjusted Coefficients & Resistances

| k | $A_k$ | $R_k$(Kilo-ohms) |
|---|---|---|
| -5 | .03536 | 46.2 |
| -4 | .01571 | 63.45 |
| -3 | -.40078 | 3.8 |
| -2 | -.61689 | 1.56 |
| -1 | .29194 | 9.023 |
| 0 | 1. | .05 |
| 1 | .29273 | 2.32 |
| 2 | -.61297 | 1.263 |
| 3 | -.40078 | 5.000 |
| 4 | .06287 | 63.45 |
| 5 | .07269 | 46.2 |

The pulse inputs listed in Table IV.II are used. Figure 6-11 illustrates the impulse response of the filter at sampling frequencies.

$$f_s = 50 \text{ KHz}, 500 \text{ KHz}, 1.25 \text{ MHz}.$$

The maximum peak amplitude noise observed is about 21.6% of $A_o$.

The theoretical and measured curves of bandpass filter magnitude frequency response are shown in Figure 6-12. There is no wiggling at the main lobe region and some improvement is obtained at the side lobes, which have the following amplitudes:

- 6% of maximum amplitude for $f_s$ = 1.25 MHz
- 10% of maximum amplitude for $f_s$ = 500 KHz
- 14% of maximum amplitude for $f_s$ = 50 KHz.

Using the computer program shown in Appendix E, the measured magnitude frequency response for $f_s$ equal to 500 KHz and the response corresponding to the measured impulse response listed in Table VI.VI are plotted in Figure 6-13 with DB scale on Y axis and normalized frequencies on X axis. The main lobes of the two curves are the same but there are some differences at the side lobe regions. This shows that the technique using the sample and hold circuit to adjust the tapping resistor to get better impulse response is quite accurate and very useful to the filter implementation.

## 5. Distortion Measurements of Bandpass Filter

For the case described in V.B.3 where the tapping resistances are set according to theoretical design with $R_{min}$ equal to 50 ohms, the second harmonic distortion defined by:

$$DB = 20 \log \frac{\text{2nd harmonic voltage}}{\text{fundamental voltage}}$$

are illustrated respectively in Figures 6-14 and 6-15, for sampling frequency of 500 KHz and three different peak to peak input voltages:

$$V_{in} = 3V, \quad 0.8V, \quad 0.1\,V$$

From the Figure 6-14 where the input frequency is equal to 50 KHz, the second harmonic and clock noise at 85 KHz have the relative values expressed in percentage of fundamental as shown in Table VI.VII.

TABLE VI.VII Second Harmonic & Clock Noise

| $V_{in}$ ppk | 3 Volts | .8 Volts | .1 Volt |
|---|---|---|---|
| 2nd Harmonic | 16.7% | 6.5% | 6.8% |
| Clock Noise | 5.8% | 14.9% | 88.8% |

When the amplitude of the input voltage decreases, the relative value of second harmonic decreases but the relative value of clock noise increases. In the Figure 6-14c, one can observe many spurious responses which occur at 63 KHz, 85 KHz, 112 KHz, 126 KHz, and are due principally to the clock noise and fixed pattern noise.

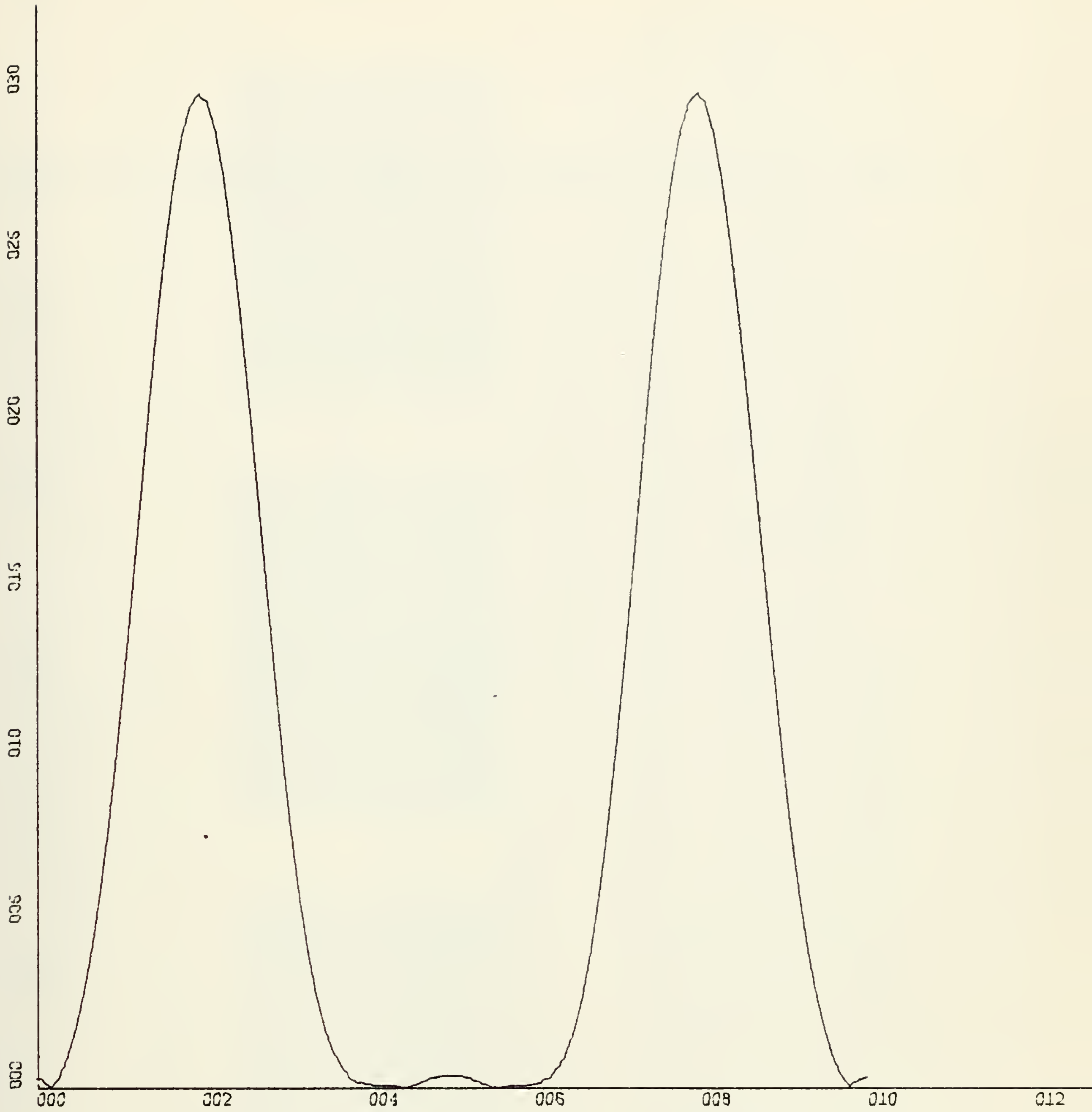


FIGURE 6.1 Amplitude Frequency Response of Bandpass Filter
Length = 11 / Hamming Window
X - Scale = .2 units/inch for normalized frequency
Y - Scale = 10 units/inch for amplitude frequency response.

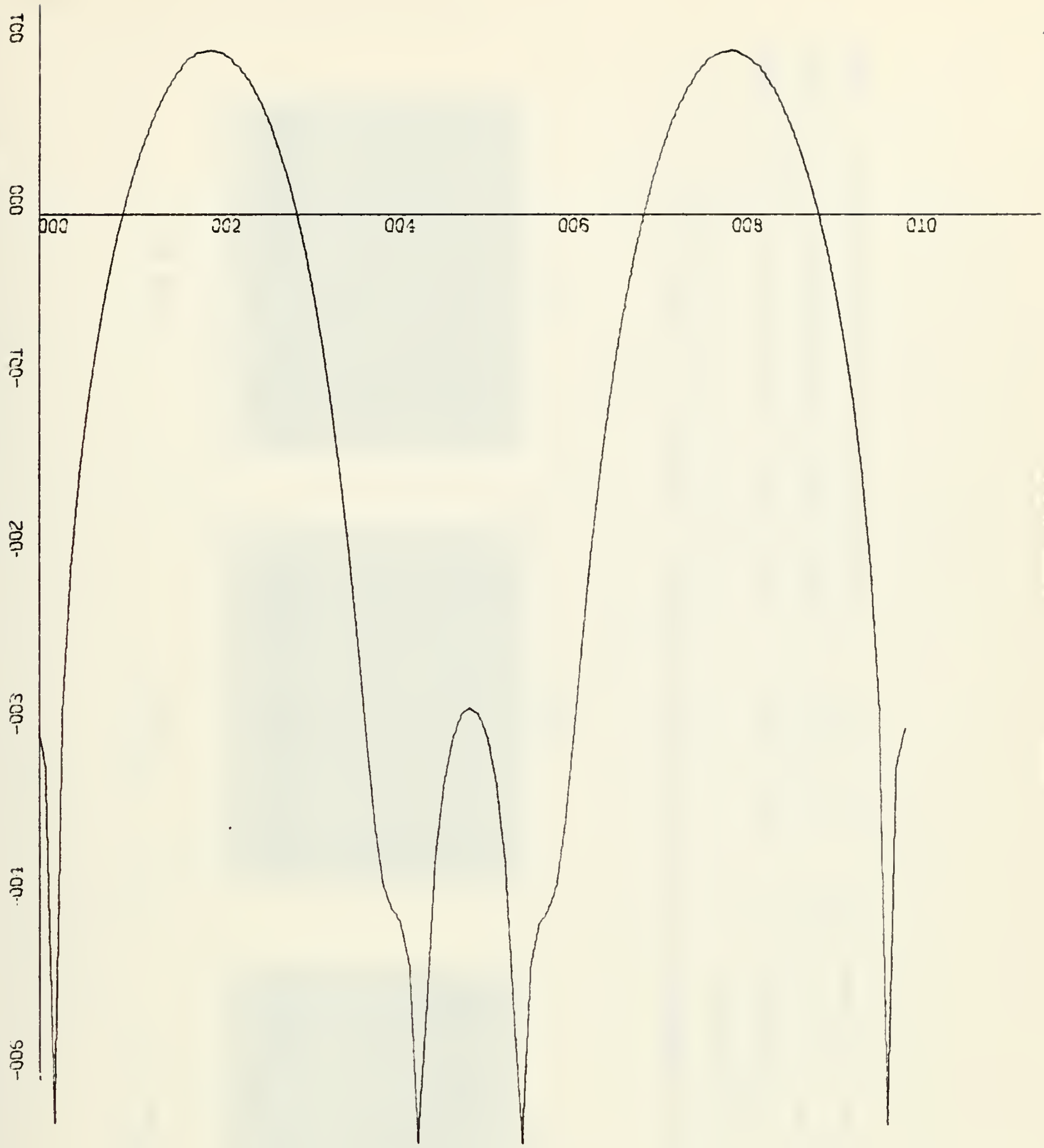


FIGURE 6.2 Amplitude Frequency Response of Bandpass Filter .
Length = 11 / Hamming Window
X - Scale = .2 units/inch for normalized frequency
Y - Scale = 10 units/inch in DB for amplitude frequency response.

| $F_{samp}$ | 50 KHz | 500 KHz | 1.25 MHz |
|---|---|---|---|

Impulse
Response

Input

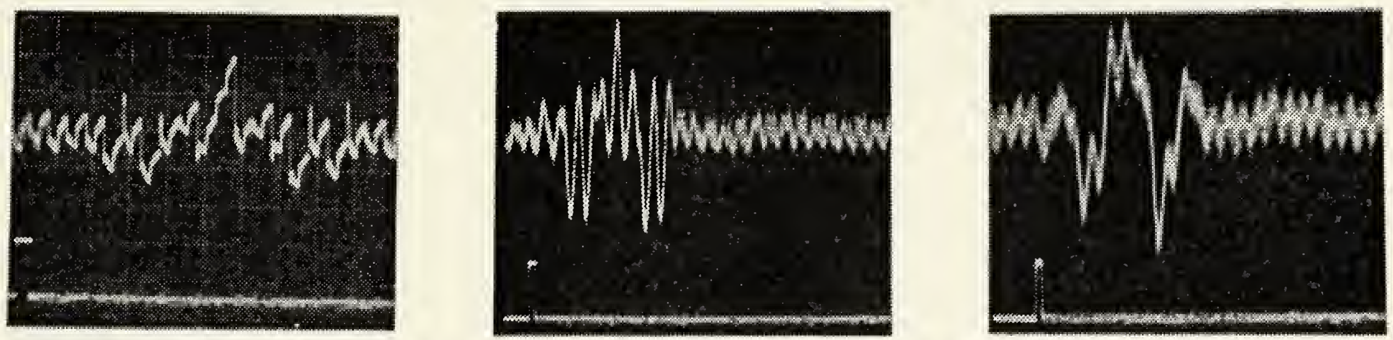

(a) (b) (c)

FIGURE 6.3 Impulse Response of Bandpass Filter with Tapping Resistors According to Theoretical Design. $R_{min}$ = 10 Kilo-ohms.

(a) Upper Scale: H=20 microsec./div. V=.05 V/div.; Lower Scale: H=5 microsec./div. V=1 V/div

(b) Upper Scale: H=5 microsec./div. V=.02 V/div.; Lower Scale: H=5 microsec./div. V=1 V/div

(c) Upper Scale: H=2 microsec./div. V=.01 V/div.; Lower Scale: H=2 microsec./div. V=1 V/div

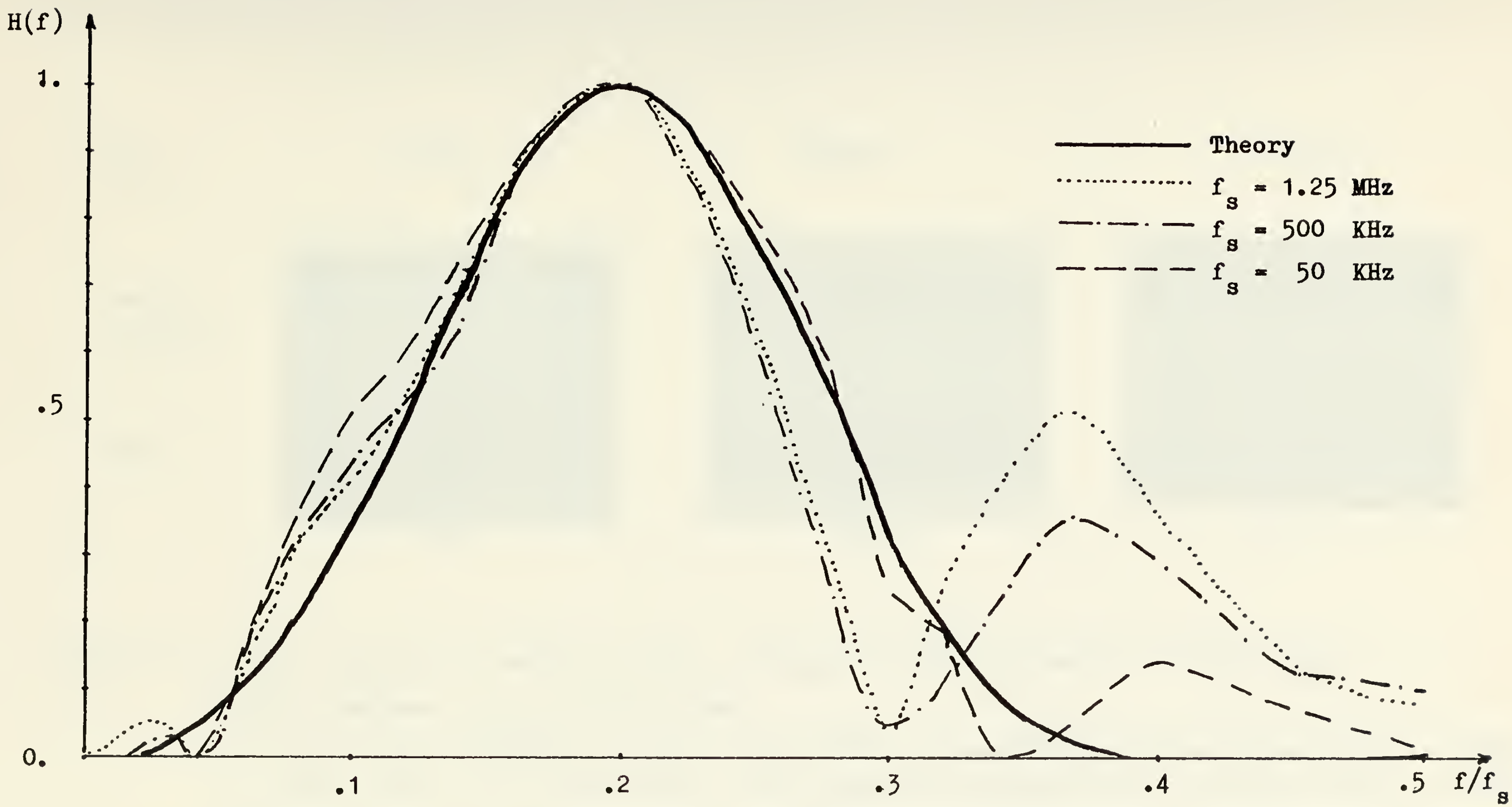


FIGURE 6.4 Bandpass Filter Magnitude Frequency Response.
Tapping Resistors According to Design. $R_{min}$ = 10 Kilo-ohms

$F_{samp}$ 50 KHz 500 KHz 1.25 MHz

Impulse Response

Input

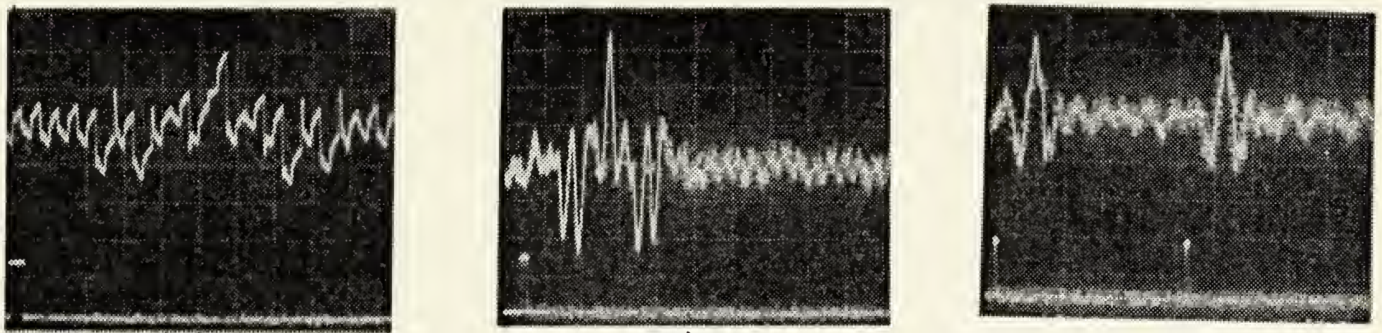

(a) (b) (c)

FIGURE 6.5 Impulse Response of Bandpass Filter. Tapping Resistors Adjusted to Yield Better Impulse Response. $R_{min}$ = 10 Kilo-ohms.

(a) Upper Scale: H=20 microsec./div. V=.05 V/div; Lower Scale: H=20 microsec./div. V=1 V/div

(b) Upper Scale: H=5 microsec./div. V=.02 V/div; Lower Scale: H=5 microsec./div. V=1 V/div

(c) Upper Scale: H=5 microsec./div. V=.02 V/div; Lower Scale: H=5 microsec./div. V=1 V/div

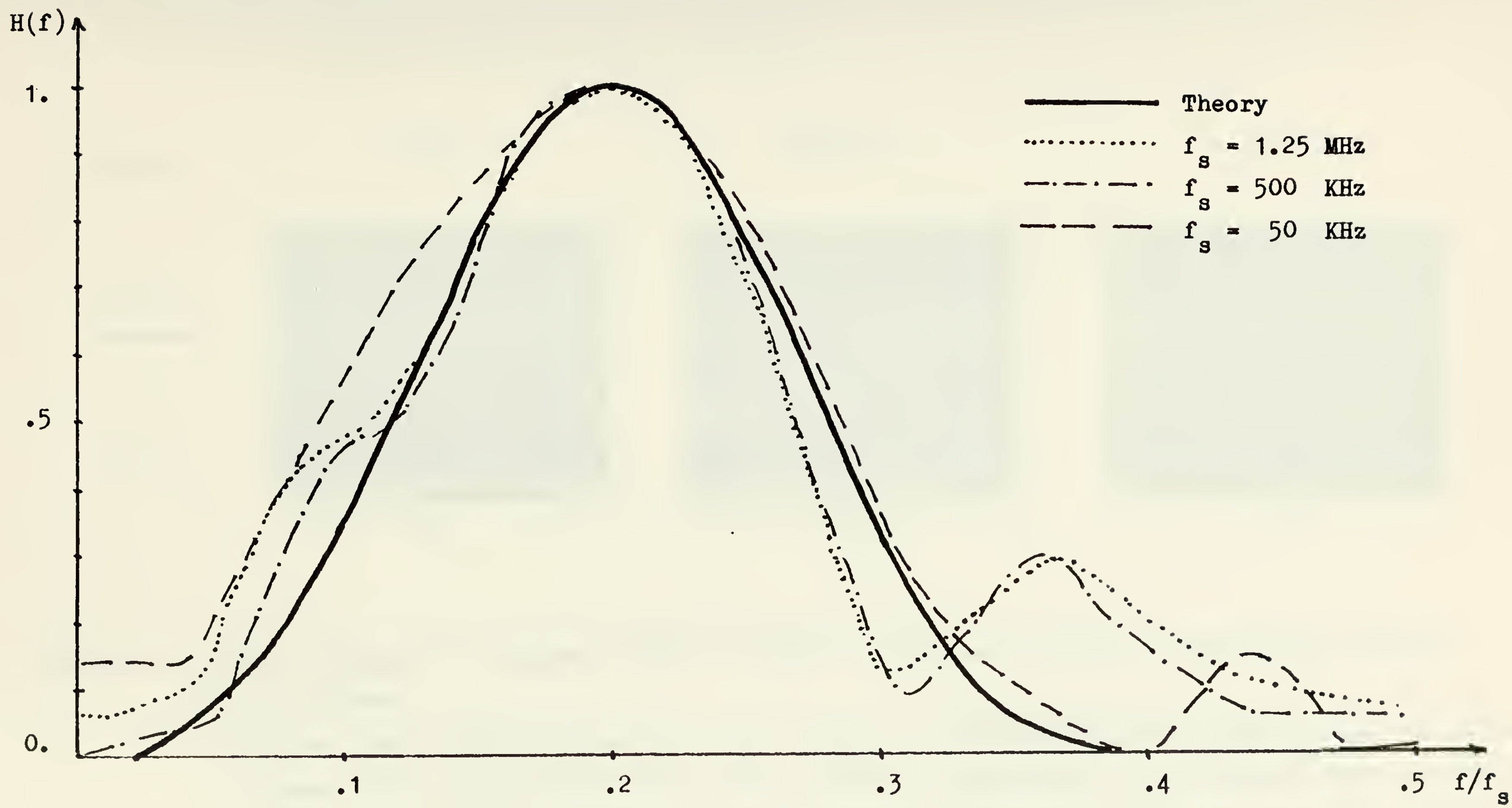


FIGURE 6.6 Bandpass Filter Magnitude Frequency Response.
Tapping Resistors Adjusted to Yield Better Impulse Response. $R_{min}$ = 10 Kilo-ohms

$F_{samp}$ 50 KHz 500 KHz 1.25 MHz

Impulse Response

Input

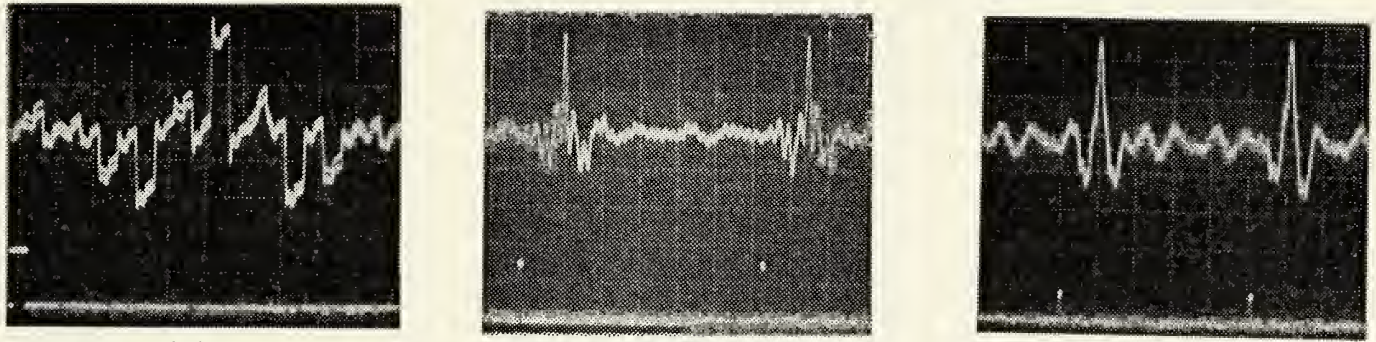

(a) (b) (c)

FIGURE 6.7 Impulse Response of Bandpass Filter. Tapping Resistors According to Theoretical Design.

$R_{min}$ = 50 ohms.

(a) Upper Scale: H=20 microsec./div. V=.1 V/div.; Lower Scale: H=20 microsec./div. V=1 V/div

(b) Upper Scale: H=10 microsec./div. V=.1 V/div.; Lower Scale: H=10 microsec./div. V=1 V/div

(c) Upper Scale: H=5 microsec./div. V=.05 V/div.; Lower Scale: H=5 microsec./div. V=2 V/div

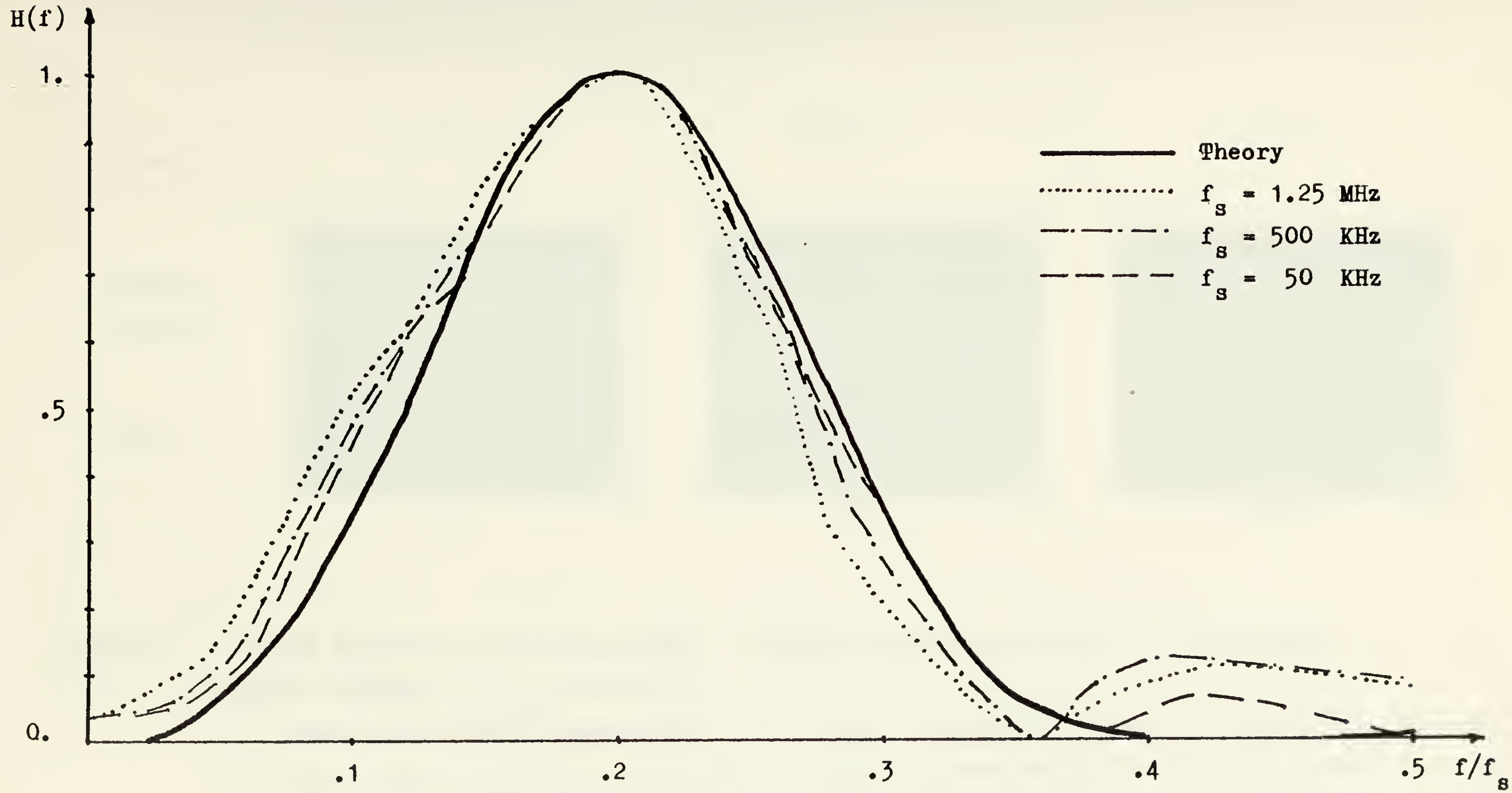


FIGURE 6.8 Bandpass Filter Magnitude Frequency Response.
Tapping Resistors According to Design. $R_{min}$ = 50 ohms

$F_{samp}$ 50 KHz 500 KHz 1.25 MHz

Impulse Response

Input

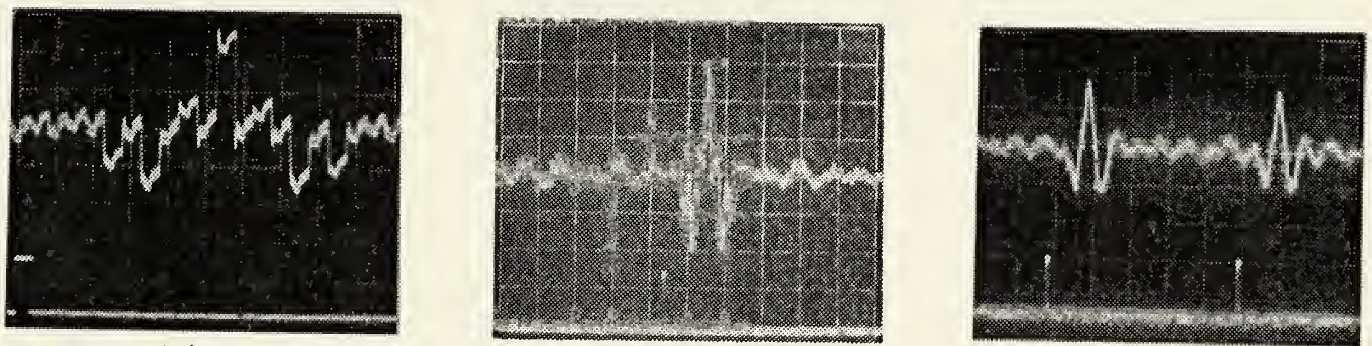

(a) (b) (c)

FIGURE 6.9 Impulse Response of Bandpass Filter. Tapping Resistors Adjusted to Yield Better Impulse Response. $R_{min}$ = 50 ohms.

(a) Upper Scale: H=20 microsec./div. V=.1 V/div.; Lower Scale: H=20 microsec./div. V=1 V/div

(b) Upper Scale: H=10 microsec./div. V=.1 V/div.; Lower Scale: H=10 micrisec./div. V=1 V/div

(c) Upper Scale: H=5 microsec./div. V=.1 V/div.; Lower Scale: H=5 microsec./div. V=1 V/div

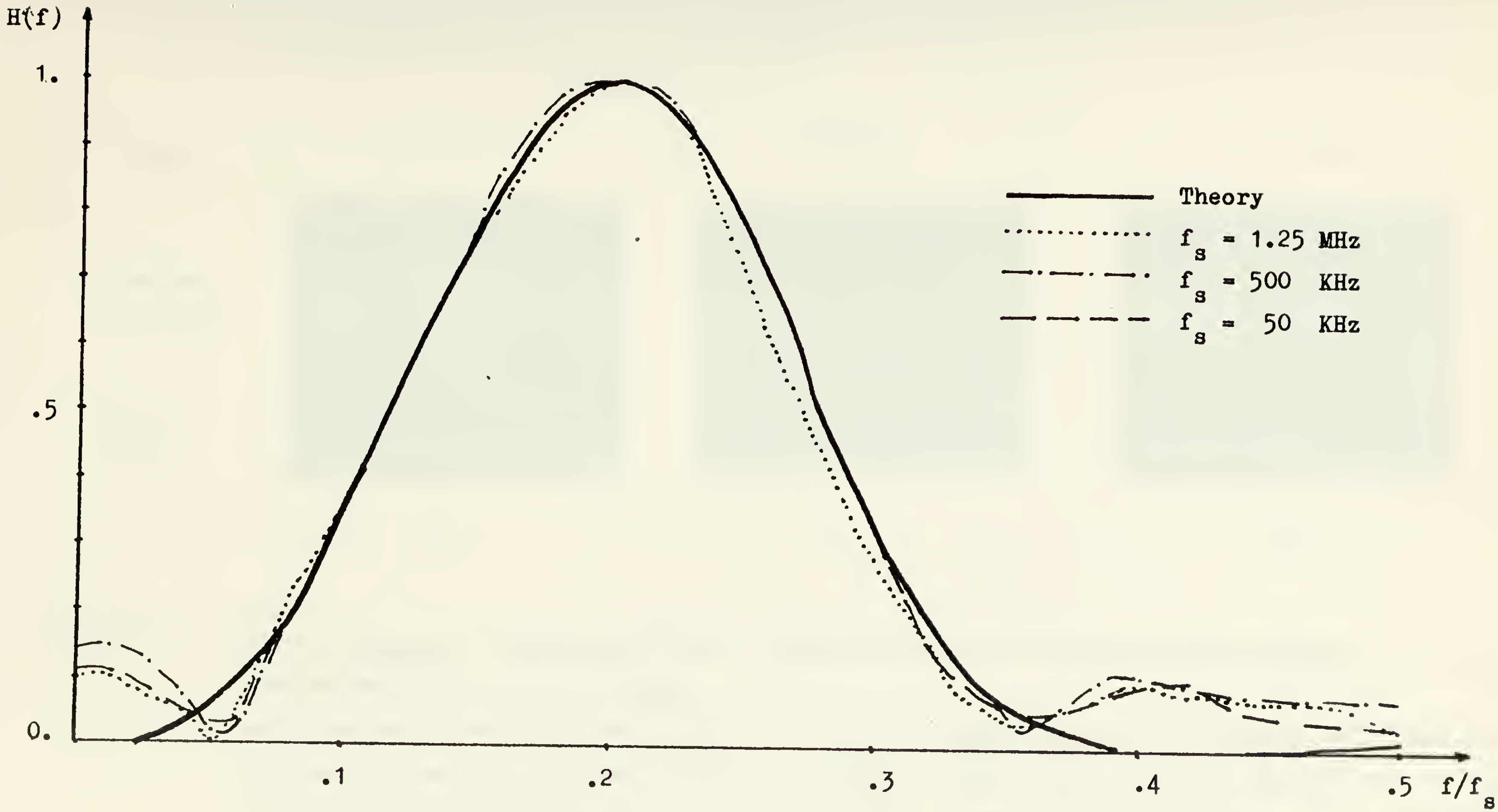


FIGURE 6.10 Bandpass Filter Magnitude Frequency Response.
Tapping Resistors Adjusted to Yield Better Impulse Response. $R_{min}$ = 50 ohms

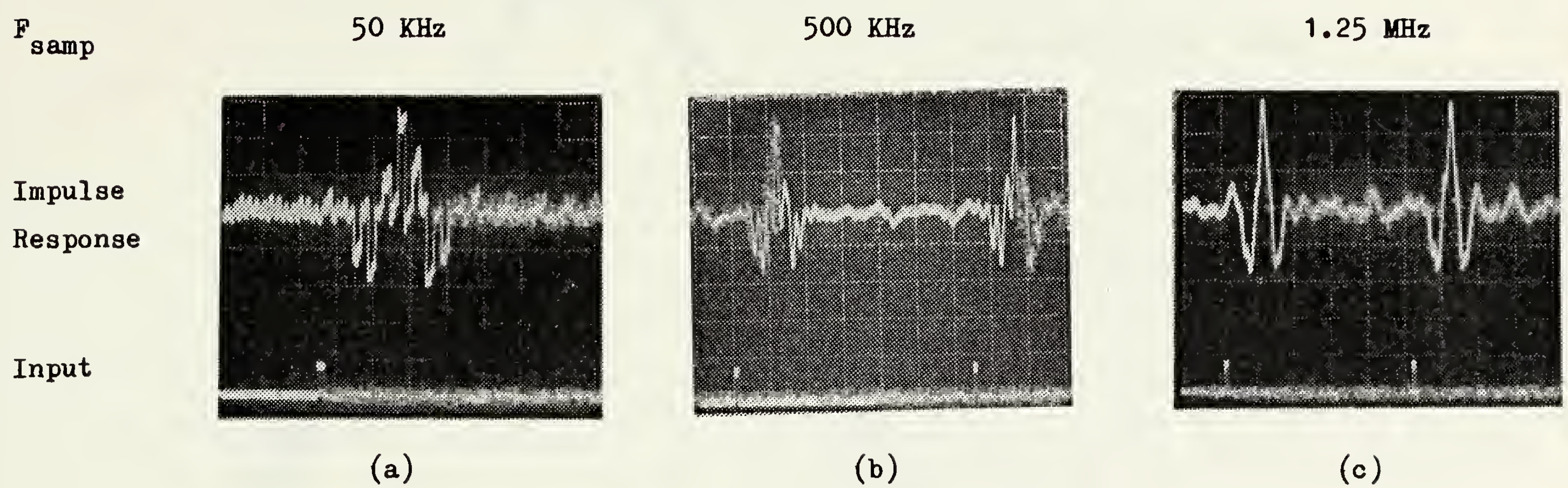


FIGURE 6.11 Impulse Response of Bandpass Filter. Tapping Resistors Adjusted to Yield Better Impulse Response. $R_{min} = 50$ ohms.

(a) Upper Scale: H=50 microsec./div. V=.1 V/div.; Lower Scale: H=50 microsec./div. V=2 V/div

(b) Upper Scale: H=10 microsec./div. V=.1 V/div.; Lower Scale: H=10 microsec./div. V=2 V/div

(c) Upper Scale: H=5 microsec./div. V=.05 V/div; Lower Scale: H=5 microsec./div. V=2 V/div

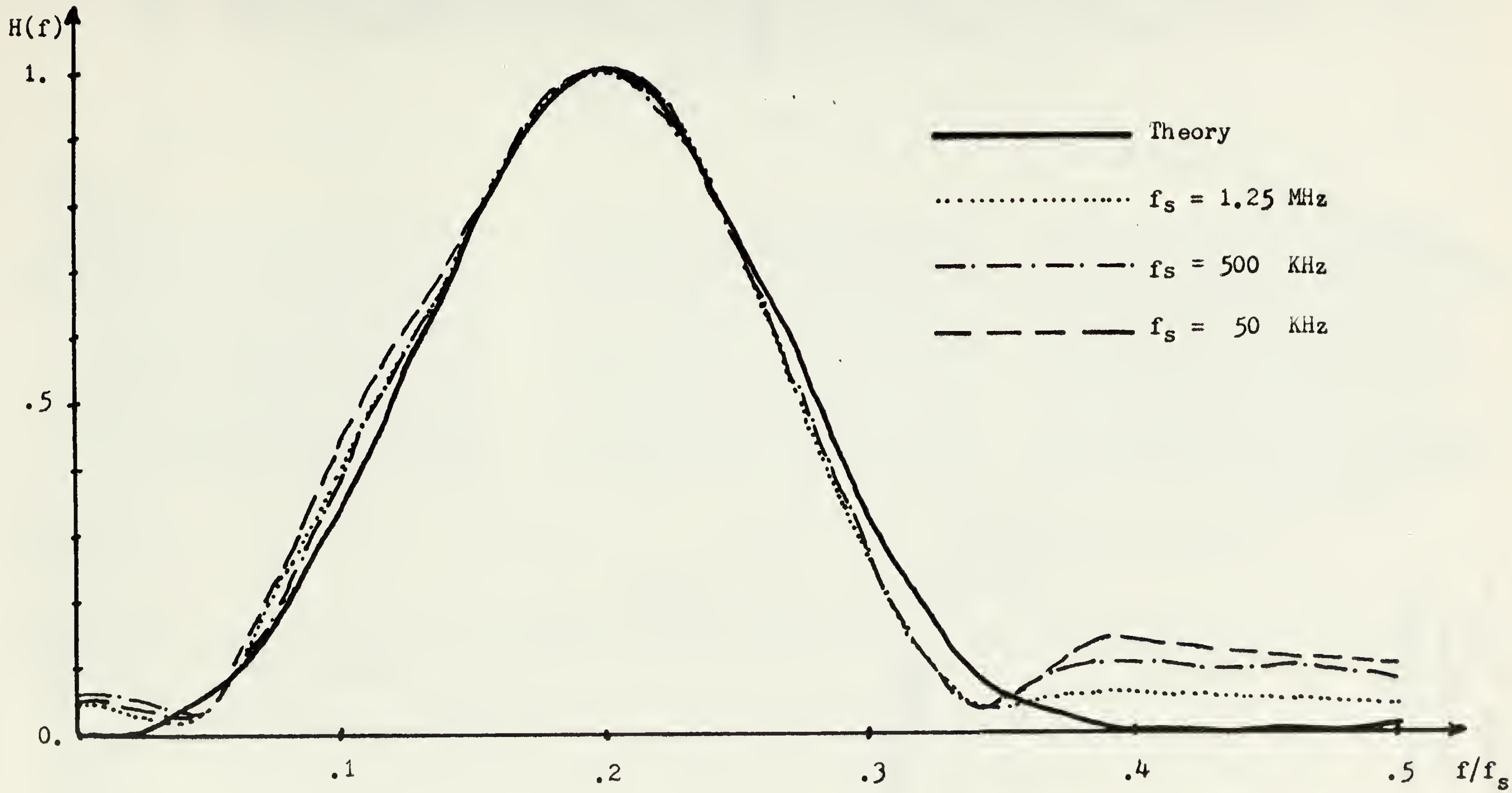


FIGURE 6-12 Bandpass Filter Magnitude Frequency Response.

Tapping Resistors Adjusted to Yield Better Impulse Response. $R_{min}$ = 50 ohms

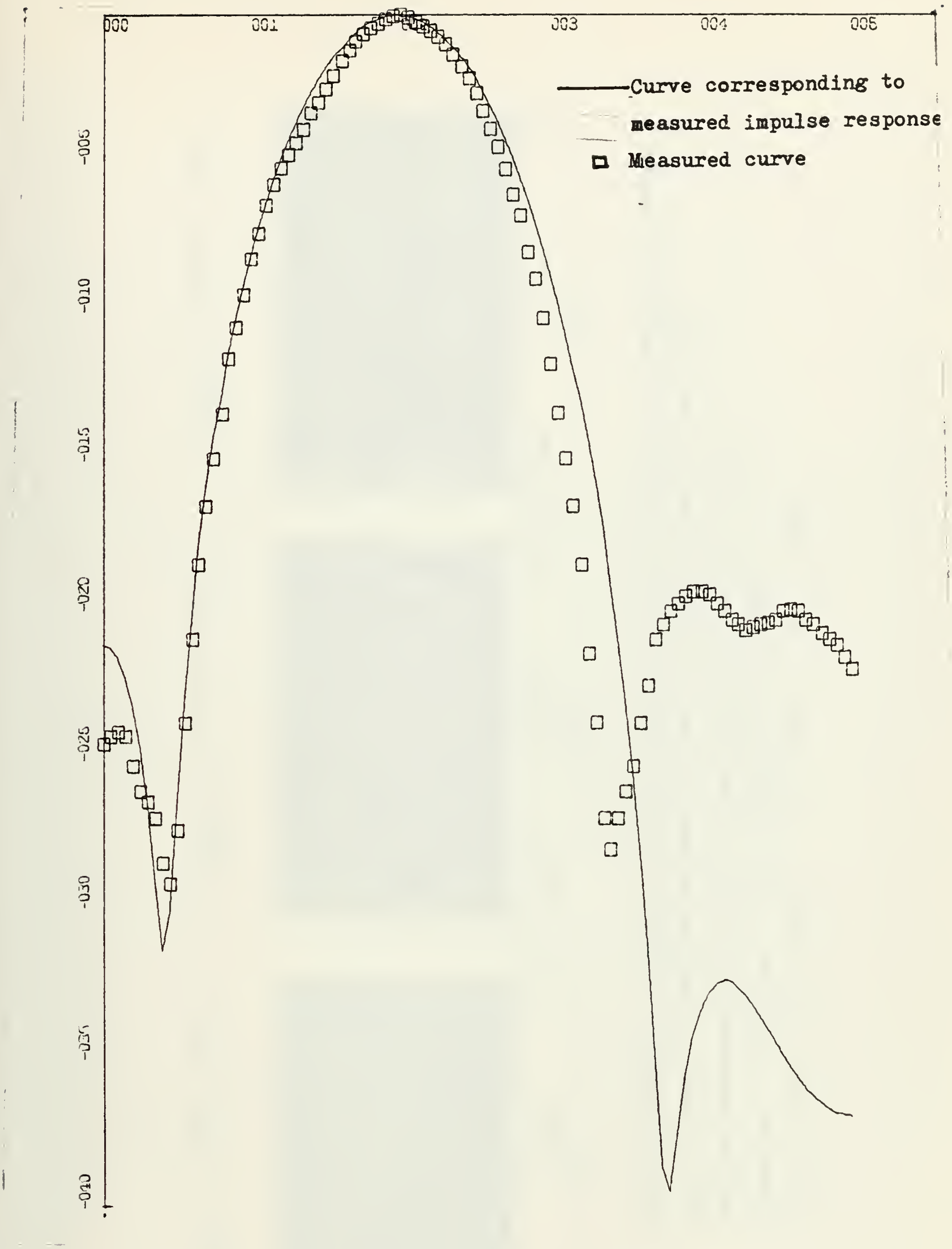


FIGURE 6.13 Bandpass Filter Magnitude Frequency Response.
Tapping Resistors Adjusted Using Impulse Response.
Rmin = 50 ohms. Q = 250. fsamp = 500 KHz.
X - Scale = .1 units/inch for normalized frequency
Y - Scale = 5 units/inch in DB

$V_{input}$ = 3 V peak to peak

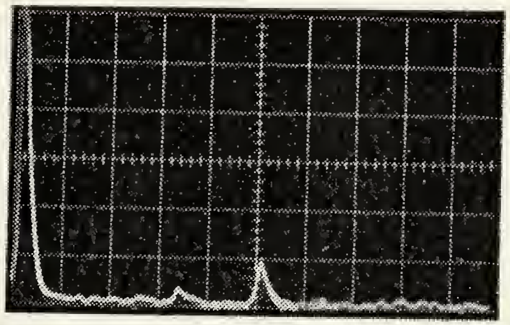

50 KHz 100 KHz 150

(a)

$V_{input}$ = .8 V peak to peak

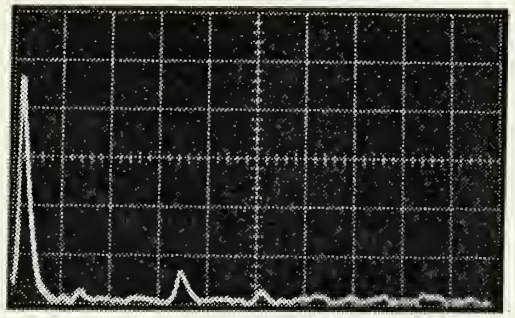

50 KHz 100 KHz 150

(b)

$V_{input}$ = .1 V peak to peak

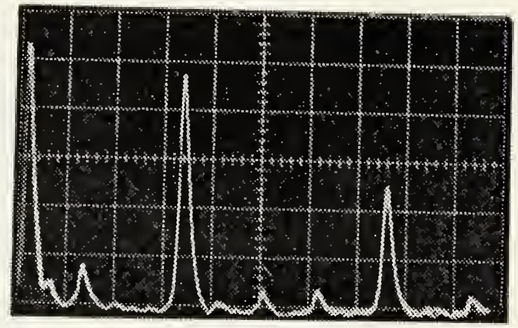

50 KHz 100 KHz 150

(c)

FIGURE 6.14 Spectral Analysis of Bandpass Filter (Tapping Resistors According to Theoretical Design. $R_{min}$ = 50 ohms). Spurious Response occured at 85 KHz is due to clock noise. Sampling Frequency $f_s$ = 500 KHz. Input Signal Frequency = 50 KHz Dispersion = 10 KHz/cm. Center Frequency = 100 KHz Vertical Scale = (a) 5 V/div.; (b) 2 V/div.; (c) .2 V/div.

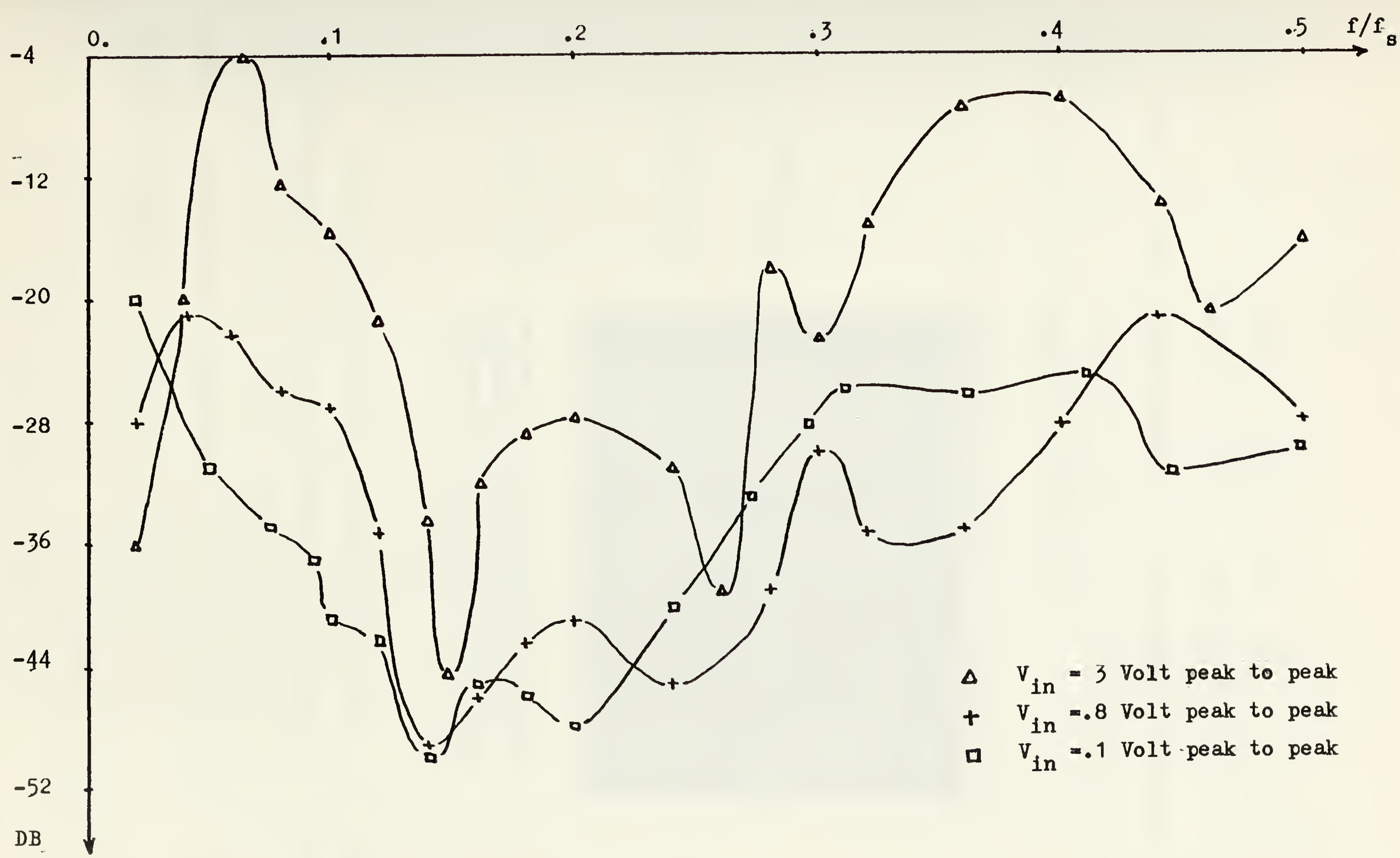


FIGURE 6.15 Second Harmonic Distortion of Bandpass Filter with Tapping Resistors According to Design and $R_{min}$ = 50 ohms for Different Input Signal Amplitudes. $f_{samp}$ = 500 KHz

6. Observations

The characteristic feature of the filter realized by the electronic tapped analog delay line is that one can scan the center frequency of the bandpass filter to the left or right by simply decreasing or increasing the clock frequency. Figure 6-16 illustrates this feature for Q = constant at two different sampling frequencies:

$$f_s = 500 \text{ KHz}, 835 \text{ KHz}$$

$f_s$=500 KHz

$f_s$=835 KHz

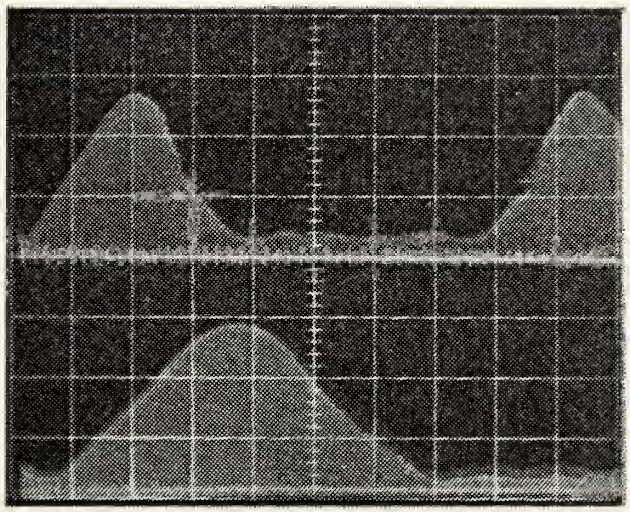

FIGURE 6-16. Bandpass Filters Amplitude Frequency response at 2 different sampling frequencies $f_s$=500 KHz & $f_s$=835 KHz. Scale: H = .2 nsec/Div V = .1 V/Div.

Another observation is that the transversal filter implementation is not very sensitive to high specifications for moderate number of taps. The tapping coefficients are almost the same for different values of Q required. The impulse response of bandpass filters for:

$$f_o = 0.2\, f_s \quad (f_o = \text{center frequency})$$

$$Q = 50, \ 250, \ 500$$

using 11 taps is listed in Table VI.VIII, and using 23 taps in Table I.IX.

TABLE VI.VIII Tapping Coefficients (11 Taps)

| k | $A_k$ Q=50 | Q=250 | Q=500 |
|---|---|---|---|
| 0 | 1. | 1. | 1. |
| 1 | 0.28644 | 0.28647 | 0.28640 |
| 2 | -0.59140 | -0.59148 | -0.59148 |
| 3 | -0.38382 | -0.38389 | -0.38395 |
| 4 | 0.07375 | 0.7378 | 0.07378 |
| 5 | 0.09857 | 0.09863 | 0.09863 |

TABLE VI.IX Tapping Coefficients (23 Taps)

| k | $A_k$ Q=50 | Q=250 | Q=500 |
|---|---|---|---|
| 0 | 1. | 1. | 1. |
| 1 | 0.30373 | 0.30377 | 0.30370 |
| 2 | -0.75475 | -0.75486 | -0.75486 |
| 3 | -0.69072 | -0.69086 | -0.69095 |
| 4 | 0.23217 | 0.23227 | 0.23227 |
| 5 | 0.63317 | 0.63357 | 0.63358 |
| 6 | 0.15702 | 0.15717 | 0.15718 |
| 7 | -0.31184 | -0.31222 | -0.31224 |
| 8 | -0.22189 | -0.22225 | -0.22226 |
| 9 | 0.05648 | 0.05660 | 0.05660 |
| 10 | 0.11777 | 0.11807 | 0.11808 |
| 11 | 0.02596 | 0.02604 | 0.02605 |

# VI. CONCLUSION

Digital non-recursive filters have been extensively developed for the implementation of "finite impulse response" (FIR) filters using software on digital computers. In recent years, new CTD (charge transfer device) tapped delay lines make it possible to implement real time FIR filters using these hardware devices. However, because the signal is sampled analog instead of digital and because the device principle and technology are new, careful investigation is needed for the successful development of these hardware sampled analog signal processors. In this thesis, the new Reticon TAD-12 tapped delay line with external programmable tap weights is investigated in detail. In addition to a thorough evaluation of its device performance, the properties of three sampled analog FIR filters using TAD-12 are investigated. They are the prewhitening, dewhitening and bandpass filters.

Both the frequency response of TAD-12 devices have been evaluated for sampling frequency up to 2.5 MHz. It was found that the output showed the following limitations:

1. Frequency response limitation:

Tap outputs generally roll-off faster than predicted by the effect of sample and hold. The roll-off depends on the location of the tap and its tapping resistance.

2. Time response limitation:

Output at one tap generally takes more than the delay period between adjacent taps to settle down and affect the output of the following taps. The settling time depends on the location of the tap, its tapping resistance and the sampling frequency.

3. Non-uniformities:

Tap outputs are not uniform among the taps. The non-uniformity varies with the location of the tap, its tapping resistance and signal frequency.

4. Loading effect:

Tap outputs vary with tapping resistance. However, it should be pointed out that these limitations are large at higher sampling frequencies and signal frequencies. At sampling frequencies less than 100 KHz and signal frequencies less than 10 KHz, TAD-12 behaves satisfactorily.

The properties of three sampled analog FIR filters using TAD-12 have been evaluated following three design procedures.

1. Tap resistances are selected using the same design procedure developed for digital non-recursive filters.
2. Tap resistances are corrected using the frequency response.
3. Tap resistances are corrected using the impulse time response.

It was found that the device limitation causes considerable deviation of the filter performance from theoretical prediction especially when the sampling frequency is high. Furthermore, the deviation is relatively smaller in bandpass filter and becomes worse in dewhitening filter followed by prewhitening filter. This trend is the result of the relative magnitudes

of the tap outputs with respect to the noises caused by the device limitations.

These problems encountered in the Reticon TAD-12 tapped delay line just showed that it is still in its developing stage. Improved results can be expected when the causes of the device limitations are better understood and corrected.

APPENDIX A

```
C*****************************************************************
C   PROGRAM OF DESIGNING NONRECURSIVE PREWHITENING FILTER BY
C   WINDOW METHOD
C*****************************************************************
C
C
C   THIS PROGRAM CALCULATES AND PLOTS AMPLITUDE AND PHASE OF
C   FIR DIGITAL FILTER WITH TRANSFER FUNCTION
C   H(Z) = C(0)+C(1)*Z**(-1)+C(2)*Z**(-2)+....+C(M)*Z**(-M)
C   C(M)   FINITE IMPULSE RESPONSE
C   A      SLOPE OF FREQUENCY AMPLITUDE RESPONSE FROM F0 TO
C          HIGHEST FREQUENCY FP
C   B      CONSTANT FREQUENCY AMPLITUDE RSEPONSE FROM 0 TO F0
C   T = 1. (NORMALIZED DELAY UNIT) AND FP=0.5*(1/T) AND
C   E = F0/FP
C
C
      COMPLEX ZINV,G,P
      COMPLEX CEXP,CMPLX
      DIMENSION F(150),C(30),W(30),D(30),DD(30),CW(30),
     1AMP(150),PHASE(150)
      INTEGER*4  ITB(12)/12*0/
      REAL*4     RTB(28)/28*0.0/
      DATA R/0.1/,A/1./,E/119.048/,N/5/
      PI=3.14159265
      CONVRT=180./PI
      M=2*N+1
      WRITE(6,500) M
  500 FORMAT(1X,'LENGTH OF FILTER IS:',I4///)
C
C   TO COMPUTE FINITE IMPULSE RESPONSE AND WINDOW FUNCTION
C
      W(N+1)=1.
      C(N+1)=R+A/(2*PI)*(.5-1./(2.*E))**2
      DO 600 K=1,N
      D(K)=A*(COS(K*PI)-COS(K*PI/E))/(2.*PI**3*K**2)
      C(N+1-K)=D(K)
      C(N+1+K)=C(N+1-K)
      DD(K)=0.54+0.46*COS(2.*PI*K/M)
      W(N+1-K)=DD(K)
      W(N+1+K)=W(N+1-K)
  600 CONTINUE
      WRITE(6,650)(C(I),I=1,M)
  650 FORMAT(//2X,'COEFFICIENTS ARE:'/8(1X,F10.5))
      CMAX=ABS(C(N+1))
      DO 700 I=1,M
      IF(ABS(C(I)).GT.CMAX) CMAX=ABS(C(I))
  700 CONTINUE
      DO 750 I=1,M
C
C   NORMALIZE FIR
C
      C(I)=C(I)/CMAX
  750 CONTINUE
      WRITE(6,800)(C(I),I=1,M)
  800 FORMAT(//2X,'NORMALIZED COEFFICIENTS ARE:'/8(1X,F10.5))
      WRITE (6,900) (W(I),I=1,M)
  900 FORMAT(//2X,'HAMMING WINDOW ARE:'/8(1X,F10.5))
      DO 9 I=1,M
    9 CW(I)=C(I)*W(I)
      WRITE(6,1000)(CW(I),I=1,M)
 1000 FORMAT(//2X,'COEFFICIENTS IMPROVED BY HAMMING ARE'
     1/8(1X,F10.5))
      WRITE(6,50)
   50 FORMAT(///5X,'FREQUENCY',8X,'AMPLITUDE',13X,'PHASE'///)
      DO 10 J=1,101
C
C   F IS FREQUENCY IN FRACTIONS OF NYQUIST FREQUENCY
```

```
C
      F(J)=0.005*FLOAT(J-1)
      ZINV=CEXP(CMPLX(0.,-2.*F(J)*PI))
      P=CMPLX(1.,0.)
      G=CMPLX(0.,0.)
      DO 6 I=1,M
      G=G+P*CW(I)
    6 P=P*ZINV
      AMP(J)=CABS(G)
      X=REAL(G)
      Y=AIMAG(G)
      IF(ABS(X).GT.1.E-8) GO TO 60
      PHASE(J)=SIGN(90.,Y)
      GO TO 8
   60 PHASE(J)=ATAN2(Y,X)*CONVRT
    8 WRITE(6,20) F(J),AMP(J),PHASE(J)
   20 FORMAT(5X,F6.3,4X,E16.8,4X,E16.8)
   10 CONTINUE
      EQUIVALENCE(TITLE,RTB(5))
      REAL*8  TITLE(12)
      READ(5,300) TITLE
  300 FORMAT(6A8)
      CALL DRAWP(101,F,AMP,ITB,RTB)
      READ(5,300) TITLE
      CALL DRAWP(101,F,PHASE,ITB,RTB)
      STOP
      END
//GO.SYSIN DD *
AMPLITUDE FREQUENCY RESPONSE OF PREWHITENING
FILTER / LENGTH = 11 / HAMMING WINDOW
PHASE RESPONSE OF PREWHITENING FILTER
LENGTH = 11 / HAMMING WINDOW
```

APPENDIX B

```
C***********************************************************************
C   PROGRAM OF DESIGNING DWF FROM GIVEN IMPULSE RESPONSE OF
C   DWF BY FREQUENCY SAMPLING METHOD
C   THE PRESCRIBED CHARACTERISTIC AND DESIGNED FREQUENCY
C   CHARACTERISTIC OF DWF ARE PLOTTED ON THE SAME GRAPH
C***********************************************************************
C
C
C   THIS PROGRAM CALCULATES AND PLOTS AMPLITUDE AND PHASE OF
C   FIR DIGITAL FILTER WITH TRANSFER FUNCTION
C   H(Z) = C(0)+C(1)*Z**(-1)+C(2)*Z**(-2)+....+C(M)*Z**(-M)
C   C(M)  FINITE IMPULSE RESPONSE
C
C
      COMPLEX ZINV,G,P,H(150)
      COMPLEX CEXP,CMPLX
      DIMENSION F(150),C(30),W(30),D(30),DD(30),CW(30),
     1AMP(150),PHASE(150),HH(150)
      INTEGER*4  ITB(12)/12*0/
      REAL*4     RTB(28)/28*0.0/
      FACTOR=1.13
      MM=0
      N=5
      PI=3.14159265
      CONVRT=180./PI
      M=2*N+1
      WRITE(6,500) M
  500 FORMAT(1X,'LENGTH OF FILTER IS:',I4///)
      READ(5,1)(C(I),I=1,M)
    1 FORMAT(8F10.5)
  610 WRITE(6,650)(C(I),I=1,M)
  650 FORMAT(//2X,'COEFFICIENTS ARE:'/8(1X,F10.5))
C
C   COMPUTE HAMMING WINDOW
C
      W(N+1)=1.
      DO 600 K=1,N
      DD(K)=0.54+0.46*COS(2.*PI*K/M)
      W(N+1-K)=DD(K)
      W(N+1+K)=W(N+1-K)
  600 CONTINUE
      CMAX=ABS(C(N+1))
      DO 700 I=1,M
      IF(ABS(C(I)).GT.CMAX) CMAX=ABS(C(I))
  700 CONTINUE
      DO 750 I=1,M
C
C   NORMALIZE FIR
C
      C(I)=C(I)/CMAX
  750 CONTINUE
      WRITE(6,800)(C(I),I=1,M)
  800 FORMAT(//2X,'NORMALIZED COEFFICIENTS ARE:'/8(1X,F10.5))
      DO 9 I=1,M
    9 CW(I)=C(I)*W(I)
      WRITE(6,1000)(CW(I),I=1,M)
 1000 FORMAT(//2X,'COEFFICIENTS IMPROVED BY HAMMING ARE'
     1/8(1X,F10.5))
      WRITE(6,50)
   50 FORMAT(///5X,'FREQUENCY',8X,'AMPLITUDE',13X,'PHASE'///)
      DO 10 J=1,101
C
C   F IS FREQUENCY IN FRACTIONS OF NYQUIST FREQUENCY
C
      F(J)=0.005*FLOAT(J-1)
      ZINV=CEXP(CMPLX(0.,-2.*F(J)*PI))
      P=CMPLX(1.,0.)
      G=CMPLX(0.,0.)
```

```
      DC 6 I=1,M
      IF(MM.EC.1) GO TO 11
      G=G+P*CW(I)
      GC TO 6
   11 G=G+P*CW(I)*FACTOR
    6 P=P*ZINV
      AMP(J)=CABS(G)
C
C   FRECUENCY SAMPLE POINTS CF DWF
C
      H(J)=1./G
      HH(J)=CABS(H(J))
      X=REAL(G)
      Y=AIMAG(G)
      IF(ABS(X).GT.1.E-8) GO TO 60
      PHASE(J)=SIGN(90.,Y)
      GC TO 8
   60 PHASE(J)=ATAN2(Y,X)*CONVRT
    8 WRITE(6,20) F(J),AMP(J),PHASE(J)
   20 FCRMAT(5X,F6.3,4X,E16.8,4X,E16.8)
   10 CCNTINUE
      ECUIVALENCE(TITLE,RTB(5))
      REAL*8  TITLE(12)
      IF(MM.EC.1) GO TO 301
      GC TO 302
  301 ITB(1)=3
      ITB(2)=0
      CALL DRAWP(101,F,AMP,ITB,RTB)
  302 L=N+1
C
C   CF DWF
C
      DC 1500 I=1,L
      K=I-1
      GG=CMPLX(0.,0.)
      DC 1100 J=1,101
      Z=CEXP(CMPLX(0.,2.*PI*F(J)*K))
      GG=GG+Z*H(J)
 1100 CCNTINUE
      C(I)=GG/101.
      C(N+1-I)=C(I)
 1500 CCNTINUE
      MM=MM+1
      IF(MM.EQ.2) GO TO 2100
      READ(5,300) TITLE
  300 FCRMAT(6A8)
      ITB(1)=1
      ITB(2)=1
C
C   PLCT THE PRESCRIBED FREQUENCY CHARACTERISTIC CF DWF
C
C   USING INVERSE DISCRETE FCURIER TRANSFCRM TO CALCULATE THE
C   IMPULSE RESPONSE OF DWF
      CALL DRAWP(101,F,HH,ITB,RTB)
C
C   GC BACK TO PLOT THE AMPLITUDE FREQUENCY RESPONSE OF DWF
C
      GC TO 610
 2100 STCP
      END
//GO.SYSIN DD *
  -0.00091   0.0000   -0.01219   0.0000   -0.21427   1.0000
  -0.21427   0.0      -0.01219   0.0      -0.00091
AMPLITUDE FRECUENCY RESPCNSE OF DEWHITENING
FILTER / LENGTH = 11 / HAMMING WINDOW
```

# APPENDIX C

```
C*****************************************************************
C* PROGRAM OF DESIGNING NONRECURSIVE BANDPASS FILTER
C*****************************************************************
C
C
C   THIS PROGRAM CALCULATES AND PLOTS AMPLITUDE AND PHASE OF
C   FIR DIGITAL FILTER WITH TRANSFER FUNCTION
C   H(Z) = C(0)+C(1)*Z**(-1)+C(2)*Z**(-2)+....+C(M)*Z**(-M)
C   C(M)  FINITE IMPULSE RESPONSE
C   A   AMPLITUDE OF BANDPASS
C   F1 & F2   I CRITICAL FREQUENCIES
C
C
      COMPLEX ZINV,G,P
      COMPLEX CEXP,CMPLX
      DIMENSION F(150),C(30),W(30),D(30),DD(30),CW(30),
     1AMF(150),PHASE(150)
      INTEGER*4  ITB(12)/12*0/
      REAL*4     RTB(28)/28*0.0/
      DATA A/1./,F1/0.1980/,F2/0.2020/,N/5/
      PI=3.14159265
      CONVRT=180./PI
      M=2*N+1
      WRITE(6,500) M
  500 FORMAT(1X,'LENGTH OF FILTER IS:',I4///)
C
C
      W(N+1)=1.
      C(N+1)=2.*A*(F2-F1)
      DO 600 K=1,N
      D(K)=A*(SIN(2.*PI*K*F2)-SIN(2.*PI*K*F1))/(K*PI)
      C(N+1-K)=D(K)
      C(N+1+K)=C(N+1-K)
      DD(K)=0.54+0.46*COS(2.*PI*K/M)
      W(N+1-K)=DD(K)
      W(N+1+K)=W(N+1-K)
  600 CONTINUE
      WRITE(6,650)(C(I),I=1,M)
  650 FORMAT(//2X,'COEFFICIENTS ARE:'/8(1X,F10.5))
      CMAX=ABS(C(N+1))
      DO 700 I=1,M
      IF(ABS(C(I)).GT.CMAX) CMAX=ABS(C(I))
  700 CONTINUE
      DO 750 I=1,M
C
C   NORMALIZE FIR
C
      C(I)=C(I)/CMAX
  750 CONTINUE
      WRITE(6,800)(C(I),I=1,M)
  800 FORMAT(//2X,'NORMALIZED COEFFICIENTS ARE:'/8(1X,F10.5))
      WRITE (6,900) (W(I),I=1,M)
  900 FORMAT(//2X,'HAMMING WINDOW ARE:'/8(1X,F10.5))
      DO 9 I=1,M
    9 CW(I)=C(I)*W(I)
      WRITE(6,1000)(CW(I),I=1,M)
 1000 FORMAT(//2X,'COEFFICIENTS IMPROVED BY HAMMING ARE'
     1/8(1X,F10.5))
      WRITE(6,50)
   50 FORMAT(///5X,'FREQUENCY',8X,'AMPLITUDE',13X,'PHASE'///)
      DO 10 J=1,101
C
C   F IS FREQUENCY IN FRACTIONS OF NYQUIST FREQUENCY
C
      F(J)=0.01*FLOAT(J-1)
      ZINV=CEXP(CMPLX(0.,-2.*F(J)*PI))
      P=CMPLX(1.,0.)
      G=CMPLX(0.,0.)
```

```
      DO 6 I=1,M
      G=G+P*CW(I)
    6 P=P*ZINV
      AMP(J)=CABS(G)
      X=REAL(G)
      Y=AIMAG(G)
      IF(ABS(X).GT.1.E-8) GO TO 60
      PHASE(J)=SIGN(90.,Y)
      GO TO 8
   60 PHASE(J)=ATAN2(Y,X)*CONVRT
    8 WRITE(6,20) F(J),AMP(J),PHASE(J)
   20 FORMAT(5X,F6.3,4X,E16.8,4X,E16.8)
   10 CONTINUE
      EQUIVALENCE(TITLE,RTB(5))
      REAL*8  TITLE(12)
      READ(5,300) TITLE
  300 FORMAT(6A8)
      CALL DRAWP(101,F,AMP,ITB,RTB)
      READ(5,300) TITLE
      CALL DRAWP(101,F,PHASE,ITB,RTB)
      STOP
      END
//GO.SYSIN DD *
AMPLITUDE FREQUENCY RESPONSE OF BANDPASS
FILTER / LENGTH = 11 / HAMMING WINDOW
PHASE RESPONSE OF BANDPASS FILTER
LENGTH = 11 / HAMMING WINDOW
```

APPENDIX D

```
C   THIS PROGRAM CALCULATES IMPULSE RESPONSE GIVEN AMPLITUDE
C   FREQUENCY RESPONSE OF FILTER
      COMPLEX CEXP,CMPLX
      DIMENSION F(150),C(30),W(30),CW(30),DD(30),H(150)
      N=5
      PI=3.14159265
      M=2*N+1
      WRITE(6,500) M
  500 FORMAT(1X,'LENGTH OF FILTER IS:',I4//)
C
C   COMPUTE HAMMING WINDOW
C
      W(N+1)=1.
      DO 600 K=1,N
      DD(K)=0.54+0.46*COS(2.*PI*K/M)
      W(N+1-K)=DD(K)
      W(N+1+K)=W(N+1-K)
  600 CONTINUE
      READ(5,700) (H(J),J=1,101)
  700 FORMAT(8F10.5)
      WRITE(6,750) (H(J),J=1,101)
  750 FORMAT(//2X,'DATA ARE:',///(8(1X,F10.5),/))
C
C   NORMALIZE H(J)
C
      HMAX=H(89)
      DO 2000 J=1,101
      IF(H(J).GT.HMAX) HMAX=H(J)
 2000 CONTINUE
      DO 2100 J=1,101
      H(J)=H(J)/HMAX
 2100 CONTINUE
C
C   USING INVERSE DISCRETE FOURIER TRANSFORM
C   TO CALCULATE THE IMPULSE RESPONSE
C
      L=M
      DO 1500 I=1,L
      K=I-1
      GG=CMPLX(0.,0.)
      DO 1100 J=1,101
      F(J)=0.01*FLOAT(J-1)
      Z=CEXP(CMPLX(0.,2.*PI*F(J)*K))
      GG=GG+Z*H(J)
 1100 CONTINUE
      C(I)=GG/101.
 1500 CONTINUE
      WRITE(6,650)(C(I),I=1,M)
  650 FORMAT(//2X,'COEFFICIENTS ARE:'/8(1X,F10.5))
C
C   NORMALIZE FIR
C
      CMAX=ABS(C(N+1))
      DO 800 I=1,M
      IF(ABS(C(I)).GT.CMAX) CMAX=ABS(C(I))
  800 CONTINUE
      DO 900 I=1,M
      C(I)=C(I)/CMAX
  900 CONTINUE
      WRITE(6,850)(C(I),I=1,M)
  850 FORMAT(//2X,'NORMALIZED COEFFICIENTS ARE:'/8(1X,F10.5)
      DO 9 I=1,M
    9 CW(I)=C(I)*W(I)
      WRITE(6,1000)(CW(I),I=1,M)
 1000 FORMAT(//2X,'COEFFICIENTS IMPROVED BY HAMMING'
     1/8(1X,F10.5))
      STOP
      END
```

## APPENDIX E

```
C*****************************************************************
C   PROGRAM FOR PLOTTING 100 CALCULATED AND MEASURED POINTS
C   OF ANY NONRECURSIVE FILTER WITH GIVEN IMPULSE RESPONSE
C*****************************************************************
C
C
C   THIS PROGRAM CALCULATES AND PLOTS AMPLITUDE AND PHASE OF
C   FIR DIGITAL FILTER WITH TRANSFER FUNCTION
C   H(Z) = C(0)+C(1)*Z**(-1)+C(2)*Z**(-2)+....+C(M)*Z**(-M)
C   C(M)  FINITE IMPULSE RESPONSE
C
C
      COMPLEX ZINV,G,P
      COMPLEX CEXP,CMPLX
      DIMENSION F(150),C(30),AMP(150),PHASE(150),B(150),
     1BB(150),BA(150),AMPL(150),AMPLT(150)
     1AMPL(150),AMPLT(150)
      INTEGER*4   ITB(12)/12*0/
      REAL*4     RTB(28)/28*0.0/
      PI=3.14159265
      M=11
      CONVRT=180./PI
      READ(5,500)(C(I),I=1,M)
  500 FORMAT(8F10.5)
      READ(5,500) (B(K),K=1,101)
      WRITE(6,850) (B(K),K=1,101)
  850 FORMAT(//2X,'DATA ARE:',///(8(1X,F10.5),/))
      BMAX=B(89)
      DO 1000 J=1,101
 1000 IF(B(J).GT.BMAX) BMAX=B(J)
      DO 1100 J=1,101
      BB(J)=B(J)/BMAX
 1100 BA(J)=20.*ALOG10(BB(J))
      WRITE(6,800)(C(I),I=1,M)
  800 FORMAT(//2X,'NORMALIZED COEFFICIENTS ARE:'/8(1X,F10.5))
      WRITE(6,50)
   50 FORMAT(///5X,'FREQUENCY',8X,'AMPLITUDE',13X,'PHASE'///)
      DO 10 J=1,101
C
C   F IS FREQUENCY IN FRACTIONS OF NYQUIST FREQUENCY
C
      F(J)=0.005*FLOAT(J-1)
      ZINV=CEXP(CMPLX(0.,-2.*F(J)*PI))
      P=CMPLX(1.,0.)
      G=CMPLX(0.,0.)
      DO 6 I=1,M
      G=G+P*C(I)
    6 P=P*ZINV
      AMP(J)=CABS(G)
      X=REAL(G)
      Y=AIMAG(G)
      IF(ABS(X).GT.1.E-8) GO TO 60
      PHASE(J)=SIGN(90.,Y)
      GO TO 8
   60 PHASE(J)=ATAN2(Y,X)*CONVRT
    8 WRITE(6,20) F(J),AMP(J),PHASE(J),B(J)
   20 FORMAT(5X,F6.3,4X,E16.8,4X,E16.8,6X,E16.8)
   10 CONTINUE
      AMAX=AMP(51)
      DO 2000 J=1,101
      IF(AMP(J).GT.AMAX) AMAX=AMP(J)
 2000 CONTINUE
      DO 2100 J=1,101
      AMPL(J)=AMP(J)/AMAX
 2100 AMPLT(J)=20.*ALOG10(AMPL(J))
      ITB(1)=1
      ITB(2)=0
      EQUIVALENCE(TITLE,RTB(5))
```

```
      REAL*8   TITLE(12)
      READ(5,7) TITLE
    7 FORMAT(6A8)
      CALL DRAWP(101,F,AMPLT,ITB,RTB)
      ITB(1)=3
      ITB(2)=3
      CALL DRAWP(101,F,BA,ITB,RTB)
      STOP
      END
```

## APPENDIX F

## TAPPING RESISTANCES FOR NON-RECURSIVE FILTER

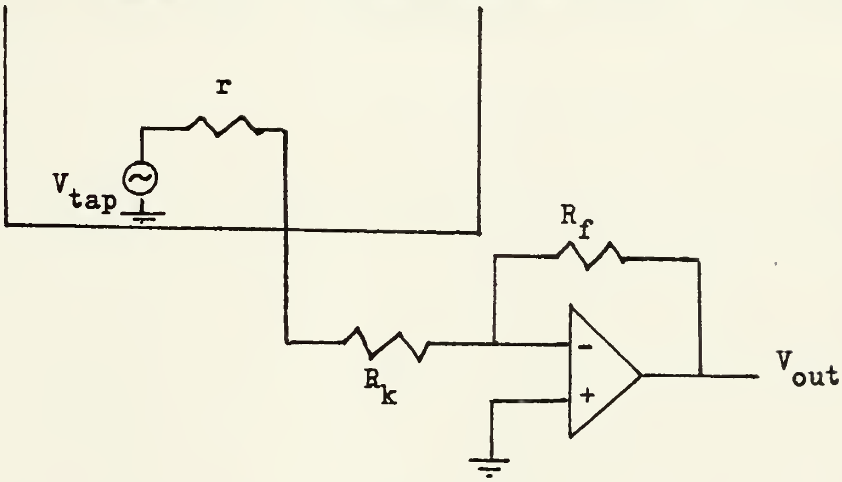


**FIGURE F.1 Coefficient Implementation**

The contribution of a single tap, $V_k$, to the output, $V_{out}$, is the product of $V_k$ and the coefficient, $A_k$, or

$$|A_k| = \left|\frac{V_{out}}{V_k}\right| = \frac{R_f}{r + R_k}$$

The expression indicates that $R_k$ is inversely proportional to $A_k$, therefore the largest coefficient will correspond to the minimum resistance, $R_{min}$, so

$$A_{max} = \frac{R_f}{r + R_{min}}$$

Solving this equation for $R_f$ and substituting that result into the $A_k$ expression yields:

$$|A_k| = \frac{A_{max}\ (r + R_{min})}{r + R_k}$$

or,

$$R_k = \frac{A_{max}}{A_k} (r + R_{min}) - r$$

For the TAD-12, the output impedance for a tap, r, is about 5 Kilo-ohms.

## LIST OF REFERENCES

1. Oppenheim, Alan V. and Schafer, Ronald W., Digital Signal Processing, Prentice-Hall, 1975.

2. Gold, B. and Rader, C. M., Digital Processing of Signals, McGraw-Hill, 1969.

3. Taub, H. and Schilling, D. L., Principles of Communication Systems, McGraw-Hill, 1971.

## INITIAL DISTRIBUTION LIST

| | | No. Copies |
|---|---|---|
| 1. | Defense Documentation Center<br>Cameron Station<br>Alexandria, Virginia 22314 | 2 |
| 2. | Library, Code 0212<br>Naval Postgraduate School<br>Monterey, California 93940 | 2 |
| 3. | Department Chairman, Code 62<br>Department of Electrical Engineering<br>Naval Postgraduate chool<br>Monterey, California 93940 | 2 |
| 4. | Assoc. Professor T. F. Tao, Code 62 TV<br>Department of Electrical Engineering<br>Naval Postgraduate School<br>Monterey, California 93940 | 10 |
| 5. | Ang Vong Mongkol<br>P.O. Box BF<br>Pacific Grove, CA 93950 | 3 |